THERMAL STRUCTURAL INSTABILITY AND MAGNETORESISTANCE IN $EuTiO_3$

QIU HONGFEI

NATIONAL UNIVERSITY OF SINGAPORE

2017

THERMAL STRUCTURAL INSTABILITY AND MAGNETORESISTANCE IN $EuTiO_3$

Qiu Hongfei

(*B. Sci. , Sichuan University*)

Supervisor: Prof. Wang Jian-sheng

A THESIS SUBMITTED

FOR THE DEGREE OF DOCTOR OF

PHILOSOPHER

DEPARTMENT OF PHYSICS

NATIONAL UNIVERSITY OF SINGAPORE

2017

DECLARATION

I hereby declare that the thesis is my original work and it has been written by me in its entirety. I have duly acknowledged all the sources of information which have been used in the thesis.

This thesis has also not been submitted for any degree in any university previously.

Qiu Hongfei

21st August 2017

Acknowledgment

I would like to thank my supervisor, Prof. Wang Jian-Sheng. His insightful opinions and suggestions are most valuable to me. His immense patience and calm pieces of advice have made this thesis possible

I would like to express my gratitude towards to my colleagues Chen Ruofan, Ren Jichang, Yang Kaike for helpful discussions.

Lastly but most importantly, I would like to thank and delicate this thesis to my parents, especially to my father.

Contents

Abstract

Due to the potential for being multiferroics, the interests on $EuTiO_3$ (ETO) have aroused in recent year. Rich phenomena due to coupling between magnetism, electron and phonon, make ETO so fascinating.

Among all these properties, magnetoresistance and soft mode are studied in this thesis. Firstly, the influence of second-order Jahn-Teller effect on anharmonic phonon is investigated, and find second-order coupling can enhance the softness of soft mode frequency. And the anharmonic oscillation is also stabilized by such coupling under proper condition. Secondly, a combination of NEGF and Boltzmann equation is used to inspect some possible causes for large colossal magnetoresistance, and it confirms the important contribution of molecular field. Thirdly, an algorithm to solve spin Green's function of arbitrary nano-size spin system is proposed, which suggest a possible way to investigate transport of nano-size spintronic device within NEGF framework.

List of Tables

List of Figures

Chapter 1

Introduction

Searching for novel functional materials is one of major tasks for nowadays scientific research. Transition metal oxides are already widely utilized in modern electronic technology, due to their various physical properties, e.g. thermal, magnetic and electronic properties. For example, high temperature superconductivity in copper oxides [7] has draw huge interests for both scientist and engineer.

Magnetoresistance is important phenomenon due to coupling between electronic and magnetic properties. Magnetoresistance was discovered in 19th century. Since giant magnetoresistive was discovered by Perter Gruenberg [8, 9] and Albert Fert [9] in late 1980s, Magnetoresistance plays crucial roles in IT industry, especially used for storage technology. For last 30 years, mechanical hard disk is primary storage device for computers, until recent year solid state hard disk progressed quickly and potential to replace mechanical hard disk. The fast development of solid state storage is due to the, better utilization of ferroelectricity, which is the key for non-voltage memory unit. Ferroelectricity related structural instability and magnetoresistance of $EiTiO_3$ are two main topics for this thesis.

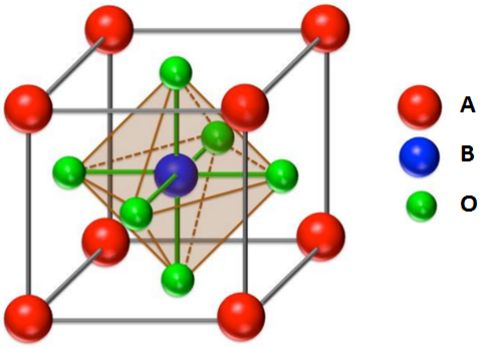

Fig. 1.1. Structure of perovskite oxide ABO_3

1.1 Perovskite and $EuTiO_3$

As a member of perovskite , $EuTiO_3$ (ETO) have basic perovskite structure. Perovskite is originally a name for calcium titanium oxide $CaTiO_3$ by Russian mineralogist Lev Perovski. But now it is extended to a name for a class of compounds which share same structure of $CaTiO_3$. Perovskite oxide is generally of formula ABO_3. Ideal cubic unit structure is shown in Fig. 1.1. A site cation is a Trivalant rare earth ion, e.g. Pr, La, Gd etc. or divalent alkaline earth, e.g. Ca, Sr, Ba etc. and occupies a corner position. B site cation is a transition metal ion, like Mn, Ti, Co, Fe etc. and locates at the body center with oxygen octahedral cage as BO_3. However general formula contains oxygen, there are few perovskite compounds replaced oxygen with other compound, such as $NaMgF_3$.

Perovskite oxides drew intensive research interests due to its fascinating magnetic, electrical and optical properties and be already implemented in various applications[10, 11].

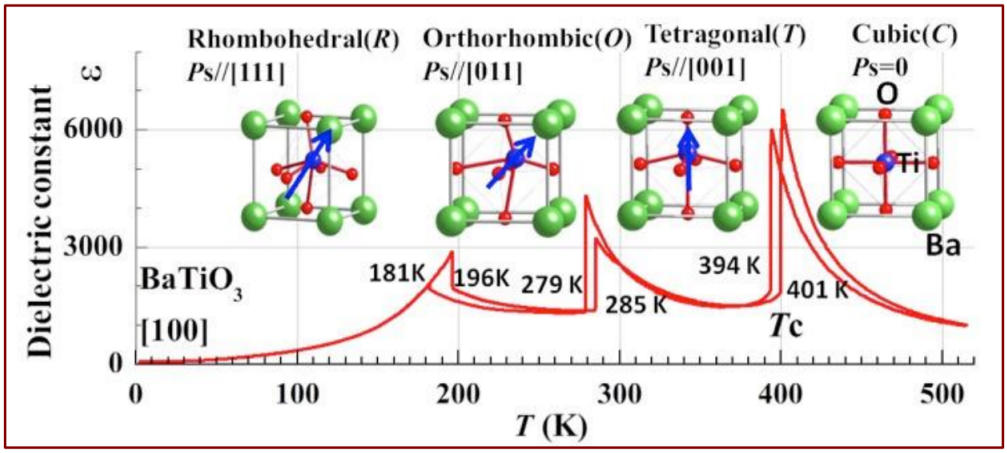

Fig. 1.2. Temperature dependence of dielectric constant of BTO single crystal. Insets show the schematics of Ti displacement in the oxygen octahedron of the perovskite structure. TC represents the paraelectric-to-ferroelectric phase transition. Figure from Ref.[1]

1.1.1 Alkaline-earth Titanates

Alkaline earth titanate ($ATiO_3$, A: Ca, Ba and Sr) is a important group of perovskite materials for electronic industry. $BaTiO_3$(BTO) was discovered during W.W.II and detailed structure in high temperature is firstly given by H.D. Megaw [12]. And series of phase transition was revealed by A. Von Hippel[13, 13], as shown in Fig. 1.2. As the first ferroelectric materials without hydrogen bond, which is known as displasive ferroelectricity nowadays, it initiated a new area of research. BTO is ideal cubic form at above ferroelectric transition temperature (around 400K), in which All Ba^{2+} resides at eight corner, Ti^{4+} stays at body center with O^{2-} at each surface center. Distortion appeared below 400K, as mutual displace of positive and negative charge center which leads to spontaneous polarization. Due to the large dielectric constant. ferroelectric and piezoelectric properties, BTO is most widely used among Alkaline-earth titanates.

However both $CaTiO_3$(CTO) and $SrTiO_3$(STO) [14] undergo structural phase transition, both Bulk CTO and STO are paraelectric down to lowest temperature. CTO is cubic structure at above 1636K[14], and

STO have transition temperature at only 110K. At room temperature cubic STO, with lattice constant $a = 3.905\mathring{A}$, is a band insulator with band gap of 3.2eV. Series of structural phase transition, cubic $\rightarrow$ tetragonal $\rightarrow$ orthorhombic $\rightarrow$ rhombohedra, happen at 110K, 60K, 30K respectively[15, 16, 17]. Although ferroelectricity is not shown in normal bulk STO sample at even low temperature, it could be induce by structural perturbation by either strain [18, 19] or chemical substitution [20, 21].

1.1.2 Rare-earth Titanates

Intensive research is conduced on STO since 1980s, but recent year, ETO, as a magnetic relative to STO, is gaining its own attention. ETO belongs to Rare-earth titanates, in which A-site cation is occupied by La, Gd, Eu, Sm, Pr etc. and usually have Ti^{3+} $(t_{2g}^1 e_g^0)$ rather than Ti^{4+} in alkaline-earth titanates. But ETO is a exception that it have teravalent Ti as in alkaline-earth titanate. Other trivalent rare-earth titanate $RTiO_3$ have pseudo-cubic perovskite structure with TiO_6 orthorhombic distortion, in which magnitude is directly related to ionic radii of A-site cation. Larger radius leads to weaker distortion, i.e. Ti-O-Ti is more stabilized as a straight line rather than decrease bond angle from 180°. Trivalent $RTiO_3$ is Mott insulator, with each Ti^{3+} have one electron occupying t_{2g} orbital. So it is possible to undergo a transition to metal by doping with divalent alkaline [22, 23, 24];

1.1.3 $EuTiO_3$

Eu is divalent with half filled $4f^7$ orbital and show strong magnetic properties. As ETO is structurally similar to STO, with almost equal lattice constant, $a = 3.905\mathring{A}$, they often undergo comparative study[25]. Main difference is the magnetic properties of ETO due to $4f^7$ spins. ETO is in G-type anti-ferromagnetic ordering below $T_N = 5.3K$ as shown in Fig. 1.3.

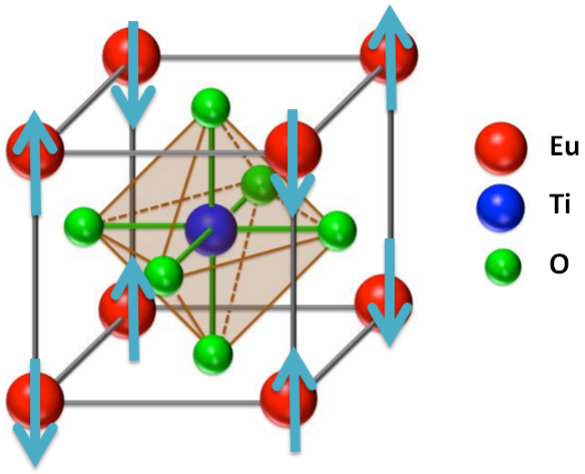

Fig. 1.3. G-type configuration of $EuTiO_3$

For long time, ETO was considered having ground state of cubic structure, but later it is realized that ETO also undergoes cubic-tetragonal transition at around 282K, just like similar transition of STO at 105k. And first principle calculation predicts rotation and oxygen octahedra tilting at ground state. However, ETO undergoes structural phase transition, no ferroelectricity is observed in bulk ETO. But strained film [26] and nanotube [27] are predicated to be ferroelectric.

Magnetoresistance is change in electrical resistance under the influence of magnetic field, which was found in thin layers of alternating nonmagnetic and ferromagnetic materials[8, 9]. Colossal magnetoresistance (CMR) is dramatic magnetoresistance change. Although Extensive study was conducted on manganese-based perovskite oxides [28, 29, 30, 31, 32, 33, 34, 35]. Large CMR is also observed in ETO by Km Rubi [36], and it is the first observation of CMR among the rare earth titanates.

1.2 Objective

As a promising materials for creating multiferroics, extensive researches have been conducted on ETO. But many aspects are still unclear, such as the colossal negative magnetoresistance is not well explained. Usual double-exchange mechanism is definitely not applicable here. And the better utilization of multiferroics need deeper understanding of ferroelectricity and structural instabilities. The aim of my study is to have deeper understanding of these two aspects of bulk $EuTiO_3$. Firstly, thermal instability in Titanate is studied, which is directly link to structural phase transition. I do not stick to real $EuTiO_3$ system, but a toy model as generalization of $EuTiO_3$ and $SrTiO_3$. And I calculate influence of second-order Jahn-Teller effect on soft mode frequency. Secondly, I investigate magnetoresistance in $EuTiO_3$. Thirdly, I proposed a method to calculated spin Green's function at finite temperature. The method is not directly linked to bulk $EuTiO_3$, but is potential for modeling of nano-size functional structure on thin-film $EuTiO_3$.

This thesis is organized as following. In Chapter 2, I introduce theories which I used for my model calculation. In Chapter 3, I review theories of displasive ferroelectricity. Then I use a dynamic covalence model and use non-equilibrium Green's function method to do calculation, and show the roles of mediated electron on harmonically ionic oscillation. In Chapter 4, I study spin-scattering model to investigate colossal magnetoresistance due to interaction of spin and electron system. In Chapter 5, I formulate computable spin Green's function for arbitrary nano-size system and proposeda algorithm to perform tedious expansion procedure automatically.

Chapter 2

Methods

2.1 Nonequilibrium Green's Function

2.1.1 Interaction Picture

Schrodinger picture and Heisenberg picture, which evolve only states and operator respectively, are two basic formalism to treat dynamic evolution of quantum system. However interaction picture, which evolve both wave function and operator, is more preferred in NEGF formalism.

Considering a system with Hamiltonian H, the state at time t is denoted as$|\psi(t)\rangle_\alpha$, subscript α can be "S", "H", or "I", denoting Schrodinger, Heisenberg, Interaction picture respectively, the same for observable $A_\alpha(t)$. t_0 means initial synchronization time, i.e. $|\psi(t_0)\rangle_S = |\psi(t_0)\rangle_H = |\psi(t_0)\rangle_I$.

In Schrodinger picture:

$$|\psi(t)\rangle_S = U_S(t,t_0)\,|\psi(t_0)\rangle_S,$$

$U_S(t,t_0)$ is evolution operator, and formally written as

$$U_S(t,t_0) = Te^{-\frac{i}{\hbar}\int_{t_0}^{t} H(t')dt'},$$

notation T means time-order operator which always arrange the operator with earlier time to the right. Conversely, anti-time-order operator $\bar{T}$ put earlier operator to left.

$$U_S(t_1,t_2) = U_S^{-1}(t_2,t_1) = U_S^{\dagger}(t_2,t_1) = \bar{T}e^{-\frac{i}{\hbar}\int_{t_0}^{t} H(t')dt'}.$$

So that, the quantum average of observable A is $\langle\psi(t)|_S A_s(t)|\psi(t)\rangle_S$.

Alternatively, states themselves can remain unchanged but only operators evolve. So operator in Heisenberg picture is defined as

$$\begin{aligned} A_H(t) &= U_S(t_0,t) A_s(t) U_S(t,t_0) \\ |\psi(t)\rangle_H &= |\psi(t_0)\rangle_H \end{aligned}$$

and

$$\begin{aligned} & \langle\psi(t)|_H A_H(t)|\psi(t)\rangle_H \\ = & \langle\psi(t)|_H U_S(t_0,t) A_s(t) U_S(t,t_0)|\psi(t)\rangle_H \\ = & \langle\psi(t_0)|_S U_S(t_0,t) A_s(t) U_S(t,t_0)|\psi(t_0)\rangle_S \\ = & \langle\psi(t)|_S A_s(t)|\psi(t)\rangle_S . \end{aligned}$$

Hence the selection of picture is just a choice of calculation tool. The quantum average, which is we are really care about, don't change. It also hold for interaction picture. Assuming Hamiltonian H consists of two parts,

$$H(t) = H_0 + V(t), \tag{2.1}$$

in which $H_0$is assumed solvable, i.e. eigenfunctions and eigenvalues of H_0 are known, and V is interaction.

In interaction picture, both states and operators evolve, but they evolve

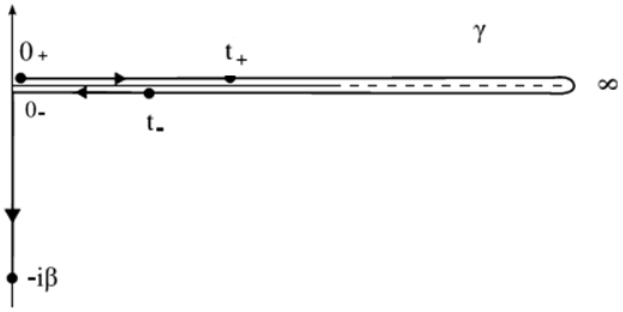

Fig. 2.1. Keldysh contour

with H_0 and V respectively.

$$\begin{aligned} |\psi(t)\rangle_I &= e^{\frac{i}{\hbar}H_0 t} |\psi(t_0)\rangle_S \\ A_I(t) &= e^{\frac{i}{\hbar}H_0 t} A_s(t) e^{-\frac{i}{\hbar}H_0 t} \end{aligned}$$

$$\begin{aligned} U_I(t,t_0) &= e^{\frac{i}{\hbar}H_0 t} U_S(t,t_0) e^{-\frac{i}{\hbar}H_0 t_0} \\ &= T e^{-\frac{i}{\hbar}\int_{t_0}^{t} V(t')dt'}. \end{aligned}$$

Although interaction picture looks more complicated as both states and operators evolve, it facilitate calculation due to the separation of solvable part H_0 and interaction V.

2.1.2 Keldysh Contour

Before introducing contour-ordered Green's functions, which are the central roles in NEGF formalism, forward-backward time contour is shown as Fig. 2.1.

Evolution process starts from particular time t_0 and forwards to some target time t_f then return back to initial time t_0. Arbitrary time point denoted as t, can be in either forward branch or backward branch, denoted

t^+ and t^- respectively. The advantage of this loop process is that lots of quantities can be calculated at time point t_0 when system are determined by solvable part H_0 only and easily be calculated.

2.1.3 Adiabatic Switch-on

Aiming for simplifying calculation by calculate quantities at the time when interaction is off, the transition process have to be properly chosen. Starting with the Hamiltonian Eq. 2.1, the time depended part is written as

$$V(t) = \lim_{\epsilon \to 0_+} e^{-|t|\epsilon} V_0,$$

which means the interaction is fully switched on at time point $t = 0$, and the system has no interaction at $t = \pm\infty$. Then let $t_0 = -\infty$,

$$|\psi(t)\rangle_I = U_\epsilon(t, t_0) |\psi(t_0)\rangle_I \tag{2.2}$$

$$i\hbar \frac{\partial}{\partial t} U_\epsilon(t, t_0) = e^{-\epsilon|t|} V_0 U_\epsilon(t, t_0).$$

After integration, it gives

$$U_\epsilon(t, t_0) = T e^{-\frac{i}{\hbar}\int_{t_0}^{t} e^{-\epsilon|t'|} V_0 dt'}. \tag{2.3}$$

According to 2.2 and 2.3:

$$|\psi(t_0)\rangle_I = e^{\frac{i}{\hbar} H_0 t_0} |\psi(t_0)\rangle_S.$$

Since $t_0 \to -\infty$, total Hamiltonian $H \to H_0$, initial state $|\psi(t_0)\rangle_S$ is exactly only determined by solvable part H_0. The evolution along imaginary time axis is no longer needed, and I only used Schwinger-Keldysh Contour (Fig. 2.2) rather than normal Keldysh contour in this thesis. Because the switch-on process of interaction is gradual and infinitesimally slow, the

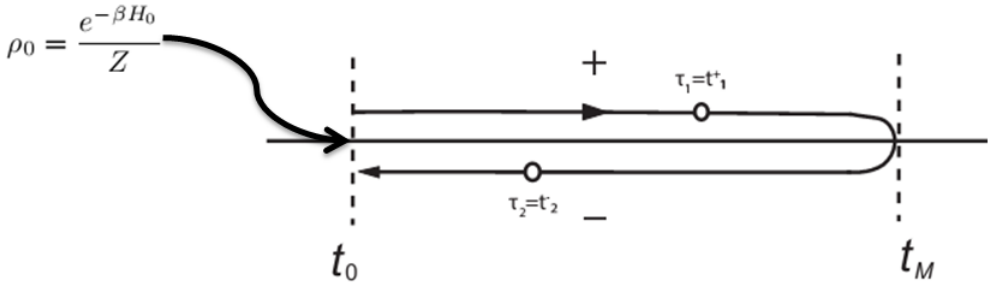

Fig. 2.2. Schwinger-Keldysh contour

states with full interaction is able to expressed by non-interactive state via propagator $U(t, -\infty)$.

2.1.4 Fermionic Green's Functions

Starting with fermionic Green's function, we define contour ordered Green's function firstly

$$G(r,t;r',t') = -\frac{i}{\hbar}\left\langle T_c \hat{C}(r,t)\,\hat{C}^{\dagger}(r',t')\right\rangle .$$

Green's functions are defined in different way for fermionic and bosonic operator.

The following 4 Green's functions are defined on real time axis,

$$\begin{aligned}
G^{>}(r,t;r',t') &= -\frac{i}{\hbar}\left\langle \hat{C}(r,t)\,\hat{C}^{\dagger}(r',t')\right\rangle \\
G^{<}(r,t;r',t') &= \frac{i}{\hbar}\left\langle \hat{C}^{\dagger}(r',t')\,\hat{C}(r,t)\right\rangle \\
G^{t}(r,t;r',t') &= \theta(t-t')\,G^{>}(r,t;r',t') + \theta(t'-t)\,G^{<}(r,t;r',t') \\
G^{\bar{t}}(r,t;r',t') &= \theta(t'-t)\,G^{>}(r,t;r',t') + \theta(t-t')\,G^{<}(r,t;r',t'),
\end{aligned}$$

where $\langle \ldots\ldots \rangle$ denotes an appropriately defined average. Although it can be either equilibrium or non-equilibrium average, only equilibrium average is used in this thesis. It averages over full Hamiltonian H by default, and is denoted with "0" when averages over non-interactive part H_0. $>$ and

$<$ denote greater and less Green's function respectively, and "t" and "$\bar{t}$" mean time ordered and anti-time ordered Green's function. Due to both t' and t can be in either upper branch (+) or lower branch (-) , it get 4 ways of paring and contour ordered Green's function is corresponding to one of aforementioned Green's functions as

$$\begin{array}{ccc} & t'_+ & t'_- \\ t_+ & G^t\left(r,t;r',t'\right) & G^{>}\left(r,t;r',t'\right) \\ t_- & G^{<}\left(r,t;r',t'\right) & G^{\bar{t}}\left(r,t;r',t'\right) \end{array} . \tag{2.4}$$

However, two more Green's are needed to have simpler formalism. Retarded Green's function (denoted with "r") and advanced Green's function ("a") are more preferred in actual calculation. they can be obtained by rotation of Eq. 2.4,

$$\begin{aligned} G^r\left(r,t;r',t'\right) &= -\frac{i}{\hbar}\theta\left(t-t'\right)\left\langle\left\{\hat{C}\left(r,t\right)\hat{C}^{\dagger}\left(r',t'\right)\right\}\right\rangle \\ G^a\left(r,t;r',t'\right) &= \frac{i}{\hbar}\theta\left(t'-t\right)\left\langle\left\{\hat{C}\left(r,t\right)\hat{C}^{\dagger}\left(r',t'\right)\right\}\right\rangle . \end{aligned}$$

$\theta\left(t\right)$ is Heaviside step function defined as

$$\theta\left(t\right)=\begin{cases} 1 & t>0 \\ \frac{1}{2} & t=0 \\ 0 & t<0 \end{cases}$$

By definition, it is easy to get two useful relations

$$G^r\left(r,t;r',t'\right)-G^a\left(r,t;r',t'\right) = G^{>}\left(r,t;r',t'\right)-G^{<}\left(r,t;r',t'\right) \tag{2.5}$$

$$G^r\left(r,t;r',t'\right)+G^a\left(r,t;r',t'\right) = G^t\left(r,t;r',t'\right)-G^{\bar{t}}\left(r,t;r',t'\right) . \tag{2.6}$$

If the calculation is for quantities in equilibrium or static case, calculation can be substantially simplified by working in frequency domain. For a translational invariant function

$$F_{AB}(t,t') = F_{AB}(t-t').$$

Fourier transformation is defined as

$$F_{AB}(\omega) = \int_{-\infty}^{\infty} dt e^{i\omega t} F_{AB}(t).$$

Be noted, the reverse transformation is with normalization factor

$$F_{AB}(t) = \frac{1}{2\pi}\int_{-\infty}^{\infty} d\omega e^{-i\omega t} F_{AB}(\omega).$$

Spectral density is defined as

$$A(\omega) = -2ImG^{r}(\omega) = 2ImG^{a}(\omega), \tag{2.7}$$

which always satisfies the normalization condition

$$\frac{1}{2\pi}\int_{-\infty}^{\infty} A(\omega) = 1$$

For solvable system, assuming eigenvalue is ε, it produce the Green's function in Fourier space

$$\begin{aligned}
G^{0,r}(\omega) &= \frac{1}{\omega\hbar - \varepsilon + i\eta} \\
G^{0,a}(\omega) &= \frac{1}{\omega\hbar - \varepsilon - i\eta} \\
G^{0,>}(\omega) &= 2\pi f(-\omega)\,\delta(\omega\hbar - \varepsilon) \\
G^{0,<}(\omega) &= 2\pi f(\omega)\,\delta(\omega\hbar - \varepsilon)
\end{aligned}$$

in which $f(\omega)$ is Fermi function $f(\omega) = \frac{1}{e^{\beta\omega\hbar}+1}$.

2.1.5 Phonon Green's Functions

Bosonic Green's function is similar to fermionic Green's function. Six Green's functions are defined as fermionic case. However it could simply replace fermionic creation and annihilation operators with bosonic creation and annihilation operators, displacement operator $u == \sqrt{\frac{\hbar}{2m\omega_0}}\left(a^\dagger + a\right)$ is used,

$$\begin{aligned}
D^r(r,t;r',t') &= -\frac{i}{\hbar}\theta(t-t')\langle[u(r,t),u(r',t')]\rangle \\
D^a(r,t;r',t') &= \frac{i}{\hbar}\theta(t'-t)\langle[u(r,t),u(r',t')]\rangle \\
D^>(r,t;r',t') &= -\frac{i}{\hbar}\langle u(r,t)\,u(r',t')\rangle \\
D^<(r,t;r',t') &= -\frac{i}{\hbar}\langle u(r',t')\,u(r,t)\rangle \\
D^t(r,t;r',t') &= \theta(t-t')D^>(r,t;r',t') + \theta(t'-t)D^<(r,t;r',t') \\
D^{\bar{t}}(r,t;r',t') &= \theta(t'-t)D^>(r,t;r',t') + \theta(t-t')D^<(r,t;r',t').
\end{aligned}$$

Noted that $u^\dagger = u$. By this definition, the important relation 2.5 and 2.6 are hold as well here,

$$\begin{aligned}
D^r(r,t;r',t') - D^a(r,t;r',t') &= D^>(r,t;r',t') - D^<(r,t;r',t') \\
D^r(r,t;r',t') + D^a(r,t;r',t') &= D^t(r,t;r',t') - D^{\bar{t}}(r,t;r',t')
\end{aligned}$$

But due to the choice of operator u, non-interactive Green's functions in Fourier space are,

$$\begin{aligned} D_{u,u}^{>}(\omega) &= -\frac{i\pi}{m\omega_0}\sum_{\sigma=\pm 1}\delta(\omega+\sigma\omega_0)\,\sigma n(\sigma\omega_0) \\ D_{u,u}^{<}(\omega) &= -\frac{i\pi}{m\omega_0}\sum_{\sigma=\pm 1}\delta(\omega-\sigma\omega_0)\,\sigma n(\sigma\omega_0) \\ D_{u,u}^{r}(\omega) &= \frac{1}{m}\lim_{\eta\to 0^+}\frac{1}{(\omega+i\eta)^2-\omega_0^2} \\ D_{u,u}^{a}(\omega) &= \frac{1}{m}\lim_{\eta\to 0^+}\frac{1}{(\omega-i\eta)^2-\omega_0^2}, \end{aligned}$$

$n(\omega)$ is boson distribution $n(\omega)=\frac{1}{e^{\beta\omega\hbar}-1}$.

Wick's Theorem

When doing perturbative expansion, it produce infinite series which always contain terms of product of multiple operators like $\left\langle \hat{O}_0\hat{O}_1\cdots\hat{O}_{n-1}\right\rangle$. Wick's theorem says,

$$\left\langle T_c\hat{O}_0\hat{O}_1\cdots\hat{O}_{n-1}\right\rangle = \sum_{i_1,i_2,\cdots i_n}\alpha^{N_p}\left\langle T_c\hat{O}_{i_1}\hat{O}_{i_2}\right\rangle\left\langle T_c\hat{O}_{i_3}\hat{O}_{i_4}\right\rangle\cdots\left\langle T_c\hat{O}_{i_{n-1}}\hat{O}_{i_n}\right\rangle,$$

where $i_1, i_2, \cdots i_n$ are permutation of $0, 1, 2, \cdots, n$ that make $\left\langle T_c\hat{O}_{i_m}\hat{O}_{i_n}\right\rangle$ paired with annihilation operator at left and creation operator at right. And N_p are numbers of permutation. $\alpha = 1$ for boson, and $\alpha = -1$ for fermion, i.e. every adjacent permutation bring sign change for fermion. For example, for electron operator C_i, $\left\langle T_cC_1^\dagger C_2C_3C_4^\dagger\right\rangle = -\left\langle T_cC_3C_4^\dagger\right\rangle\left\langle T_cC_2C_1^\dagger\right\rangle + \left\langle T_cC_3C_1^\dagger\right\rangle\left\langle T_cC_2C_4^\dagger\right\rangle$.

Wick's theorem is only applicable to contour Green's function at finite temperature, i.e. Wick's theorem have be applied before aftermentioned Langreth's theorem.

2.1.6 Fluctuation-dissipation Theorem

Greater and less Green's function represent the the time dependent correlation. Retarded and advanced Green's funcions, we will see in later section, represent the responses. Correlation and response functions are usually the keys to the quantities that we care about, or even themselves are quantities of huge interests.

It is tough task to calculate aforementioned Green's functions in non-trivial system, but it is possible to easily relate retarded and advanced Green's function to greater and less green function in equilibrium system. The relation is terms as Fluctuation-dissipation theorem,

$$\begin{aligned} G^{<}(\omega) &= if(\omega) A(\omega) \\ G^{>}(\omega) &= e^{-\beta\omega} G^{<}(\omega), \end{aligned}$$

which could be proved via Lemann representation.Combining with Eq. 2.7, we will see that retarded Green's function would be of significant interest. If retarded Green's function is gotten, we will have all other Green's function naturally. It is crucial relation to investigate magnetic property via spin Green's function in later chapter. Due to Eq.2.7, spectral is imaginary part of retarded Green's function but of only real value, so the greater and less functions are purely imaginary.

2.1.7 Langreth's Theorem

The six Green's functions are directly linked to contour ordered Green's function according to on which branch the two time points t and t' are. But things get complicated when multiple terms get involved, like arbitrary function with 2 contour time $F(t_n, t_i) = \int_C dt_1 dt_2 \cdots dt_{n-1} A(t_0, t_1) B(t_1, t_2) \cdots\cdots Z(t_{n-1}, t_n)$, C means integrate over contour loop. This kind of collective contour terms,

that could be multiplied or convolved, is common when doing perturbative expansion. To dealing with it, one have to find the way to map these terms of contour loop to real time axis. It is called Langreth's theorem, which is consisted of several mapping rules.

Let's start with a simple case:

$$A(t,t') = \int_C B(t,\tau)\, C(\tau,t')\, d\tau,$$

assuming $t < t'$, and τ is dummy variable. Firstly we consider less function

$$A^<(t,t') = \int_{C_1} B(t,\tau)\, C^<(\tau,t')\, d\tau + \int_{C_2} B^<(t,\tau)\, C(\tau,t')\, d\tau,$$

here the full contour C is divided to 2 parts, $C_1$and C_2. C_1 is $(-\infty_+, t')$ and C_2 is $(t, -\infty_-)$,noted that there is overlapping part between t, t' . "$-\infty_+$" , "$-\infty_-$ " mean beginning and end of contour loop correspondingly, which are both in $-\infty$.

$$\begin{aligned}
& A^<(t,t') \\
= & \begin{cases} & \int_{-\infty_+}^{t} B^<(t,\tau)\, C^<(\tau,t')\, d\tau + \int_{t}^{-\infty_-} B^<(t,\tau)\, C^<(\tau,t')\, d\tau \\ + & \int_{-\infty_+}^{t'} B^<(t,\tau)\, C^<(\tau,t')\, d\tau + \int_{t'}^{-\infty_-} B^>(t,\tau)\, C^>(\tau,t')\, d\tau \end{cases} \\
= & \begin{cases} & \int_{-\infty}^{t} \left(B^>(t,\tau) - B^<(t,\tau)\right) C^<(\tau,t')\, d\tau \\ + & \int_{-\infty}^{t'} B^<(t,\tau) \left(C^<(\tau,t') - C^>(\tau,t')\right) d\tau \end{cases} \\
= & \begin{cases} & \int_{-\infty}^{+\infty} \theta(t-\tau) \left(B^>(t,\tau) - B^<(t,\tau)\right) C^<(\tau,t')\, d\tau \\ + & \int_{-\infty}^{+\infty} \theta(t'-\tau)\, B^<(t,\tau) \left(C^<(\tau,t') - C^>(\tau,t')\right) d\tau \end{cases} \\
= & \int_{-\infty}^{+\infty} B^r(t,\tau)\, C^<(\tau,t')\, d\tau + \int_{-\infty}^{\infty} B^<(t,\tau)\, C^a(\tau,t')\, d\tau,
\end{aligned}$$

which can be symbolically simplied as

$$A^{<} = B^{r} C^{<} + B^{<} C^{a}, \tag{2.8}$$

similarly, for greater function,

$$A^{>} = B^{r} C^{>} + B^{>} C^{a}, \tag{2.9}$$

and retarded function,

$$A^{r}(t,t') \;=\; \theta(t-t')\left[A^{>}(t,t') - A^{<}(t,t')\right],$$

Substituting greater and less Green's function with Eq.2.8 & 2.9,

$$\begin{aligned}
A^{r}(t,t') &= \theta(t-t') \begin{cases} & \int_{-\infty}^{+\infty} B^{r}(t,\tau)\, C^{>}(\tau,t')\, d\tau + \int_{-\infty}^{\infty} B^{>}(t,\tau)\, C^{a}(\tau,t')\, d\tau \\ - & \int_{-\infty}^{+\infty} B^{r}(t,\tau)\, C^{<}(\tau,t')\, d\tau - \int_{-\infty}^{\infty} B^{<}(t,\tau)\, C^{a}(\tau,t')\, d\tau \end{cases} \\
&= \theta(t-t') \begin{cases} & \int_{-\infty}^{+\infty} B^{r}(t,\tau)\, \theta(\tau-t') \left[C^{>}(\tau,t') - C^{<}(\tau,t')\right] d\tau \\ + & \int_{-\infty}^{+\infty} B^{r}(t,\tau)\, \theta(t'-\tau) \left[C^{>}(\tau,t') - C^{<}(\tau,t')\right] d\tau \\ + & \int_{-\infty}^{\infty} \theta(t-\tau) \left[B^{>}(t,\tau) - B^{<}(t,\tau)\right] C^{a}(\tau,t')\, d\tau \\ + & \int_{-\infty}^{\infty} \theta(\tau-t) \left[B^{>}(t,\tau) - B^{<}(t,\tau)\right] C^{a}(\tau,t')\, d\tau \end{cases} \\
&= \theta(t-t') \int_{-\infty}^{+\infty} \left[B^{r}(t,\tau)\, C^{r}(\tau,t') - B^{a}(t,\tau)\, C^{a}(\tau,t')\right] d\tau \\
&= \int_{-\infty}^{+\infty} B^{r}(t,\tau)\, C^{r}(\tau,t').
\end{aligned}$$

Similarly for advanced function, symbolic form is given as

$$A^{r} \;=\; B^{r} C^{r} \tag{2.10}$$

$$A^{a} \;=\; B^{a} C^{a} \tag{2.11}$$

Table 2.1
Langreth Theorem

Contour	Real time
$C(\tau,\tau') = A(\tau,\tau')\,B(\tau,\tau')$	$C^{<}(t,t') = A^{<}(t,t')\,B^{<}(t,t')$
	$C^{r}(t,t') = \begin{cases} & A^{<}(t,t')\,B^{r}(t,t') \\ + & A^{r}(t,t')\,B^{<}(t,t') \\ + & A^{r}(t,t')\,B^{r}(t,t') \end{cases}$
	$C^{<}(\omega) = \int d\omega' A^{<}(\omega-\omega')\,B^{<}(\omega')$
	$C^{r}(\omega) = \int d\omega' \begin{cases} & A^{<}(\omega-\omega')\,B^{r}(\omega') \\ + & A^{r}(\omega-\omega')\,B^{<}(\omega') \\ + & A^{r}(\omega-\omega')\,B^{r}(\omega') \end{cases}$
$D(\tau,\tau') = A(\tau,\tau')\,B(\tau',\tau)$	$D^{<}(t,t') = A^{<}(t,t')\,B^{>}(t',t)$
	$D^{r}(t,t') = \begin{cases} & A^{<}(t,t')\,B^{a}(t',t) \\ + & A^{r}(t,t')\,B^{<}(t',t) \end{cases}$
	$D^{<}(\omega) = A^{<}(\omega+\omega')\,B^{>}(\omega')$
	$D^{r}(\omega) = \int d\omega' \begin{cases} & A^{<}(\omega+\omega')\,B^{a}(\omega') \\ + & A^{r}(\omega+\omega')\,B^{<}(\omega') \end{cases}$

,with Eqs. 2.8,2.9,2.10,2.11m one could summarize general form

$$\begin{aligned} A^{>,<} &= \begin{cases} A_1^r \cdots A_{n-1}^r A_n^{>,<} + A_1^r \cdots A_{n-2}^r A_{n-1}^{>,<} A_n^a + \cdots + \\ A_1^r \cdots A_{i-1}^r A_i^{>,<} A_{i+1}^a \cdots A_n^a + \cdots + A_1^{>,<} A_2^a \cdots A_n^a \end{cases} \\ A^{r,a} &= A_1^{r,a} A_2^{r,a} \ldots A_n^{r,a}. \end{aligned}$$

Besides these simple serial multiplication terms, parallel or looped multiplication terms are also common. And due to the overlapping, they lead to convolution. The relations are listed in Table 2.1.

For other product which is more than 3 terms can be done with the combination of formula in table. For instance, triple terms $F(\tau,\tau') = A(\tau,\tau')\,B(\tau,\tau')\,C(\tau',\tau)$ will be seen later in Section 3.2, and can be expanded to

$$
\begin{aligned}
F^r &= F^t - F^< \\
&= A^t(\tau,\tau')\,B^t(\tau,\tau')\,C^{\bar{t}}(\tau',\tau) - A^<(\tau,\tau')\,B^<(\tau,\tau')\,C^>(\tau',\tau) \\
&= \begin{cases} & [A^r(\tau,\tau') + A^<(\tau,\tau')]\,[B^r(\tau,\tau') + B^<(\tau,\tau')]\,[C^r(\tau',\tau) + C^<(\tau',\tau)] \\ - & A^<(\tau,\tau')\,B^<(\tau,\tau')\,C^>(\tau',\tau) \end{cases} \\
&= \begin{cases} + & A^r(\tau,\tau')\,B^r(\tau,\tau')\,C^r(\tau',\tau) \\ + & A^r(\tau,\tau')\,B^<(\tau,\tau')\,C^r(\tau',\tau) \\ + & A^<(\tau,\tau')\,B^r(\tau,\tau')\,C^r(\tau',\tau) \\ + & A^<(\tau,\tau')\,B^<(\tau,\tau')\,C^a(\tau',\tau)\,\cdot \\ + & A^r(\tau,\tau')\,B^r(\tau,\tau')\,C^<(\tau',\tau) \\ + & A^r(\tau,\tau')\,B^<(\tau,\tau')\,C^<(\tau',\tau) \\ + & A^<(\tau,\tau')\,B^r(\tau,\tau')\,C^<(\tau',\tau) \end{cases}
\end{aligned}
\tag{2.12}
$$

2.2 Boltzmann Equation

2.2.1 Bloch-Boltzmann Theory

Bloch-Boltzmann theory is a semi-classical theory to investigate electronic transport in solids. Although this theory is originally developed for dilute classical gases, it has been successfully applied to metal and semiconductor which are neither classical nor dilute. the core of Bloch-boltzmann theory is Boltzmann equation.

Drude Model

In 1900 Paul Drude proposed Drude model [37, 38], which is historically the first model dealing with electronic transport in metals. Drude model consider electrons as classical particles, ignore interaction between electrons.

Electrons are driven by electric field and accelerating until collision, the average time between subsequent collisions is relaxation time τ. and its equation of motion is

$$m_e \frac{d\langle v \rangle}{dt} + m_e \frac{\langle v \rangle}{\tau} = eE$$

in which , m_e is the mass of electron. By which it is easy to find a linear relation between current density J and electric field E

$$J = \frac{nq^2\tau}{m_e} E.$$

As the first microscopic model , it is pretty crude model by kinetic theory without accounting for the temperature dependence. As the fact that Drude model consider electron as free electron from beginning, the band structure of electrons are disregarded. Furthermore, origin of relaxation time τ is crucial quantity in this model, but it is not well elucidated.

2.2.2 Boltzmann Equation

Boltzmann equation is proposed by Ludwig Boltzmann. It provide a microscopic model to describe statistical behavior of thermodynamic system in non-equilibrium. When it is applied to electric transport problem, it require a semi-classical model for electron system, in which electrons are described by two vectors, position vector $\mathbf{r}$ and wave vector $\mathbf{k}$, wave vector $\mathbf{k}$ may be contraction of $(\mathbf{k}, n)$, n is band index. For particular temperature T, the distribution function of electrons is written as $f(\mathbf{r}, \mathbf{k})$. By which mean number is $\frac{2}{(2\pi)^3} f(\mathbf{r}, \mathbf{k}) \, d\mathbf{r} d\mathbf{k}$, factor 2 is for spin degeneracy. Local density of electrons (of particular band) is

$$n(\mathbf{r}) = \frac{2}{(2\pi)^3} f(\mathbf{r}, \mathbf{k}) \, d\mathbf{k}.$$

Distribution function $f(\mathbf{r},\mathbf{k})$, is usually implicit function of temperature T, and chemical potential μ for equilibrium case. For transient case it is also function of time t. So Boltzmann equation is

$$\frac{\partial f}{\partial t}+\mathbf{v_k}\cdot\nabla_{\mathbf{r}}f+\mathbf{F}\cdot\nabla_{\mathbf{k}}f=\left(\frac{\partial f}{\partial t}\right)_{coll}, \tag{2.13}$$

where force $F=e\left[E(\mathbf{r},t)+v_{\mathbf{k}}\times B(\mathbf{r},t)\right]$ is the Lorentz force. And the equilibrium distribution at temperature T is Fermi-Dirac distribution

$$f_0(\varepsilon_k)=\frac{1}{e^{\beta(\varepsilon_k-\mu)}+1},$$

$\left(\frac{\partial f}{\partial t}\right)_{coll}$ is collision integral.

2.2.3 Collision Process

Collision integral is formally

$$\left(\frac{\partial f}{\partial t}\right)_{coll}=\sum_{k'}P_{k,k'}-P_{k',k}$$

$P_{f,i}$ means the probability of transition from initial state $|i\rangle$ to state $|f\rangle$. Obviously, $\left(\frac{\partial f}{\partial t}\right)_{coll}$ is zero when system reaches equilibrium. the origin of collision is due to various sources. If more than one process contributes to collisions, collision integral should be the sum of all processes. For dilute electron gas, electron-electron interaction is consider weekly interacted and usually omitted. At high temperature, the interaction between electron and thermal vibration is more important than other interactions. but at low temperature, it is impurity that dominate scattering process.

2.2.4 Local Equilibrium

Local equilibrium is that the system is globally in non-equilibrium and locally in equilibrium. So local equilibrium distribution is characterized

by local chemical potential $\mu(\mathbf{r},t)$ and local temperature $T(\mathbf{r},t)$. Local Fermi-Dirac distribution is

$$f^0(\varepsilon_k) = \frac{1}{e^{\frac{[\varepsilon_k - \mu(\mathbf{r},t)]}{\beta(\mathbf{r},t)}} + 1}$$

if system is slightly out of steady local equilibrium, distribution function f_k could be written as $f_k = f_k^0 + \delta f_k$.

The deviation of distribution function is possibly due to various sources. For our interests, the current is commonly driven by electric and magnetic field, as well as temperature gradient and chemical potential gradient. However, electric field and magnetic field affect differently on electrons. Primarily, electric field exchange energy with electron, but magnetic field does not. δf_k is first order perturbative term with respect to electric field, chemical potential gradient and temperature gradient, but contain all orders with respect to the magnetic field.

It is more convenient to define electrochemical potential

$$\bar{\mu}(\mathbf{r},t) = \mu(\mathbf{r},t) + e\Phi(\mathbf{r},t)$$

where $\Phi(\mathbf{r},t)$ is electric potential and $\nabla_r \Phi(\mathbf{r},t) = E(\mathbf{r},t)$. Now, electric field and chemical potential gradient are combined. And in this thesis chemical potential is always constant $\mu(\mathbf{r},t) = \mu_0$. For simplicity, bar is omitted in this thesis, chemical potential μ refer to electrochemical potential $\bar{\mu}(\mathbf{r},t)$. since original chemical potential $\mu(\mathbf{r},t)$ is constant, only electric field contributes to spatial difference, i.e. $\nabla_r \mu = e\nabla_r \Phi(\mathbf{r},t) = eE(\mathbf{r},t)$.

Substituting f_k into Eq. (2.13)2.13, by using

$$\begin{aligned}
\nabla_r f_k(r) &= -\frac{\partial f_k^0}{\partial \varepsilon_k}[\varepsilon_k - \mu(r)]\frac{\nabla_r T(r)}{T(r)} \\
\nabla_k f_k &= \frac{\partial f}{\partial \varepsilon_k}\hbar v_k + \nabla_k \delta f_k \\
(v_k \times B)\cdot v_k &= 0,
\end{aligned}$$

it gives linearized Boltzmann equation

$$-\frac{\partial f_k^0}{\partial \varepsilon_k}\left\{\left[\varepsilon_k-\mu\left(r\right)\right]v_k\cdot\frac{\nabla_r T\left(r\right)}{T\left(r\right)}+ev_k\cdot E\right\}-e\left[E\cdot\nabla_k\delta f_k+B\cdot\left(v_k\times\nabla_k\delta f_k\right)\right]=\left(\frac{\partial f}{\partial t}\right)_{coll}$$

Single mode approximation is the commonest way to solve Boltzmann equation. According to which, the collision term $\left(\frac{\partial f}{\partial t}\right)_{coll}$ is to make system relaxed to local equilibrium states. the collision term is approximately written as

$$\left(\frac{\partial f}{\partial t}\right)_{coll}\approx-\frac{f_k-f^0\left(\varepsilon_k\right)}{\tau\left(k\right)}=-\frac{\delta f_k}{\tau\left(k\right)},$$

$\tau\left(k\right)$ is relaxation time, the dependence of k is related to the details of collision mechanisms. Conventionally δf_k could be re-written as

$$\delta f_k=\frac{\partial f_k^0}{\partial \varepsilon_k}\delta\phi,$$

$\delta\phi$ is small value.

2.2.5 Transport Coefficients

Without magnetic field, i.e. $B=0$, particle current is calculated by:

$$J_N=\frac{2}{\left(2\pi\right)^3}\int\delta f_k\mathbf{v_k}d\mathbf{k}$$

and heat flux:

$$J_Q=\frac{2}{\left(2\pi\right)^3}\int\delta f_k\left(\varepsilon_k-\mu\right)\mathbf{v_k}d\mathbf{k}.$$

And it naturally gives a general form like Onsager relation:

$$\begin{aligned}J_N &= L_{11}\nabla_r\mu+L_{12}\frac{\nabla_r T}{T}\\ J_Q &= L_{21}\nabla_r\mu+L_{22}\frac{\nabla_r\mu}{T}\end{aligned}$$

$$\begin{aligned} L_{11} &= L_0 \\ L_{12} = L_{21} &= L_1 \\ L_{22} &= L_2 \end{aligned}$$

where

$$L_n = -\frac{1}{3}\int d\mathbf{k} g\left(k\right) v_k^2 \left(\varepsilon_k - \mu\right)^n \frac{\partial f_k^0}{\partial \varepsilon_k} \qquad n = 0, 1, 2.$$

And by considering case of no temperature gradient, i.e. $\frac{\nabla_r T}{T} = 0$, it gives electric conductivity

$$\sigma = -e^2 L_0.$$

Similarly for thermal conductivity

$$\kappa = \frac{L_0 L_2 - L_1^2}{K_0 T},$$

as well as Seebeck coefficients

$$S = -\frac{L_1}{L_0 T}.$$

2.2.6 Transport Coefficients with Magnetic Field

Considering magnetic case, i.e. $B \neq 0$, linearized Boltzmann equation gives solution of infinite series in terms of $\mathbf{B}$. By cutting off at second order, it gives

$$\delta\phi = -\frac{\tau_k}{1 + \mathbf{s}^2}\left[\mathbf{v_k} \cdot \mathbf{F} + \mathbf{v_k} \cdot \left(\mathbf{s} \times \mathbf{F}\right) + \left(\mathbf{v_k} \cdot \mathbf{s}\right)\left(\mathbf{s} \cdot \mathbf{F}\right)\right],$$

in which $\mathbf{F} = \nabla\mu + \frac{\varepsilon_k - \mu}{T}\nabla T$, $\mathbf{s} = \frac{e\tau_k}{m^\star}\mathbf{B}$, $m^\star$ is effective mass.

Particle current J_N and heat current J_Q can be written as:

$$\begin{aligned} J_N &= \begin{cases} \alpha_{11}^0 \nabla_{\mathbf{r}}\mu + \alpha_{11}^1 \mathbf{B} \times \nabla_{\mathbf{r}}\mu + \alpha_{11}^2 \mathbf{B}\left(\mathbf{B}\cdot\nabla_{\mathbf{r}}\mu\right) \\ \alpha_{12}^0 \frac{\nabla_{\mathbf{r}}T}{T} + \alpha_{12}^1 \mathbf{B} \times \frac{\nabla_{\mathbf{r}}T}{T} + \alpha_{12}^2 \mathbf{B}\left(\mathbf{B}\cdot\frac{\nabla_{\mathbf{r}}T}{T}\right) \end{cases} \\ J_Q &= \begin{cases} \alpha_{21}^0 \nabla_{\mathbf{r}}\mu + \alpha_{21}^1 \mathbf{B} \times \nabla_{\mathbf{r}}\mu + \alpha_{21}^2 \mathbf{B}\left(\mathbf{B}\cdot\nabla_{\mathbf{r}}\mu\right) \\ \alpha_{22}^0 \frac{\nabla_{\mathbf{r}}T}{T} + \alpha_{22}^1 \mathbf{B} \times \frac{\nabla_{\mathbf{r}}T}{T} + \alpha_{22}^2 \mathbf{B}\left(\mathbf{B}\cdot\frac{\nabla_{\mathbf{r}}T}{T}\right) \end{cases} \end{aligned}$$

where

$$\alpha_{\mu\nu}^{\eta} = \frac{1}{3}\int dk g\left(k\right) v_k^2 \frac{\tau_k}{1+s^2}\left(\varepsilon_k - \mu_0\right)^{\mu+\nu-2}\left(\frac{e\tau_k}{m^*}\right)^{\eta}\frac{\partial f_k^0}{\partial \varepsilon_k}$$

By assuming electric field is applied in x direction, and magnetic field is in z direction, it gives longitudinal conductivity and transverse conductivity,

$$\begin{aligned} \sigma_{xx} &= \frac{D_2}{D_0} \\ \sigma_{xy} &= -\frac{D_2}{D_1}, \end{aligned} \tag{2.14}$$

Seebeck coefficient

$$S = \frac{eD_5}{D_2}$$

and thermal conductivity

$$\kappa = \frac{D_7}{D_2}$$

in which

$$
\begin{aligned}
D_0 &= e\alpha_{11}^0 \\
D_1 &= e\alpha_{11}^1 B_z \\
D_2 &= e^2 \begin{vmatrix} \alpha_{11}^0 & -\alpha_{11}^1 B_z \\ \alpha_{11}^1 B_z & \alpha_{11}^0 \end{vmatrix} \\
D_3 &= e^2 \begin{vmatrix} \alpha_{11}^1 B_z & \alpha_{11}^0 \\ -\alpha_{21}^0 & \alpha_{21}^1 B_z \end{vmatrix} \\
D_4 &= \begin{vmatrix} \alpha_{21}^0 & \alpha_{11}^0 \\ \alpha_{21}^1 B_z & \alpha_{11}^1 B_z \end{vmatrix} \\
D_5 &= \frac{e}{T} \begin{vmatrix} -\alpha_{11}^1 B_z & \alpha_{12}^0 \\ \alpha_{11}^0 & \alpha_{12}^1 B_z \end{vmatrix} \\
D_6 &= \frac{e}{T} \begin{vmatrix} \alpha_{11}^0 & \alpha_{12}^0 \\ \alpha_{11}^1 B_z & \alpha_{12}^1 B_z \end{vmatrix} \\
D_7 &= \frac{e^2}{T} \begin{vmatrix} \alpha_{11}^0 & -\alpha_{11}^1 B_z & \alpha_{12}^0 \\ \alpha_{11}^1 B_z & \alpha_{11}^0 & \alpha_{12}^1 B_z \\ -\alpha_{21}^0 & \alpha_{21}^1 B_z & \alpha_{22}^0 \end{vmatrix}.
\end{aligned}
$$

Magento-effect is explicitly due to Lorentz force in this method, but magnetic field could also play roles in relaxation time and other aspects. the quantity $\mathbf{s} = \frac{e\tau_k}{m^\star}\mathbf{B}$ is the key figure shows the importance of Lorentz force, $|s| \ll 1$ indicate magneto-effect due to Lorentz force is trivial.

2.3 Green's Function for Spin System

Green's function is a powerful tool for many-body problem, however it is usually used for electron and phonon system. In this section, I firstly review the basic formula for spin Green's function. then I introduce approximation

to decouple high order terms to make iterative formula closed and how to solve isotropic bulk system at first order approximation.

2.3.1 Basic Green's Function

For this method, the primary Green's function is double time Green's function, which is exactly retarded Green's function in NEGF language. In this Chapter, we follow the convention of this community, and use double pointy brackets notation

$$G^r_{AB,\eta}(t) = \langle\langle A; B\rangle\rangle_{t,\eta} = -\frac{i}{\hbar}\theta(t)\left\langle [A(t), B]_\eta \right\rangle,$$

η denotes commutation operation, $\eta = -1$ for commutator or $\eta = 1$ for anti-commutator. As operator A and B are spin operators, which are neither bosonic nor fermionic, either one works here, but preferring commutator will lead to simpler formalism. So all notation "[,]" that omitted η notation, ans it always imply commutator ($\eta = -1$).

Fourier transformation is defined as,

$$\langle\langle A; B\rangle\rangle_\omega = \int_{-\infty}^{\infty} e^{i\omega t} \langle\langle A(t); B\rangle\rangle_t \, dt \tag{2.15}$$

2.3.2 Equation of Motion

In contrast to Section 2.1, where formula are in interaction picture, Heisenberg picture are used here. Equation of motion is obtained by taking time derivative of 2.15, together with $\frac{\partial}{\partial t}\theta(t - t') = \sigma(t - t')$,

$$\frac{\partial}{\partial t}\langle\langle A(t); B\rangle\rangle_t = -\frac{i}{\hbar}\delta(t)\langle [A(t), B]\rangle + \left\langle\left\langle \dot{A}(t); B\right\rangle\right\rangle_t.$$

By Fourier transformation on both side

$$\begin{aligned}\int_{-\infty}^{\infty} e^{i\omega t+\eta t}\frac{\partial}{\partial t}\left\langle\langle A;B\rangle\right\rangle_t dt &= e^{-i\omega t-\eta t}\left\langle\langle A,B\rangle\right\rangle_t\Big|_{-\infty}^{\infty} - i\tilde{\omega}\left\langle\langle A;B\rangle\right\rangle_\omega \\ &= -i\tilde{\omega}\left\langle\langle A;B\rangle\right\rangle_\omega ,\end{aligned}$$

$$\int_{-\infty}^{\infty} e^{-i\omega t-\eta t}\left\{-\frac{i}{\hbar}\delta(t)\left\langle[A(t),B]\right\rangle + \left\langle\left\langle \dot{A}(t);B\right\rangle\right\rangle_t\right\} dt = -\frac{i}{\hbar}\left\langle[A,B]\right\rangle + \left\langle\left\langle \dot{A};B\right\rangle\right\rangle_\omega .$$

which gives

$$-i\tilde{\omega}\left\langle\langle A,B\rangle\right\rangle_\omega = -\frac{i}{\hbar}\left\langle[A,B]\right\rangle + \left\langle\left\langle \dot{A};B\right\rangle\right\rangle_\omega . \tag{2.16}$$

The same for $\left\langle\left\langle \dot{A};B\right\rangle\right\rangle_\omega$, it give second order,

$$\tilde{\omega}^2\hbar^2\left\langle\langle A;B\rangle\right\rangle_{\omega-\eta i} = \tilde{\omega}\hbar\left\langle[A,B]\right\rangle + \left\langle\left[i\hbar\dot{A},B\right]\right\rangle + \left\langle\left\langle -\hbar^2\ddot{A};B\right\rangle\right\rangle_{\omega-\eta i} . \tag{2.17}$$

In Heisenberg picture

$$i\hbar\dot{A} = [A,H] , \tag{2.18}$$

by which linear operator will produce closed equation at first order. But most commonly, it's impossible to close at some order, like in spin system.

2.3.3 Decoupling Rule for Spins

Expansion of Heisenberg equation Eq. 2.18 lead to terms of multiple spin operators, $S_{i_1}^{\alpha_1}S_{i_2}^{\alpha_2}\cdots\cdots S_{i_n}^{\alpha_n}$, where $\alpha_n = \pm$ or z. difficulty for spin system is the validation of wick's theorem for general spin operator at finite temperature, however for spin one-half system wick's theorem hold at zero temperature[39]. one way to overcome this obscure is introducing decoupling rule, which productive terms are approximated by single operator. The simplest decoupling rules are introduced by Tyablikov[40], and called

random phase approximation(RPA).

$$S_i^z S_j^{\pm} \approx \langle S_i^z \rangle S_j^{\pm}. \tag{2.19}$$

In later chapter, we will see terms like$\langle\langle S_i^z S_j^+; S_i^- \rangle\rangle$ occurs in transverse Green's functions. By implementing Eq. (2.19) ,

$$\langle\langle S_i^z S_j^+; S_l^- \rangle\rangle \approx \langle S_i^z \rangle \langle\langle S_j^+; S_l^- \rangle\rangle . \tag{2.20}$$

When calculating Green's functions of longitudinal component in later section 4.2.2, it is necessary to expand to second order. It involve more complicated triple terms as [41, 42].

$$\begin{aligned} S_i^+ S_j^- S_j^+ &= \langle S_j^- S_j^+ \rangle S_i^+ + \langle S_i^+ S_j^- \rangle S_j^+ \\ \left(S_j^z\right)^2 S_i^+ &= \left\langle \left(S_j^z\right)^2 \right\rangle S_i^+. \end{aligned} \tag{2.21}$$

Several other decoupling have been proposed for dealing with different problem. More detail about decoupling will be discussed in **??**.

2.3.4 Magnetism in Bulk Magnet

In bulk system with periodic lattice, translational invariance hold, which make it more convenient to work in k space. So spatial Fourier transformation is defined as,;

$$G_q = \frac{1}{N} \sum_{R_A, R_B} G_{A,B} e^{i\mathbf{q}\cdot(R_A - R_B)}$$

Considering simplest ferromagnetic Heisenberg model

$$H = -\frac{J}{2} \sum_{\langle i,j \rangle} \mathbf{S}_i \cdot \mathbf{S}_j - h \sum_i S_i^z,$$

where $\langle i,j\rangle$ means nearest-neighbor site and total spin is S.

Green's function $\left\langle\left\langle S_q^+; S_{-q}^{(n)-}\right\rangle\right\rangle$ is considered, i.e. $A = S_q^+$ and $B = S_{-q}^{(n)-}$ in Eq. 2.16. Assuming model have been solved via applying decoupling rule,

$$G(k,E) = \frac{1}{2\pi}\frac{\Theta(a)}{E - E(k)},$$

in which $\Theta(a) = \left\langle\left[S^+, e^{aS^z}S^-\right]\right\rangle$. Considering identity

$$\begin{aligned}
\mathbf{S}^2 &= S(S+1) \\
&= \frac{1}{2}\left(S^+S^- + S^-S^+\right) + (S^z)^2 \\
&= (S^z)^2 + S^-S^+ + S^z \\
&= (S^z)^2 + S^+S^- - S^z,
\end{aligned}$$

and it gives

$$\Psi = \frac{1}{N}\sum_k \psi(k,0) = \left\langle S^-S^+\right\rangle = S(S+1) - \left\langle (S^z)^2\right\rangle + \langle S^z\rangle. \qquad (2.22)$$

Defining quantity

$$\Omega(a) = \left\langle e^{aS^z}\right\rangle,$$

equilibrium value is related to $\Omega(a)$,

$$\langle (S^z)^n\rangle = \frac{\partial^n \Phi(a)}{\partial a^n}|_{a=0}.$$

Due to the identity

$$\left[S^+, (S^z)^n\right] = \left\{(S^z-1)^n - (S^z)^n\right\}S^+,$$

and via Taylor expansion, it gives

$$\left[S^+, e^{aS^z}\right] = \left(e^{-a}-1\right)e^{aS^z}S^+.$$

S^+S^- terms are replaced by S^z,

$$\begin{aligned}\Theta(a) &= 2\left\langle e^{aS^z}S^z\right\rangle + \left(e^{-a}-1\right)\left\langle e^{aS^z}S^+S^-\right\rangle. \\ &= S(S+1)\left(e^{-a}-1\right)\left\langle e^{aS^z}\right\rangle + \left(e^{-a}+1\right)\left(e^{aS^z}S^z\right) - \left(e^{-a}-1\right)\left\langle e^{aS^z}(S^z)^2\right\rangle.\end{aligned}$$

Finally they gives a differential equation

$$D^2\Omega + \frac{(1+\Phi)e^a+\Phi}{(1+\Phi)e^a-\Phi}D\Omega - S(S+1) = 0.$$

This differential equation is solved by Callen , who give solution [40],

$$\Phi(a) = \frac{\Psi^{2S+1}e^{-Sa} - (1+\Psi)^{2S+1}e^{(S+1)a}}{\left[\Psi^{2S+1}-(1+\Psi)^{2S+1}\right]\left[(1+\Psi)e^a-\Psi\right]}.$$

So magnetization can be calculated,

$$\begin{aligned}\langle S^z\rangle &= \frac{\partial\Omega(a)}{\partial a}|_{a=0} \\ &\quad \frac{(S-\Psi)(1+\Psi)^{2S+1}+(S+1+\Psi)\Psi^{2S+1}}{(1+\Psi)^{2S+1}-\Psi^{2S+1}},\end{aligned} \tag{2.23}$$

and

$$\begin{aligned}\left\langle (S_s^z)^2\right\rangle &= \frac{\partial^2\Omega(a)}{\partial a^2}|_{a=0} \\ &= \begin{cases} \frac{2S\Psi^{2S+2}-\Psi^{2S+1}+2(S+1)(1+\Psi)^{2S+2}}{\Psi^{2S+1}-(1+\Psi)^{2S+1}} \\ + \quad (S+1)^2-\Psi-1+2(\Psi+1)^2 \end{cases}.\end{aligned}$$

Chapter 3

Thermal Structural Instability of $EuTiO_3$

3.1 Displasive Ferroelectricity

Ferroelectric materials are already widely used in various areas due to their robust spontaneous electrical polarization. Modern ferroelectric materials consist mainly of perovskite ferroelectric materials. In earlier era, ferroelectricity was discovered in hydrogen-bounded materials, like Rochelle salt[43] and KDP[44]. Until 1949, $BaTiO_3$(BTO), first ferroelectric materials without hydrogen bond [45, 46, 47, 48], was discovered. BTO is of relatively simple perovskite structure and led to deeper understand of the origin of ferroelectricity. There are two types of ferroelectricity, either order-disorder or displasive, which are distinguished by whether it's microscopically polar at paraelectric phase. order-disorder Ferroelectric materials are still microscopically polar at paraelectric phase, but only macroscopically non-polar in thermal average sense, which is similar to Ising spin lattice. Displasive ferroelectric materials are microscopically polar at ferroelectric phase but non-polar at paraelectric physics, which imply structural transition.

3.1.1 Soft Mode in ETO and STO

Ferroelectric transition is usually associated with soft mode condensation. Soft mode in structural phase transition was first observed by Raman and Nedungadi [49]. Cowley discovered one of $q = 0$ optical modes in $SrTiO_3$ was softened with decreased temperature, however no ferroelectric phase transition was found. Which make this problem more open, with extensive study via various experimental approach. the concept "soft mode" is sometimes ambiguous. One may define it as collective excitation whose frequency decrease anomalously as approaching transition point. Although soft mode are usually attributed to lattice dynamical mode, other causes may also lead to soft mode. The structural phase transition ,that caused by such modes triggered lattice instability, can be either first order or second order.

Structural transition triggered by zone-center soft modes are called ferrodistortive structural transition and modes condensate at other than zone-center is termed antidistortive structural transition. Displasive ferroelectrics and ferrodistortive structural transition are closely connected. Although most displasive ferroelectrics are ferrodistortive, it's possible to find some small spontaneous polarization caused by indirect coupling to antidistortive modes. For antidistortive case, whose soft modes usually condensates at zone boundary, occurs as cell-doubling transition. One of special case of antidistortive transition is antipolar transition, in which electric dipoles are of anti-parallel alignment between neighboring cells. So that no macroscopic polarization is observed in such phase. Although antidistortive transition is characterized by zone-boundary mode condensation, it usually accompanies by zone-center condensation as well. For more complicated case, it's possible to see both antidistortive and ferrodistortive condensation coexist in same system but in different direction.

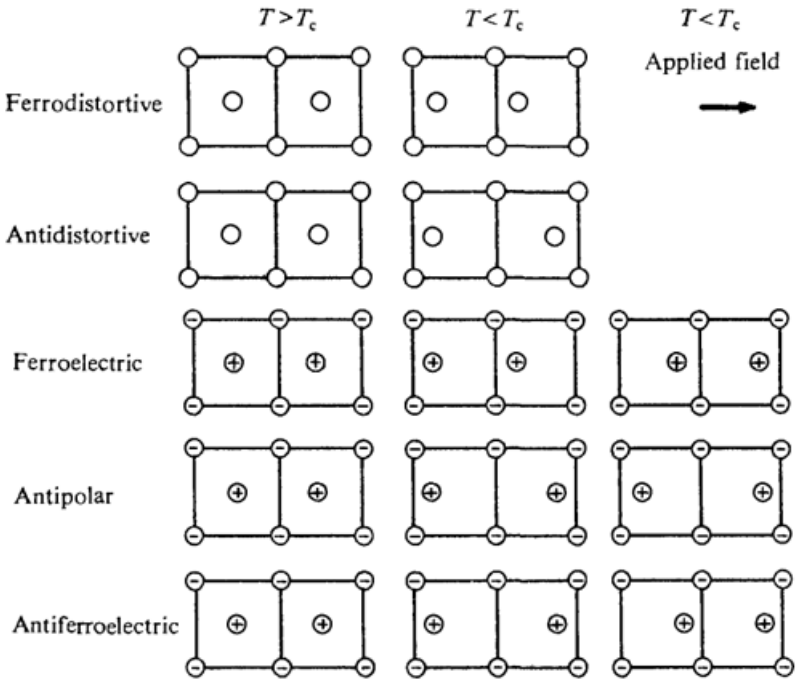

Fig. 3.1. A schematic representation of some fundamental types of structural phase transition from a centrosymmetric prototype. Figure from [2]

3.1.2 Polarizability Model

To investigating dynamics of structural instability of cubic perovskite, lattice dynamics model[50, 51, 3, 52, 53, 54, 55, 56]. It is a shell model which assumed oxygens are coupled to neighboring A-site and B-site cation by axially symmetric short-range force. each one with negative shell charge. Layer model of cubic and uni-axial ferroelectrics is of the Hamiltonian,

$$H_{ph} = \sum_{i,n} \frac{1}{2} m_i \dot{u}_{in}^2 + \frac{1}{2} \sum_n \begin{cases} f' \left(u_{1,n+1} - u_{1,n}\right)^2 + g_2 \left(v_{1,n} - u_{1,n}\right)^2 + \frac{1}{2} g_4 \left(v_{1,n} - u_{1,n}\right)^4 \\ + \quad f \left(u_{2,n} - v_{1,n}\right)^2 + f \left(u_{2,n+1} - v_{1,n}\right)^2 \end{cases},$$

where $g_4 > 0$ is forth order repulsive anharmonic terms, and $g_2 < 0$ is attractive. m_1 is mass for TiO_3 cluster and m_2 is mass for Eu. $u_{i,n}$ is displacement of ion i of site n, and $v_{i,n}$ is electronic shell displacement of ion i at site n. f are shell-core coupling between different type of ions. the

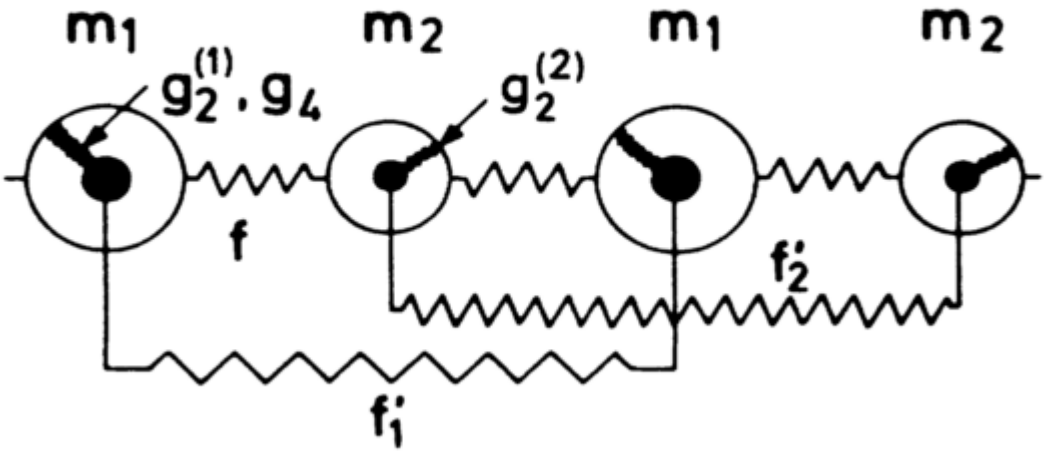

Fig. 3.2. Layer model of cubic and uni-axial ferroelectrics.[3]

model is illustrated in Fig. 3.2.

This model is classically solved via self-consistent phonon approximation. Soft optic mode frequency is shown in Fig. 3.3,

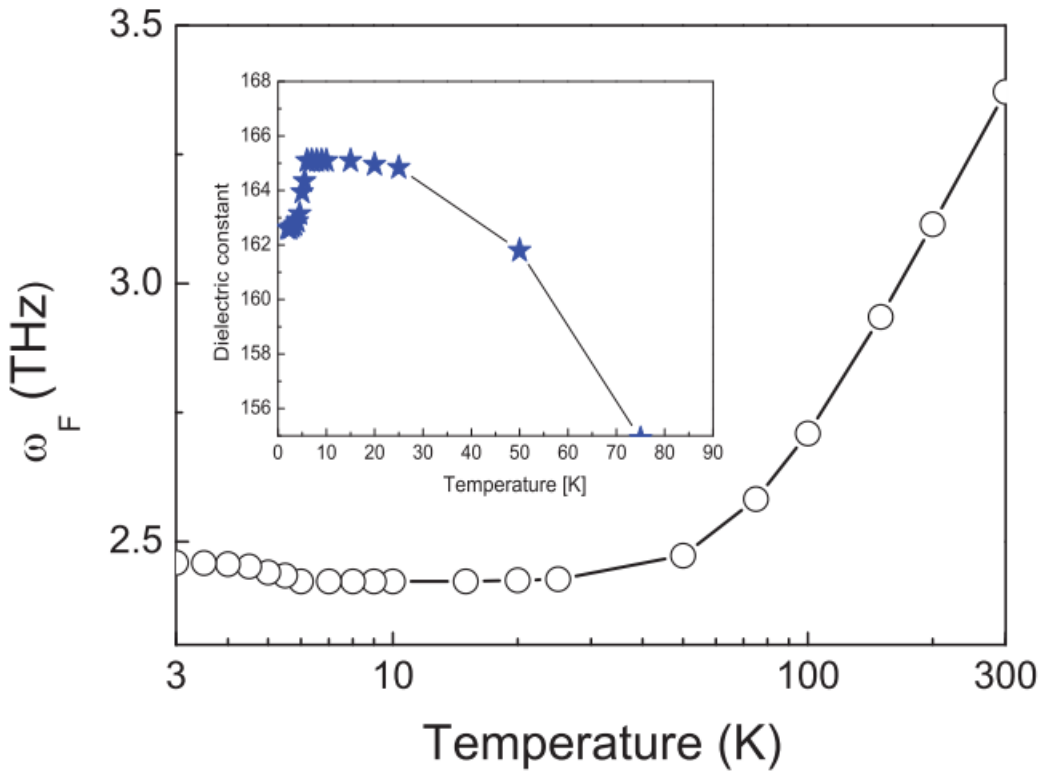

Fig. 3.3. Temperature dependence of the soft optic mode ω_F of ETO in a semi-logarithmic plot. The full stars are experimental data from [4, 5] The inset shows the related dielectric constant. Solid lines are guides to the eye. Figure from [6].

3.2 Dynamic Covalence Model

So far, polarizability model is the only model which can match experimental result of soft mode with respect to different temperature. But this model is quite phenomenological with fitting parameters. And the soft mode feature are primarily contributed by anharmonic terms. Anharmonic potential surface is also manifested in first principle calculation[55].

As the long-distance repulsion is not enough to explain the soft mode in STO or ETO. And Bersuker's argument about local origin[57] also suggest the role of second-order Jahn-Teller effect. To investigate the influence of second-order Jahn-Teller effects, I used such dynamic covalence model to investigate influence of second order Jahn-Teller effect.

$$\begin{aligned} H &= H_{ph} + H_e + H_{e-ph} \\ H_e &= \sum_i \varepsilon_i C_i^\dagger C_i \\ H_{ph} &= \sum_n g_4 x_n^4 - g_2 x_n^2 + \frac{p_n^2}{2m} \\ H_{e-ph} &= \sum_{i,j,n} M_{i,j,n} C_i^\dagger C_j x_n^2. \end{aligned}$$

Electron part is localized electrons. And for phonon system, decoupled ion is oscillating in a double-well. Both electrons and ions are coupled to each other via second-order electron-phonon interaction. next nearest localized electron on Eu are are coupled via in-between oxygen ion which lead to weakly boson mediated hopping between Eu. $M_{i,j,n}$ is non-zero for all (in Fig. 3.4). From the perspective of phonon, self-consistent phonon approximation is used to consider forth terms as an effective phonon. And similarly , isolated phonon are connected via in-between localized $4f$ electron of Eu. This coupling is similar to double-exchange mechanism, in which electrons hopping between nearest manganese are mediated by oxy-

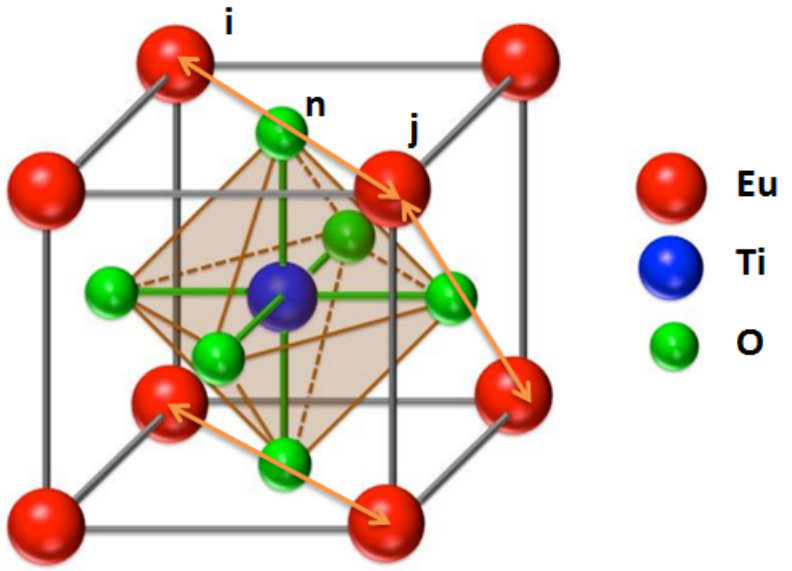

Fig. 3.4. Illustration of non-zero $M_{i,j,n}$. $\langle i, j \rangle$ are all diagonal (next-nearest) pairs of Eu, site n is the oxygen in-between paired Eu.

gen. Because potential surface is symmetrical with respect to high symmetrical reference position ,not like conventional electron-phonon coupling, the first-order coupling vanish here. However the model is 3D model, but it's symmetrical in 3 direction, however it is probably not true for real system. The structural phase transition, which is also characterized by soft mode condensation, happens in 3 direction at different temperature, which is not considered in this simplified model.

At first, we focus on low temperature case (below transition temperature). From the perspective of phonon, ion have to be localized in one of the valley. Because two valleys are symmetrical, equilibrium position is shifted to one of the valley bottom$\langle r_n \rangle$(Fig. 3.5), and define $u_n = x_n - \langle r_n \rangle$.

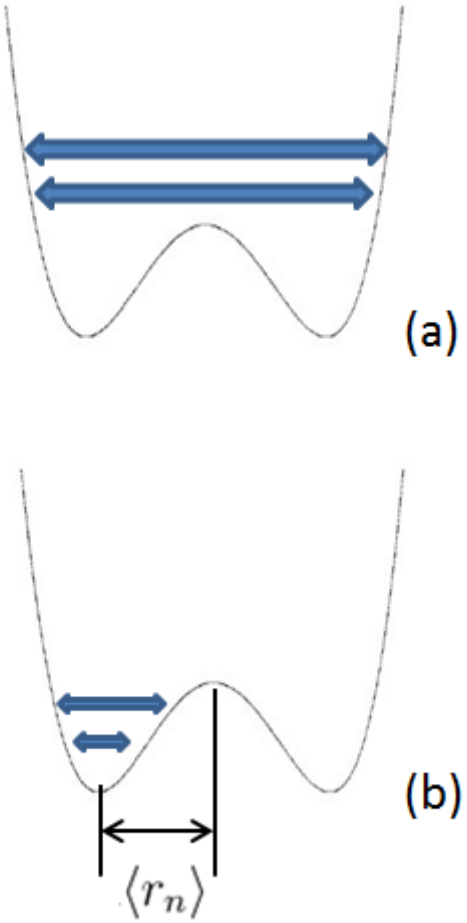

Fig. 3.5. Schematic illustration of (a) Hamiltonian H and (b) shifted Hamiltonian $\tilde{H}$.

The shifted Hamiltonian for is

$$\begin{aligned}
\tilde{H} &= \tilde{H}_{ph} + \tilde{H}_e + \tilde{H}_{e-ph} \\
\tilde{H}_{e-ph} &= \sum_{k,n} \tilde{M}_{k,n} C_k^\dagger C_k \left(u_n^2 + 2u_n \langle r_n \rangle \right) \\
\tilde{H}_e &= \sum_k \left(\varepsilon_k + \tilde{M}_k \langle r_n \rangle^2 \right) C_k^\dagger C_k \\
\tilde{H}_{ph} &= \hbar\omega_n \left(a_n^\dagger a_n + \frac{1}{2} \right).
\end{aligned}$$

Be noted that u_n is of dimension of length rather than reduced length

(corresponding Green's function is shown in Section 2.1.5) and

$$\begin{aligned} a_n &= \sqrt{\frac{m\omega_n}{2\hbar}}u + i\sqrt{\frac{1}{2m\omega_n}}p \\ a_n^\dagger &= \sqrt{\frac{m\omega_n}{2\hbar}}u - i\sqrt{\frac{1}{2m\omega_n}}p \\ \omega_n &= 2\sqrt{\frac{3g_4\left\langle u_n^2\right\rangle + g_2}{m}}. \end{aligned}$$

Because electrons are localized , electron band is actually almost a flat band. ε_k is constant, and band is slightly dispersed due to the weak phonon-mediated coupling,

$$M_{k_1,k_2,n} = 4e^{-iR_n\cdot(k_1-k_2)} \begin{cases} & \cos\left[k_{1,x}+k_{2,x}\right]\cos\left[k_{1,y}+k_{2,y}\right] \\ + & \cos\left[k_{1,y}+k_{2,y}\right]\cos\left[k_{1,z}+k_{2,z}\right] \cdot \\ + & \cos\left[k_{1,z}+k_{2,z}\right]\cos\left[k_{1,x}+k_{2,x}\right] \end{cases}$$

$M_k = M_{k,k,n}$, when $k_1 = k_2$, phase factor $e^{-iR_n\cdot(k_1-k_2)}$ don't play a role and subscript n is dumb as well. And it was calculated perturbatively via contour Green's method. By expanding up to second order,

$$
\begin{aligned}
& D_{n,n_0}(\tau,\tau_0) \\
= & \left\{ \begin{array}{lll}
 & D^0_{n,n_0}(\tau,\tau_0) & \\
+ & \frac{1}{N^2} \left\{ \begin{array}{ll}
+ & \int dt \frac{1}{N} \sum_{k',k'',n'} M_{k',k'',n'} \left(-i\hbar G^0_{k'',k'}(t,t)\right) D^0_{n,n'}(\tau,t) D^0_{n'n_0}(t,\tau_0) \\
- & 2\hbar^2 \sum_{k_1,k_1',n_1} M_{k_1,k_1',n_1} \sum_{k_2,k_2',n_2} M_{k_2,k_2',n_2} \int\int dt_1 dt_2 \times \\
 & \left\{ \begin{array}{ll}
- & D^0_{nn_2}(\tau,t_2) D^0_{n_2n_0}(t_2,\tau_0) D^0_{n_1n_1}(t=0) \left[G^0_{k_1'k_2}(t_1,t_2) G^0_{k_2'k_1}(t_2,t_1) \right] \\
+ & 2 D^0_{nn_1}(\tau,t_1) D^0_{n_1n_2}(t_1,t_2) D^0_{n_2n_0}(t_2\tau_0) G^0_{k_1'k_1}(t=0) G^0_{k_2'k_2}(t=0) \\
- & 2 D^0_{nn_1}(\tau,t_1) D^0_{n_2n_0}(t_2\tau_0) \left[D^0_{n_1n_2}(t_1,t_2) G^0_{k_2'k_1}(t_2,t_1) G^0_{k_1'k_2}(t_1,t_2) \right]
\end{array} \right.
\end{array} \right. \\
- & \frac{4i\hbar}{N^2} \sum_{k_1,k_1',n_1} M_{k_1,k_1',n_1} \sum_{k_2,k_2',n_2} M_{k_2,k_2',n_2} \langle r_{n_1} \rangle \langle r_{n_2} \rangle \int\int dt_1 dt_2 D^0_{n_1n_0}(t_1,\tau_0) D^0_{n,n_2}(\tau,t_2)
\end{array} \right.
\end{aligned}
$$

As system is translational invariant, $\langle r_{n_1} \rangle = \langle r_{n_2} \rangle = \langle r \rangle$,and using

Langreth's theorem (Table 2.1 and Section 2.1.7), self-energy is given,

$$
\Pi_n^r(\omega) = \begin{cases}
- \frac{i\hbar}{N} \sum_{k'} \tilde{M}_{k',k',n} G^0_{k',k'}(t=0) \\
- 2\hbar^2 \frac{1}{N^2} \begin{cases}
- \sum_{k_1,n_1} \tilde{M}_{k_1,k_1,n_1} \tilde{M}_{k_1,k_1,n} D^0_{n_1 n_1}(t=0) \left(\begin{cases} & G^{0,<}_{k_1k_1}(\omega') G^{0,a}_{k_1k_1}(\omega') \\ + & G^{0,r}_{k_1k_1}(\omega') G^{0,<}_{k_1k_1}(\omega') \end{cases} \right)_{\omega} \\
+ 2 \left(\sum_{k_1} \tilde{M}_{k_1,k_1,n} G^0_{k_1k_1}(t=0) \right)^2 D^{0,r}_{n,n}(\omega) \\
- 2 \sum_{k_1} \sum_{k_2} \tilde{M}_{k_1,k_2,n} \tilde{M}_{k_2,k_1,n} \int d\omega_1 \int d\omega_2 \times \\
\quad \begin{cases}
& D^{0,<}_{nn}(\omega - \omega_2 + \omega_1) G^{0,<}_{k_2k_2}(\omega_2) G^{0,a}_{k_1k_1}(\omega_1) \\
+ & D^{0,<}_{nn}(\omega - \omega_2 + \omega_1) G^{0,r}_{k_2k_2}(\omega_2) G^{0,<}_{k_1k_1}(\omega_1) \\
+ & D^{0,r}_{nn}(\omega - \omega_2 + \omega_1) G^{0,<}_{k_2k_2}(\omega_2) G^{0,<}_{k_1k_1}(\omega_1) \\
+ & D^{0,r}_{nn}(\omega - \omega_2 + \omega_1) G^{0,r}_{k_2k_2}(\omega_2) G^{0,<}_{k_1k_1}(\omega_1) \\
+ & D^{0,<}_{nn}(\omega - \omega_2 + \omega_1) G^{0,r}_{k_2k_2}(\omega_2) G^{0,r}_{k_1k_1}(\omega_1) \\
+ & D^{0,r}_{nn}(\omega - \omega_2 + \omega_1) G^{0,<}_{k_2k_2}(\omega_2) G^{0,r}_{k_1k_1}(\omega_1) \\
+ & D^{0,r}_{nn}(\omega - \omega_2 + \omega_1) G^{0,r}_{k_2k_2}(\omega_2) G^{0,r}_{k_1k_1}(\omega_1)
\end{cases}
\end{cases} \\
- 4i\hbar \frac{1}{N^2} \sum_{k_1} \sum_{k_2} \tilde{M}_{k_1,k_2,n} \tilde{M}_{k_2,k_1,n} \langle r \rangle^2 \int d\omega' \left[G^{0,<}_{k_1k_1}(\omega+\omega') G^{0,a}_{k_2k_2}(\omega') + G^{0,r}_{k_1k_1}(\omega+
\end{cases}
$$

Because all off-diagonal $G^0_{kk'}$ are vanished, $G^{0,r}_{kk'}$ is of pole structure, and $G^{0,<(>)}_{kk'}$ contain delta function the self-energy for phonon is obtained analytically via second-order Born approximation ,

$$\Pi_n^r(\omega) = \lim_{\eta\to 0^+}\begin{cases} - & \frac{1}{N}\sum_{k'}\tilde{M}_{k',k',n}\left(f(\varepsilon_{k'})+\frac{1}{2}\right) \\ + & \begin{cases} + & \frac{2}{m}\frac{1}{\omega_n}\left(\frac{1}{N}\sum_{k_1}\tilde{M}_{k_1,k_1,n}\left(f(\varepsilon_{k_1})+\frac{1}{2}\right)\right)^2\left[\frac{1}{\omega+i\eta-\omega_n}-\frac{1}{\omega+i\eta+\omega_n}\right] \\ + & \frac{8\pi^2}{m\omega_n}\frac{1}{N^2}\sum_{k_1}\sum_{k_2}\tilde{M}_{k_1,k_2,n}\tilde{M}_{k_2,k_1,n}\times \\ & \begin{cases} + & \left[f(\varepsilon_{k_1})-f(\varepsilon_{k_2})\right]\sum_{\sigma=\pm1}\sigma n(\sigma\omega_n)\frac{1}{\omega-\sigma\omega_n-\frac{\varepsilon_{k_2}-\varepsilon_{k_1}}{\hbar}+i\eta} \\ + & f(\varepsilon_{k_1})\left[f(\varepsilon_{k_2})-1\right]\left[\frac{1}{\omega-\frac{\varepsilon_{k_2}-\varepsilon_{k_1}}{\hbar}+i\eta+\omega_n}-\frac{1}{\omega-\frac{\varepsilon_{k_2}-\varepsilon_{k_1}}{\hbar}+i\eta-\omega_n}\right] \end{cases} \end{cases} \\ + & \frac{8\pi}{N^2}\langle r\rangle^2\sum_{k_1}\sum_{k_2}\tilde{M}_{k_1,k_2,n}\tilde{M}_{k_2,k_1,n}\frac{1}{\varepsilon_{k_2}-\varepsilon_{k_1}+\omega\hbar+i\eta}\left[f(\varepsilon_{k_2})-f(\varepsilon_{k_1})\right] \end{cases},$$

and imaginary part is

$$Im\Pi_n^r(\omega) = -\begin{cases} + & \frac{2}{m}\frac{\pi}{\omega_n}\left(\frac{1}{N}\sum_{k_1}\tilde{M}_{k_1,k_1,n}\left(f(\varepsilon_{k_1})+\frac{1}{2}\right)\right)^2\sum_{\sigma=\pm1}\sigma\delta(\omega-\omega_n) \\ + & \frac{8\pi^3}{m\omega_n}\frac{1}{N^2}\sum_{k_1}\sum_{k_2}\tilde{M}_{k_1,k_2,n}\tilde{M}_{k_2,k_1,n}\times \\ & \begin{cases} + & \left[f(\varepsilon_{k_1})-f(\varepsilon_{k_2})\right]\sum_{\sigma=\pm1}\sigma n(\sigma\omega_n)\delta\left(\omega-\sigma\omega_n-\frac{\varepsilon_{k_2}-\varepsilon_{k_1}}{\hbar}\right) \\ + & f(\varepsilon_{k_1})\left[f(\varepsilon_{k_2})-1\right]\sum_{\sigma=\pm1}\sigma\delta\left(\omega-\frac{\varepsilon_{k_2}-\varepsilon_{k_1}}{\hbar}+\sigma\omega_n\right) \end{cases} \\ + & \frac{8\pi^2}{N^2}\langle r\rangle^2\sum_{k_1}\sum_{k_2}\tilde{M}_{k_1,k_2,n}\tilde{M}_{k_2,k_1,n}\delta(\omega\hbar+\varepsilon_{k_2}-\varepsilon_{k_1})\left[f(\varepsilon_{k_2})-f(\varepsilon_{k_1})\right] \end{cases}$$

However the formalism is derived from shifted Hamiltonian, Hamiltonian can be calculated by specifying $\langle r\rangle = 0$. However non-interacting is used for Born approximation, Iteration is still need for phonon part as $\langle u_n^2\rangle$ in ω_n is determined self-consistent, i.e. 2 stages of self-consistency are needed. $\langle u_n^2\rangle$ is self-consistently calculated for ω_n without considering electron-phonon coupling, and another self-consistent process for interactive$\langle u_n^2\rangle$.

3.3 Result

The parameters for phonon part is estimated by fitting with double well structural via first principle calculation [55], and it is only of the same order of magnitude. As we don't considered phonon-phonon interaction and other geometry, this model only describe zone-center feature, and exact fitted value is also meaningless. The electron part is indeed localized and fully occupied band. Since we harmonically approximated phonon is not defined at high cubic center, but shifted to bottom of potential well. Which leads to weakly dispersed electron band. From the perspective of anharmonic phonon, second-order electron-phonon coupling is just modification on quadratic coefficient g_2. And we know anharmonic terms lead to soft mode, i.e. double-well potential structure itself lead to frequency softening. But in our model, quadratic term is consist of two parts, static part and dynamic part. g_2 is indeed the static part from somewhere else and dynamic part and dynamic part is $M_{i,j,n}$, which is effected by thermal fluctuation of electrons. As the electron is fully occupied, the chemical potential is selected to be positive, and it's selected to be 0.5eV above electron energy here.

The soft mode calculation is shown in Fig. 3.6, with the parameters ,$g_2 = 0.032eV/(B.r)$, $g_4 = 0.1eV/(B.r)^4$. Softness of soft mode are enhanced by second order Jahn-Teller effect. Stronger interaction lead to larger change with temperature. The dependency of temperature is due to both anharmonic forth terms and interaction. Although there is only second order Jahn-Teller is explicit in original Hamiltonian, I evaluate effect of both first and second order coupling as first order appeared when equilibrium position is shifted. By manually turn off particular terms, the enhancement is primarily due to first-order expansion of second order interaction.

However shifted Hamiltonian is assumed, it also covered non-shifted

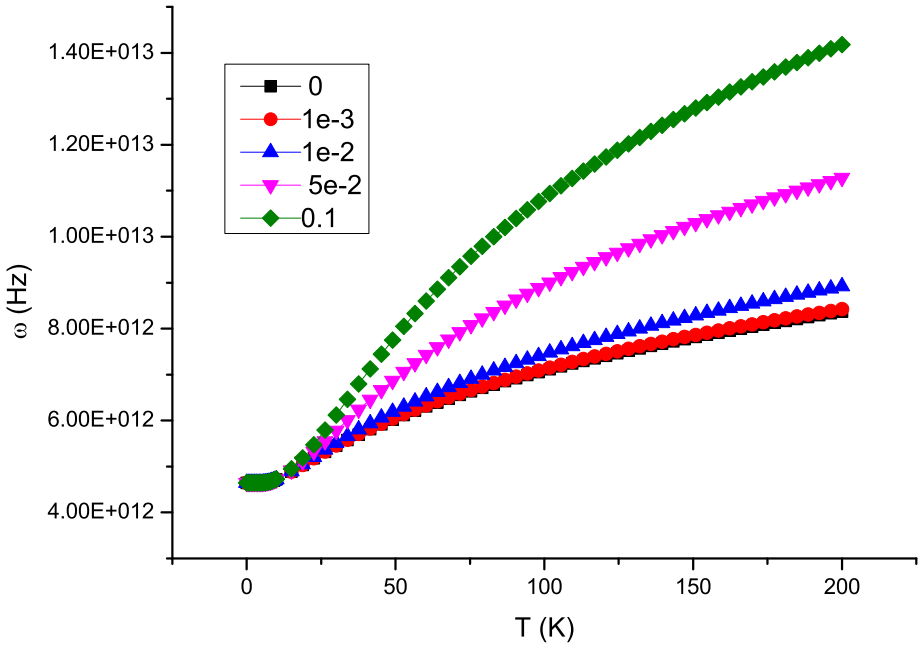

Fig. 3.6. Temperature dependence of soft mode frequency with various M_k.

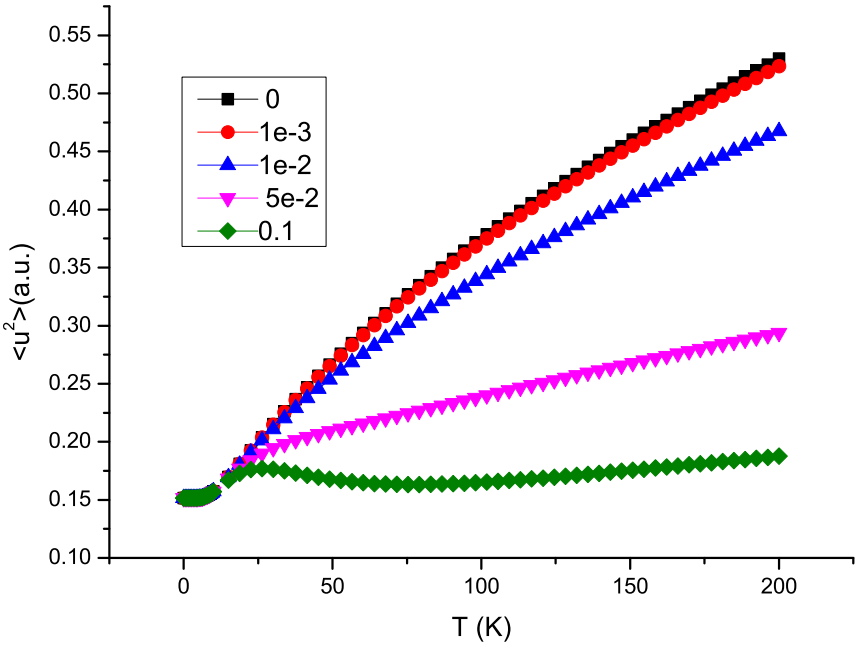

Fig. 3.7. Temperature dependence of $\langle u^2 \rangle$with various M_k.

case when $\langle r \rangle = 0$, i.e. such formalism is applicable to both distorted phase and undistorted phase in terms of temperature dependence of soft mode frequency. Nevertheless behavior near transition is unknown by perturbation. Ion oscillation is shown in Fig. 3.7 with same parameter of Fig. 3.6, it indicate the stability of distorted phase. Stronger coupling make ion more localized at bottom of potential well. When the coupling is stronger than $1e^{-3}$, fluctuation is significantly suppressed, and shifted harmonic approximation will be valid until higher temperature, i.e. the transition temperature will increase with stronger coupling. As the temperature dependency is contributed by both direct anharmonic effect and indirect electron-enhanced anharmonic effect. The small ridge of around 25K the region that two effects completing with each other. Below 25K, direct anharmonic effect play major role, and indirect electron-enhanced effect dominate at higher temperature.

In conclusion, I investigated the influence of second-order Jahn-Teller effect on anharmonic soft mode. It manifested it is possible a rectification on polarizability model. However such second-order electron-phonon interaction on $Eu : 4f^7$ electron in bulk $EuTiO_3$ make trivial contribution to conductivity but it possibly play roles in thermoelectric properties.

Chapter 4

Magnetoresistance in $EuTiO_3$

4.1 Theory of Magnetoresistance

Magnetoresistive material is characterized by the change of electrical resistivity upon influence of external magnetic field. Magnetoresistance(MR) is measured by MR rate defined as

$$MR = \frac{\rho(H) - \rho(H=0)}{\rho(H=0)} \times 100\%.$$

Positive MR means resistivity increased by application of external magnetic field, and reversely, negative MR means deceasing with magnetic field.

MR was discovered by William Thomson [58] firstly in 1856. And giant magnetoresistance (GMR) was discovered in composing multilayers of alternating ferroelectric and non-magnetic conductive layers during 1980s by A.Fert[9] and P.Grunberg [8] independently who were awarded Nobel Prize for this discovery. It have already been applied in various aspect of modern device, such as magnetic field sensor in hard disk driver and biosensors etc. In bulk ferromagnetic semiconductor $Eu_{1-x}Gd_xSe$, S. Von Molnar and Methfessel firstly found negative magnetoresistance in 1976[65]. Colossal magnetoresistance have even larger change of resistivity upon megnetic field, but is not associated with multilayer structure. Since mid-1990s, ex-

tensive researches were conducted on manganese-base perovskite oxide, e.g. in $La_{\frac{2}{3}}Ca_{\frac{1}{3}}MnO_3$ thin film Jin et. al observed huge MR up to 127000% at 77K and 6T [65, 65].

4.1.1 Colossal Magnetoresistance in Eu^{2+} Based Materials

Due to large magnetic moment of the $Eu^{2+} : 4f^7$, some europium monochalcogenides ,e.g. EuO, EuS, $EuSe$, $EuTe$ have shown wide verity of magnetic properties. EuO and EuS are ferromagnetic below 69K and 16K respectively[154, 62], and anti-ferromagnetic $EuTe$ have Neel temperature of 9.7K[74]. Colossal magnetoresistance is observed in above-mentioned EuX, but explained in different ways.

EuO is ferromagnetic semiconductor of colossal. It exhibit metallic behavior below transition temperature T_c , and such I-M transition was attributed to bound magnetic polaron and conduction band splitting[77, 88, 61, 136, 106]. $EuSe$ and $EuTe$ have positive MR and were explained by spin-disorder scattering caused conduction splitting[122, 139, 72].

Large colossal magneto resistance is newly observed in $EuTiO_3$ (ETO), and lack proper explanation for it.

4.1.2 Origin of Magnetoresistance

Giant magnetoresistivity was explained by Mott's argument[120], which says conductive metal have two conductive channels respectively for spin-up and spin-down electrons. In common metal, spin-flip scattering is usually small compared to non-flipping scattering. But due to the exchange-split, spin-up and spin-down electron have different scattering rate in ferromagnetic metals, and conduction is dominated by one transport channel. For the case, ferromagnetic layer are uniformly magnetized, one channel is always on which contribute to higher conductivity. Conversely, when ferro-

magnetic are magnetized in alternative direction, both channel are strongly scattered and lead to lower conductivity.

Colossal magnetoresistance is usually investigated in magnite. Double-exchange mechanism, which is firstly proposed by Clarence Zener[135], are considered as main contribution such strong MR effect. It happens in manganites where contains both Eu^{3+} and Eu^{4+}. Due to $Mn^{3+} - O - Mn^{4+}$ bond, electrons are possible to hop from Mn^{3+} to intermediate oxygen, and an electron of same spin at oxygen hop to Mn^{4+} simultaneously (Fig. 4.1). The transition rate between oxygen mediated Eu^{3+} and Eu^{4+} are heavily depended on magnetic orientation of them. P.W Anderson and H. Hasegawa [116] proposed effective Hamiltonian in the form of ferromagnetic Kondo model,

$$H_{DE} = -t \sum_{i,j,\sigma} c^{\dagger}_{i\sigma} c_{j\sigma} - J_H \sum_i \mathbf{s}_i \cdot \mathbf{S}_i,$$

$J_H \gg t$, and S is considered as classical. Double-exchange model have be extensively studied in late 1990s, . Magnetoresistance due to double exchange and interplay between double exchange and Jahn-Teller effect is confirmed[28, 29, 30, 31, 32, 33, 34, 35, 99]. Although I suggested double-exchange-like mechanism for Eu in Chapter 3, it definitely not the reason for CMR in ETO as double-exchange require medium level doping. In this chapter, I will investigate the possible mechanism contributing to CMR in $EuTiO3$.

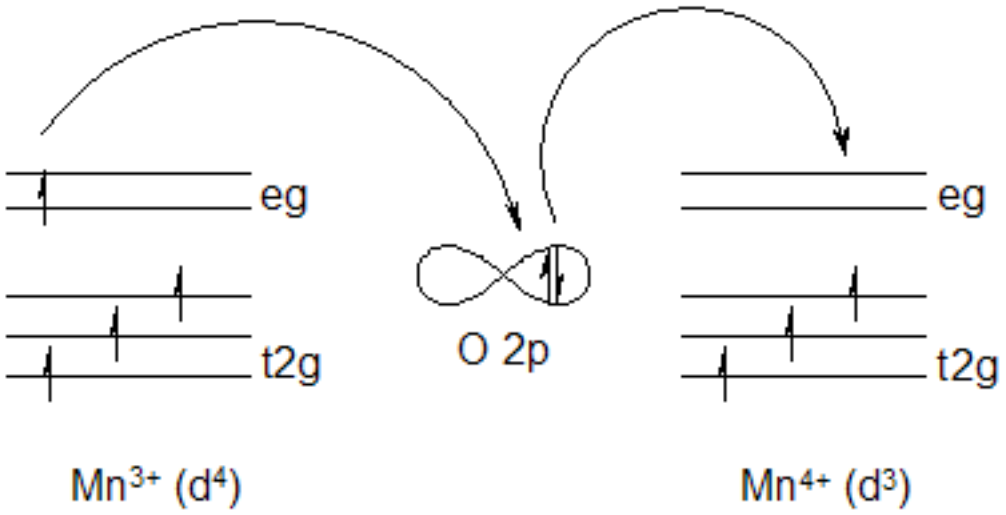

Fig. 4.1. Schematic interpretation of double exchange mechanism.

4.2 Spin Scattering Model

4.2.1 Model

As discussed in earlier section, in simpliest structural phase for $EuTiO_3$(ETO) is cubic phase as Fig. 1.3. However ETO undergoes oxygen octahedra tilting at low temperature, it still reasonable to assume ETO stay in cubic structure for my model which don't contain oxygen explicitly.

Hamiltonian of system consist of 3 parts

$$H = H_s + H_e + H_{es}, \tag{4.1}$$

H_s , H_e are Hamiltonian for localized spin system and itinerant electron system respectively, and electron-spin interaction part H_{es} .

In terms of magnetic part, is well described by $\frac{7}{2}$-spins Heisenberg model which considered both nearest neighbor $J_1 = -0.037K$ and next-nearest neighbor $J_2 = 0.069K$.

$$H_s = -J_1 \sum_{\langle i,j \rangle} \mathbf{S}_i \cdot \mathbf{S}_j - J_2 \sum_{\langle\langle i,j \rangle\rangle} \mathbf{S}_i \cdot \mathbf{S}_j + h \sum_i S_i^z, \tag{4.2}$$

$\langle , \rangle$ mean nearest pair and $\langle\langle , \rangle\rangle$denotes next nearest pair.

Electron part uses first principle calculation result,

$$H_e = \varepsilon_{k\sigma} C^\dagger_{k\sigma} C_{k\sigma}, \tag{4.3}$$

$\varepsilon_{k\sigma} = \varepsilon_k - 2\sigma^z \mu_B B$.

Interaction are

$$H_{es} = -J_{es} \sum_{\langle i,j \rangle} \mathbf{S}_i \cdot \mathbf{s}_j \tag{4.4}$$

where $\mathbf{s}_j = \sum_{\alpha\beta} C^\dagger_{i,\alpha} \sigma_{\alpha\beta} C_{i\beta}$, σ is pauli matrix, index j denotes each site of titanium. and $C^\dagger_{i,\alpha} = \sum_i e^{-ik\cdot R_i} C^\dagger_{k,\alpha}$ and $C_{i,\alpha} = \sum_i e^{ik\cdot R_i} C_{k,\alpha}$.

We assumed the itinerant electrons are hopping between 3d orbital of titanium and local magnetic spins are contributed by half filled 4f orbital of europium. So the interaction between itinerant electron and localized spin is off-site, rather than standard local s-d interaction. And this interaction is also implied by first principle calculation[148].

Such model is calculated via combination of Green's function method and Boltzmann method. And the Green's functions are solved via different method. For electron part, it is calculated via perturbation, which is consistent with the presumption of week coupling. My method is only able to consider spin-disorder scattering and mean-field band shift. Magnetic polaron is suggested to be origin as well. But molecule dynamics simulation evinced that magnetic polaron effect is quite small due to the dilute electron in ETO.

And to make perturbation valid, it is better to subtract equilibrium part for interaction H_{es}, say $\mathbf{S}_i = (\mathbf{S}_i - \langle \mathbf{S}_i \rangle) + \langle \mathbf{S}_i \rangle$, and same for electron $\mathbf{s}_j$. Albeit, in electron part is so dilute to have effect on spin sub-system. Because $\langle S^+ \rangle = \langle S^- \rangle = 0$, only longitudinal component is subtracted. Primary effect of subtraction is molecular field shift, i.e. $\varepsilon_{k\sigma}$ can be rewritten as $\varepsilon_{k\sigma} = \varepsilon_k - \sigma \left(\mu_B B + 8 J_{es} \langle S^z \rangle \right)$. Besides, subtraction don't effect much in terms of first order expansion, both symbolically and numerically(except

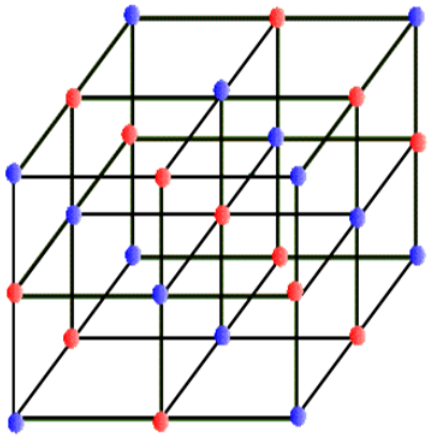

Fig. 4.2. 2 Sub-lattices. Red points denote sub-lattice “0”, and blue points denote sub-lattice “1”.

Γ point of longitudinal part). So subtraction will not be written explicitly in all formula of this chapter, but should be kept in mind.

4.2.2 Spin System

Spin part is solved by spin Green’s function method. It basically follow the method in section **??**, however we have to partially extend longitudinal part to second order as it vanished at first order for isotropic Heisenberg model.

Due to ETO is in G-type antiferromagnetic configuration at low temperature, local spins have to be separate to 2 sub-group, as shown in Fig. 4.2, where only europium left and both oxygen and titanium are omitted. two sub-groups are symmetrical and 2 sub lattices are labeled “0” and “1” respectively.

Two sets of coordination are defined. the base vectors for orthogonal

coordination

$$\begin{aligned}\mathbf{a_1'} &= (1,0,0)\\ \mathbf{a_2'} &= (0,1,0)\\ \mathbf{a_3'} &= (0,0,1)\,,\end{aligned}$$

and base vectors for skew coordination are

$$\begin{aligned}\mathbf{a_1} &= a\,(0,1,1)\\ \mathbf{a_2} &= a\,(1,0,1)\\ \mathbf{a_3} &= a\,(1,1,0)\,.\end{aligned}$$

These two coordinations are used to define Fourier transformation over each sub lattice to solve antiferromagnetic system, and Fourier transformation over all sites to consider interactive process.

Transverse spin Green's function

Here we follow the method of section 2.3. As it is isotropic Heisenberg model, we firstly focus on only transverse part. Consider first order equation (2.16) for transverse part can be written as

$$\omega \left\langle\left\langle S^+_{q,s}, S^-_{-q,s'}\right\rangle\right\rangle_\omega = \left\langle\left[S^+_{q,s}, S^-_{-q,s'}\right]\right\rangle + \left\langle\left\langle i\hbar\dot{S}^+_{q,s}, S^-_{-q,s'}\right\rangle\right\rangle_\omega , \tag{4.5}$$

where subscript $s, s' = 0, 1$ denotes sub-lattice, and $\bar{s} = 1 - s$. Although, equation 4.7 is in reciprocal space, the expansion have be done in real space,

$$\begin{aligned} ih\dot{S}^+_j &= \left[S^+_j, H_s\right]\\ &= \frac{1}{2}\sum_i J_{ij}\left(S^z_i S^+_j + S^+_j S^z_i - S^+_i S^z_j - S^z_j S^+_i\right) + hS^+_j, \end{aligned}$$

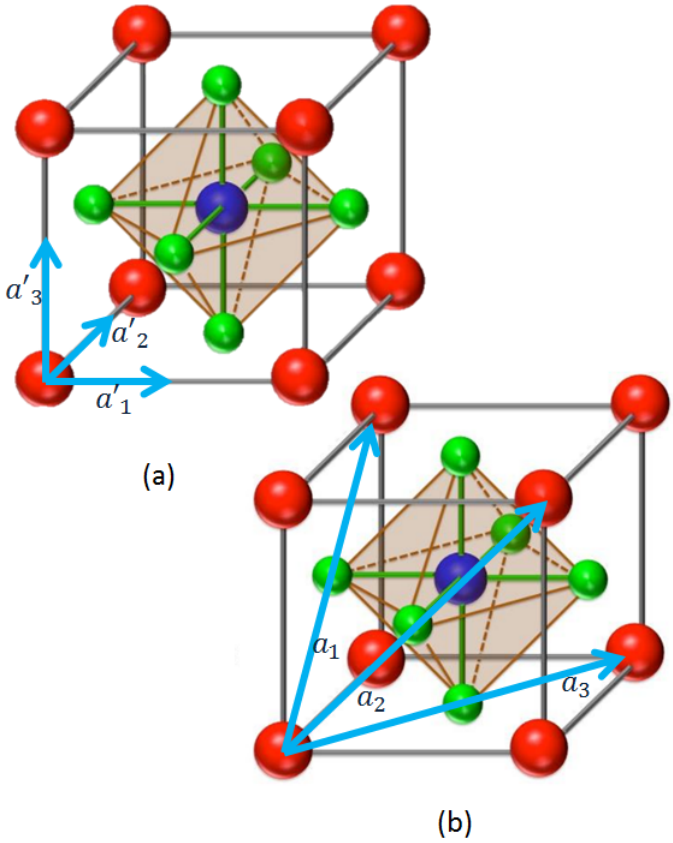

Fig. 4.3. Base vectors for (a) complete lattice and (b) sub-lattice

J_{ij} is generalization of J_1 and J_2, and it is non-zero for only nearest and next-nearest pairs. From here, we take RPA decoupling rule, Eq. (2.20),

$$ih\dot{S}_j^+ = \sum_i J_{ij}\left(\langle S_i^z\rangle S_j^+ - \langle S_j^z\rangle S_i^+\right) + hS_j^+.$$

Now separating operators of 2 sub-groups,

$$ih\dot{S}_{j,s}^+ = \left[6J_1\langle S_i^z\rangle_{\bar{s}} + 12J_2\langle S_i^z\rangle_s + h\right]S_{j,s}^+ - J_2\langle S_j^z\rangle_s\sum_{\mathbf{b}}S_{j+b}^+ - J_1\langle S_j^z\rangle_s\sum_{\mathbf{a}}S_{j+a}^+, \tag{4.6}$$

vector $\mathbf{a}$ are vectors pointing to all 6 nearest neighbors, as figure 4.4(a), and $\mathbf{b}$ are vectors pointing to all 12 next nearest neighbors as Fig. 4.4(b). In another words, both $S_{j,s}^+$ and S_{j+b}^+ are operators of sub-lattice s, and S_{j+a}^+ belongs to the the complementary sub-lattice $\bar{s}$. As $\langle S_i^z\rangle_s$ is translational invariant among sub-lattice, so site index i can be ignored, i.e. $\langle S_i^z\rangle_s = \langle S^z\rangle_s$. Implementing Fourier transformation over sub-lattice,

$$ih\dot{S}_{q,s}^+ = \left[6J_1\langle S^z\rangle_{\bar{s}} + 12J_2\langle S^z\rangle_s + h - J_2\langle S^z\rangle_s D_{nnn}(q)\right]S_{q,s}^+ - J_1\langle S^z\rangle_s D_{nn}(q)\phi_{s\bar{s}}(q)S_{q,\bar{s}}^+, \tag{4.7}$$

in which,

$$\begin{aligned} D_{nn}(q) &= \sum_{\mathbf{a}} e^{i\mathbf{q}\cdot\mathbf{R}_a} = \sum_{\mathbf{a}}\cos(\mathbf{q}\cdot\mathbf{R}_a) \\ D_{nnn}(q) &= \sum_{\mathbf{b}} e^{i\mathbf{q}\cdot\mathbf{R}_\mathbf{b}} = \sum_{\mathbf{b}}\cos(\mathbf{q}\cdot\mathbf{R}_b). \end{aligned}$$

And $\phi_{s\bar{s}}(q)$ is phase factor, which will not take effect in final result, as it can be canceled by its conjugation.

First term of right hand side of Eq. (4.5)

$$\begin{aligned} \left\langle\left[S_{q,s}^+, S_{-q,s'}^-\right]\right\rangle &= \frac{1}{N}\sum_{i,j} e^{i\mathbf{q}\cdot(\mathbf{R}_i-\mathbf{R}_j)}\left\langle\left[S_{i,s}^+, S_{j,s'}^-\right]\right\rangle \\ &= \delta_{s,s'}2\langle S^z\rangle_s, \end{aligned}$$

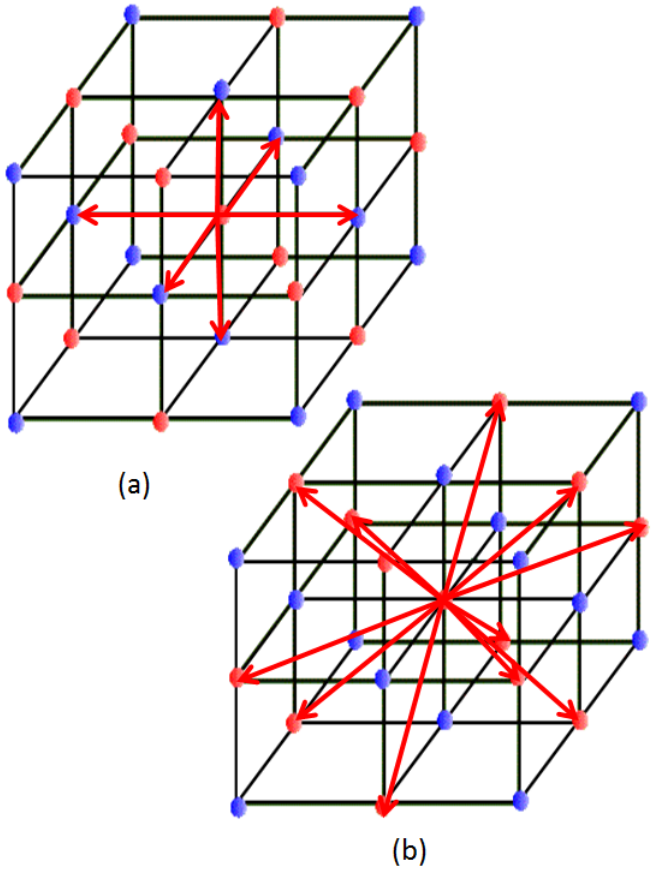

Fig. 4.4. Illustration of (a) nearest vectors **a** and (b) next-nearest vectors **b**.

is q-independent. So equation 4.5 are decoupled in reciprocal space, and we have it in matrix form,

$$\begin{bmatrix} \tilde{K}_{00} & \tilde{K}_{01}\phi_{01}(q) \\ \tilde{K}_{10}\phi_{10}(q) & \tilde{K}_{11} \end{bmatrix} \begin{bmatrix} D_{00}^{+-,r} & D_{01}^{+-,r} \\ D_{10}^{+-,r} & D_{11}^{+-,r} \end{bmatrix} = \begin{bmatrix} M_{00} & 0 \\ 0 & M_{11} \end{bmatrix}.$$

I uses notation $D_{ss'}^{+-,r}(\omega) = \left\langle\left\langle S_{q,s}^{+}, S_{-q,s'}^{-}\right\rangle\right\rangle_{\omega}$, and $M_{ss'} = \delta_{s,s'} 2\left\langle S^z\right\rangle_s$,and

$$\tilde{K}_{ss} = \hbar\omega - [6J_1\left\langle S^z\right\rangle_{\bar{s}} + 12J_2\left\langle S^z\right\rangle_s - J_2 D_{nnn}(q)\left\langle S^z\right\rangle_s + h] \quad (4.8)$$

$$\tilde{K}_{s\bar{s}}\ \phi_{s\bar{s}}(q) = J_1\left\langle S^z\right\rangle_s D_{nn}(q)\,\phi_{s\bar{s}}(q). \quad (4.9)$$

It is easy to solve it by multiply inverse of $\tilde{K}$ matrix

$$\begin{bmatrix} D_{00}^{+-,r} & D_{01}^{+-,r} \\ D_{10}^{+-,r} & D_{11}^{+-,r} \end{bmatrix} = \frac{1}{\tilde{X}_{\mathbf{q}}^{+} - \tilde{X}_{\mathbf{q}}^{-}} \left[\frac{1}{\left(\hbar\omega - \tilde{X}_{\mathbf{q}}^{+}\right)} - \frac{1}{\left(\hbar\omega - \tilde{X}_{\mathbf{q}}^{-}\right)} \right] \begin{bmatrix} \hbar\omega - \tilde{\Gamma}_{00}^{q} & \tilde{\Gamma}_{01}^{q}\phi_{01}(\mathbf{q}) \\ \tilde{\Gamma}_{10}^{q}\phi_{10}(\mathbf{q}) & \hbar\omega - \tilde{\Gamma}_{11}^{q} \end{bmatrix} \begin{bmatrix} M_{00} & 0 \\ 0 & M_{11} \end{bmatrix},$$

in which

$$\tilde{\Gamma}_{ss}^{\mathbf{q}} = h + 6J_1\langle S^z\rangle_s + 12J_2\left\langle S^z\right\rangle_{\bar{s}} - J_2\left\langle S^z\right\rangle_{\bar{s}} D_{nnn}(\mathbf{q}) \quad (4.10)$$

$$\tilde{X}_{\mathbf{q}}^{\pm} = h + \left(\frac{\langle S_1^z\rangle + \langle S_0^z\rangle}{2}\right) Y_{\mathbf{q}}^{+} \pm \sqrt{\left(\frac{\langle S_0^z\rangle - \langle S_1^z\rangle}{2}\right)^2 \left(Y_{\mathbf{q}}^{-}\right)^2 + J_1^2 D_{nn}^2(\mathbf{q})\langle S_1^z\rangle\langle S_0^z\rangle} \quad (4.11)$$

$$Y_{\mathbf{q}}^{\pm} = \pm 6J_1 + 12J_2 - J_2 D_{nnn}(\mathbf{q}).$$

Since our model are isotropic Heisenberg model, $\left\langle S^z\right\rangle_s$ are calculated self consistently via method in Section 2.3.4 . Since only diagonal terms

matter during such iterative procedure. sub-lattice version of Eq.2.22 is

$$\Psi_{ss} = \sum_{\mathbf{q}} \frac{\check{A}^{\mathbf{q}}_{ss}}{e^{\beta\tilde{X}^{+}_{q}} - 1} + \frac{\check{B}^{\mathbf{q}}_{ss}}{e^{\beta\tilde{X}^{-}_{q}} - 1},$$

where

$$\begin{aligned} \check{A}^{\mathbf{q}}_{ss} &= \frac{\hbar\omega^{(s)}_{\mathbf{q}} - \tilde{X}^{+}_{\mathbf{q}}}{\tilde{X}^{-}_{\mathbf{q}} - \tilde{X}^{+}_{\mathbf{q}}} \\ \check{B}^{\mathbf{q}}_{ss} &= \frac{\hbar\omega^{(s)}_{\mathbf{q}} - \tilde{X}^{-}_{\mathbf{q}}}{\tilde{X}^{+}_{\mathbf{q}} - \tilde{X}^{-}_{\mathbf{q}}}, \end{aligned}$$

and

$$\hbar\omega^{(s)}_{\mathbf{q}} = h + 6J_1\langle S^z\rangle_{\bar{s}} + 12J_2\left\langle S^z\right\rangle_s - J_2\left\langle S^z\right\rangle_s D_{nnn}(\mathbf{q}).$$

Finally, magnetization are achieved as Eq. 2.23,

$$\left\langle S^z\right\rangle_s = \frac{(S-\Psi_{ss})\left(1+\Psi_{ss}\right)^{2S+1} + (S+1+\Psi_{ss})\,\Psi_{ss}^{2S+1}}{\left(1+\Psi_{ss}\right)^{2S+1} - \Psi_{ss}^{2S+1}}. \tag{4.12}$$

value of $\left\langle S^z\right\rangle_s$ is used in Eq. 4.10 &4.11, and self-consistent procedure is closed.

And the transverse Green's function can be written explicitly as

$$D^{+-,r}_{ss'}(\omega) = \left(\frac{\tilde{A}^{\mathbf{q}}_{ss'}}{\hbar\omega - \tilde{X}^{+}_{\mathbf{q}}} + \frac{\tilde{B}^{\mathbf{q}}_{ss'}}{\hbar\omega - \tilde{X}^{-}_{\mathbf{q}}}\right), \tag{4.13}$$

where

$$\begin{aligned} \tilde{A}^{\mathbf{q}}_{ss} &= 2\left\langle S^z\right\rangle_s \check{A}^{\mathbf{q}}_{ss} \\ \tilde{B}^{\mathbf{q}}_{ss} &= 2\left\langle S^z\right\rangle_s \check{B}^{\mathbf{q}}_{ss} \\ \tilde{A}^{\mathbf{q}}_{s\bar{s}} &= \frac{2\left\langle S^z\right\rangle_s K^{\mathbf{q}}_{s\bar{s}}\phi_{s\bar{s}}(\mathbf{q})}{\tilde{X}^{-}_{q} - \tilde{X}^{+}_{q}} \\ \tilde{B}^{\mathbf{q}}_{s\bar{s}} &= \frac{2\left\langle S^z\right\rangle_s K^{q}_{s\bar{s}}\phi_{s\bar{s}}(\mathbf{q})}{\tilde{X}^{+}_{q} - \tilde{X}^{-}_{q}}. \end{aligned}$$

Fluctuation-dissipation theorem gives,

$$D^{+-,<}_{ss'}(\mathbf{q},\omega) = -2\pi i \left[\frac{\tilde{A}^{\mathbf{q}}_{ss'}}{e^{\beta\tilde{X^q_+}}-1}\delta(\omega\hbar - \tilde{X^{\mathbf{q}}_+}) + \frac{\tilde{B}^{\mathbf{q}}_{ss'}}{e^{\beta\tilde{X^q_-}}-1}\delta(\omega\hbar - \tilde{X^{\mathbf{q}}_-}) \right]. \tag{4.14}$$

Longitudinal Spin Green's Function

As mentioned in earlier section, It compulsory to consider up to second order for longitudinal part. Starting from Eq.2.17,

$$\tilde{\omega}^2\hbar^2 \left\langle\left\langle S^z_{\mathbf{q},s}; S^z_{-q,s}\right\rangle\right\rangle_\omega = \left\langle\left[i\hbar\dot{S}^z_{\mathbf{q},s}, S^z_{-q,s}\right]\right\rangle + \left\langle\left\langle -\hbar^2\ddot{S}^z_{\mathbf{q},s}; S^z_{-\mathbf{q},s}\right\rangle\right\rangle_{\omega+\eta i}. \tag{4.15}$$

As last section, we have first order

$$i\hbar\dot{S}^z_j = \frac{1}{2}\sum_i J_{ij}(S^+_i S^-_j - S^+_j S^-_i).$$

It looks simple in form, but complexity increase quickly with expansion up to second order. To make it clear, it it written in 2 parts,

$$-\hbar^2\ddot{S}^z_j = \left(-\hbar^2\ddot{S}^z_j\right)^{+-} + \left(-\hbar^2\ddot{S}^z_j\right)^{zz},$$

and

$$\begin{aligned}
&\left(-\hbar^2\ddot{S}^z_j\right)^{+-} \\
=\ & -\frac{1}{4}\sum_i J_{ij}\sum_{kl} J_{kl}[S^+_i S^-_j - S^+_j S^-_i, S^+_k S^-_l] \\
=\ & \frac{1}{2}\Bigg\{ \left[\begin{array}{l} J_1^2\sum_{a,a'}(S^+_{j+a}S^-_{j+a'} + S^+_{j+a'}S^-_{j+a}) + J_2^2\sum_{b,b'}(S^+_{j+b}S^-_{j+b'} + S^+_{j+b'}S^-_{j+b}) \\ +2J_1J_2\sum_{a,b}(S^+_{j+a}S^-_{j+b} + S^+_{j+b}S^-_{j+a}) \end{array} \right] S^z_j \\
& - \left[J_2^2\textstyle\sum_{b'}(S^+_{j+b+b'}S^-_j + S^+_j S^-_{j+b+b'}) + J_1J_2\sum_a(S^+_{j+a+b}S^-_j + S^+_j S^-_{j+a+b})\right] S^z_{j+b} \\
& - \left[J_1^2\textstyle\sum_{a'}(S^+_{j+a+a'}S^-_j + S^+_j S^-_{j+a+a'}) + J_1J_2\sum_b(S^+_{j+a+b}S^-_j + S^+_j S^-_{j+a+b})\right] S^z_{j+a}
\end{aligned},$$

$$
\begin{aligned}
&\left(-\hbar^2\ddot{S}_j^z\right)^{zz} \\
= \;& -\frac{1}{4}\sum_i J_{ij}\sum_{kl} J_{kl}[S_i^+S_j^- - S_j^+S_i^-, S_k^zS_l^z] \\
= \;& \frac{1}{2}\left\{\begin{array}{l}
J_1^2\sum_{a,a'}\left\{(S_{j+a'}^+S_j^- + S_j^+S_{j+a'}^-)S_{j+a+a'}^z - (S_{j+a'}^+S_j^- + S_j^+S_{j+a'}^-)S_{j+a}^z\right\} \\
+J_2^2\sum_{b,b'}\left\{(S_{j+b'}^+S_j^- + S_j^+S_{j+b'}^-)S_{j+b+b'}^z - (S_{j+b'}^+S_j^- + S_j^+S_{j+b'}^-)S_{j+b}^z\right\} \\
+J_1J_2\sum_{a,b}\left\{(S_{j+b}^+S_j^- + S_j^+S_{j+b}^-)S_{j+a+b}^z - (S_{j+b}^+S_j^- + S_j^+S_{j+b}^-)S_{j+a}^z\right\} \\
+J_1J_2\sum_{a,b}\left\{(S_{j+a}^+S_j^- + S_j^+S_{j+a}^-)S_{j+a+b}^z - (S_{j+a}^+S_j^- + S_j^+S_{j+a}^-)S_{j+b}^z\right\}
\end{array}\right\},
\end{aligned}
$$

The decoupling rules are given in Eq. 2.21, and consider two sub-lattice separately, as last section, it gives formula in reciprocal lattice

$$
\left(-\hbar^2\ddot{S}_{\mathbf{q},s}^z\right)^{+-} = E_{ss}^{\mathbf{q}(+-)}S_{q,s}^z - E_{s\bar{s}}^{\mathbf{q}(+-)}\phi_{s\bar{s}}\left(\mathbf{q}\right)S_{\mathbf{q},\bar{s}}^z,
$$

where

$$
\begin{aligned}
E_{ss}^{\mathbf{q}(+-)} &= \frac{1}{2}\left\{\begin{array}{ll}
& J_1^2\sum_{\mathbf{a},\mathbf{a}'}\left\langle S_{a-a'}^+S_0^- + S_{a'-a}^+S_0^-\right\rangle_{s'} + J_2^2\sum_{\mathbf{b},\mathbf{b}'}\left\langle S_{b-b'}^+S_0^- + S_{b'-b}^+S_0^-\right\rangle_s \\
+ & 2J_1J_2\sum_{\mathbf{a},\mathbf{b}}\left\langle S_{a-b}^+S_0^- + S_0^+S_{a-b}^-\right\rangle \\
- & \sum_b\left[J_2^2\sum_{\mathbf{b}'}\left\langle S_{b+b'}^+S_0^- + S_{-b-b'}^+S_0^-\right\rangle_s + J_1J_2\sum_{\mathbf{a}}\left\langle S_{a+b}^+S_0^- + S_0^+S_{a+b}^-\right\rangle\right]e^{i\mathbf{q}\cdot\mathbf{b}}
\end{array}\right. \qquad (4.16) \\
E_{s\bar{s}}^{\mathbf{q}(+-)} &= \frac{1}{2}\sum_{\mathbf{a}}\left[J_1^2\sum_{\mathbf{a}'}\left\langle S_{a+a'}^+S_0^- + S_{-a-a'}^+S_0^-\right\rangle_s + J_1J_2\sum_{\mathbf{b}}\left\langle S_{a+b}^+S_0^- + S_0^+S_{a+b}^-\right\rangle\right]e^{i\mathbf{q}\cdot\mathbf{a}},
\end{aligned}
$$

and $\phi_{ss'}(\mathbf{q})$ are phase factor. As this model is isotropic, and considering about the symmetry of vectors a and b, it gives

$$\begin{aligned}
\sum_{\mathbf{a},\mathbf{a}'} \left\langle S^+_{a-a'} S^-_0 + S^+_{a'-a} S^-_0 \right\rangle_{s'} &= 2 \sum_{\mathbf{a},\mathbf{a}'} \left\langle S^+_{a+a'} S^-_0 \right\rangle_{s'} \\
\sum_{\mathbf{b},\mathbf{b}'} \left\langle S^+_{b-b'} S^-_0 + S^+_{b'-b} S^-_0 \right\rangle_{s} &= 2 \sum_{\mathbf{b},\mathbf{b}'} \left\langle S^+_{b+b'} S^-_0 \right\rangle_{s} \\
\sum_{\mathbf{a},\mathbf{b}} \left\langle S^+_{a-b} S^-_0 + S^+_0 S^-_{a-b} \right\rangle &= 2 \sum_{\mathbf{a},\mathbf{b}} \left\langle S^+_{a+b} S^-_0 \right\rangle .
\end{aligned}$$

To make equation clearer, define notations:

$$
\begin{aligned}
C_1 &= \left\langle S_a^+ S_0^- + S_0^+ S_a^- \right\rangle \\
C_2^s &= \left\langle S_b^+ S_0^- + S_{-b}^+ S_0^- \right\rangle_s \\
P_{aa}^s &= \sum_{\mathbf{a},\mathbf{a}'} \left\langle S_{a-a'}^+ S_0^- + S_{a'-a}^+ S_0^- \right\rangle_s \\
P_{bb}^s &= \sum_{\mathbf{b},\mathbf{b}'} \left\langle S_{b-b'}^+ S_0^- + S_{b'-b}^+ S_0^- \right\rangle_s \\
P_{ab} &= \sum_{\mathbf{a},\mathbf{b}} \left\langle S_{a+b}^+ S_0^- + S^+ S_{a+b}^- \right\rangle \\
D_{nn}\left(\mathbf{q}\right) &= \sum_{\mathbf{a}} e^{\mathbf{q}\cdot\mathbf{a}} = \sum_{\mathbf{a}} \cos\left(\mathbf{q}\cdot\mathbf{a}\right) \\
D_{nnn}\left(\mathbf{q}\right) &= \sum_{\mathbf{b}} e^{\mathbf{q}\cdot\mathbf{b}} = \sum_{b} \cos\left(\mathbf{q}\cdot\mathbf{b}\right) \\
D_{aa}\left(\mathbf{q}\right) &= \sum_{\mathbf{a},\mathbf{a}'} e^{\mathbf{q}\cdot(\mathbf{a}+\mathbf{a}')} = \sum_{\mathbf{a},\mathbf{a}'} \cos\left[\mathbf{q}\cdot(\mathbf{a}+\mathbf{a}')\right] \\
D_{bb}\left(\mathbf{q}\right) &= \sum_{\mathbf{b},\mathbf{b}'} e^{\mathbf{q}\cdot(\mathbf{b}+\mathbf{b}')} = \sum_{\mathbf{b},\mathbf{b}'} \cos\left[\mathbf{q}\cdot(\mathbf{b}+\mathbf{b}')\right] \\
D_{ab}\left(\mathbf{q}\right) &= \sum_{\mathbf{a},\mathbf{b}} e^{\mathbf{q}\cdot(\mathbf{a}+\mathbf{b})} = \sum_{a,b} \cos\left[\mathbf{q}\cdot(\mathbf{a}+\mathbf{b})\right] \\
W_{aa,s}^a\left(\mathbf{q}\right) &= \sum_{\mathbf{a},\mathbf{a}'} \left\langle S_{a+a'}^+ S_0^- + S_{-a-a'}^+ S_0^- \right\rangle_s e^{\mathbf{q}\cdot\mathbf{a}} \\
&= \sum_{\mathbf{a},\mathbf{a}'} \left\langle S_{a+a'}^+ S_0^- + S_{-a-a'}^+ S_0^- \right\rangle_s \cos\left[\mathbf{q}\cdot\mathbf{a}\right] \\
W_{bb,s}^b\left(\mathbf{q}\right) &= \sum_{\mathbf{b},\mathbf{b}'} \left\langle S_{b+b'}^+ S_0^- + S_{-b-b'}^+ S_0^- \right\rangle_s e^{\mathbf{q}\cdot\mathbf{b}} \\
&= \sum_{\mathbf{b},\mathbf{b}'} \left\langle S_{b+b'}^+ S_0^- + S_{-b-b'}^+ S_0^- \right\rangle_s \cos\left[\mathbf{q}\cdot\mathbf{b}\right] \\
W_{ab}^a\left(\mathbf{q}\right) &= \sum_{\mathbf{a},\mathbf{b}} \left\langle S_{a+b}^+ S_0^- + S_0^+ S_{a+b}^- \right\rangle e^{\mathbf{q}\cdot\mathbf{a}} \\
&= \sum_{\mathbf{a},\mathbf{b}} \left\langle S_{a+b}^+ S_0^- + S_0^+ S_{a+b}^- \right\rangle \cos\left[\mathbf{q}\cdot\mathbf{a}\right] \\
W_{ab}^b\left(\mathbf{q}\right) &= \sum_{\mathbf{a},\mathbf{b}} \left\langle S_{a+b}^+ S_0^- + S_0^+ S_{a+b}^- \right\rangle e^{\mathbf{q}\cdot\mathbf{b}} \\
&= \sum_{\mathbf{a},\mathbf{b}} \left\langle S_{a+b}^+ S_0^- + S_0^+ S_{a+b}^- \right\rangle \cos\left[\mathbf{q}\cdot\mathbf{b}\right],
\end{aligned}
$$

Eq. 4.16 is able to rewritten as

$$\begin{aligned} E_{ss}^{\mathbf{q}(+-)} &= \frac{1}{2}\left\{J_1^2 P_{aa}^{\bar{s}} + J_2^2 P_{bb}^{s} + 2J_1 J_2 P_{ab} - J_2^2 W_{bb,s}^{b}(\mathbf{q}) - J_1 J_2 W_{ab}^{b}(\mathbf{q})\right\} \\ E_{s\bar{s}}^{\mathbf{q}(+-)} &= \frac{1}{2}\left\{J_1^2 W_{aa,s}^{a}(\mathbf{q}) + J_1 J_2 W_{ab}^{a}(\mathbf{q})\right\}. \end{aligned}$$

$$\left(-\hbar^2 \ddot{S}_{q,s}^{z}\right)^{zz} = E_{ss}^{q(zz)} S_{q,s}^{z} - E_{ss'}^{q(zz)} \phi_{ss'}(q) S_{q,s'}^{z},$$

where

$$\begin{aligned} E_{ss}^{\mathbf{q}(zz)} &= \frac{1}{2}\left(J_1^2 C_1 D_{aa}(\mathbf{q}) + J_2^2 C_2^s D_{bb}(\mathbf{q}) - 12 J_2^2 C_2^s D_{nnn}(\mathbf{q}) - 6 J_1 J_2 C_1 D_{nnn}(\mathbf{q})\right) \\ E_{s\bar{s}}^{\mathbf{q}(zz)} &= \frac{1}{2}\left(6 J_1^2 C_1 D_{nn}(\mathbf{q}) - J_1 J_2 C_2^s D_{ab}(\mathbf{q}) + 12 J_1 J_2 C_2^s D_{nn}(\mathbf{q}) - J_1 J_2 C_1 D_{ab}(\mathbf{q})\right). \end{aligned}$$

Noted that, $\sum_l [S_i^+ S_j^-, S_l^z] = 0$,so above 2 parts are complete without commuting with Zeeman terms and can be combined as

$$\begin{aligned} E_{ss}^{\mathbf{q}} &= E_{ss}^{\mathbf{q}(+-)} + E_{ss}^{\mathbf{q}(zz)} \\ E_{ss'}^{\mathbf{q}} &= E_{ss'}^{\mathbf{q}(+-)} + E_{ss'}^{\mathbf{q}(zz)}. \end{aligned}$$

Equation (4.15) can be written in matrix form as well,

$$\begin{bmatrix} (\omega\hbar)^2 - E_{00}^{\mathbf{q}} & E_{01}^{\mathbf{q}} \phi_{01}(\mathbf{q}) \\ E_{10}^{\mathbf{q}} \phi_{10}(\mathbf{q}) & (\omega\hbar)^2 - E_{11}^{\mathbf{q}} \end{bmatrix} \begin{bmatrix} D_{00}^{zz,r} & D_{01}^{zz,r} \\ D_{10}^{zz,r} & D_{11}^{zz,r} \end{bmatrix} = \begin{bmatrix} \tilde{E}_{00}^{\mathbf{q}} & \tilde{E}_{01}^{\mathbf{q}} \phi_{01}(\mathbf{q}) \\ \tilde{E}_{10}^{\mathbf{q}} \phi_{10}(\mathbf{q}) & \tilde{E}_{11}^{\mathbf{q}} \end{bmatrix}.$$

$\tilde{E}_{ss'}^{\mathbf{q}}$ are from term $\left\langle \left[i\hbar \dot{S}_{\mathbf{q},s}^{z}, S_{-\mathbf{q},s}^{z} \right] \right\rangle$, and gives

$$\begin{aligned} \tilde{E}_{ss}^{q} &= \frac{1}{2}\left(6 J_1 C_1 + 12 J_2 C_2^s - J_2 C_2^s D_{nnn}(\mathbf{q})\right) \\ \tilde{E}_{s\bar{s}}^{q} &= -\frac{J_1}{2} C_1 D_{nn}(\mathbf{q}). \end{aligned}$$

$$
\begin{aligned}
&\begin{bmatrix} D_{00}^{zz,r} & D_{01}^{zz,r} \\ D_{10}^{zz,r} & D_{11}^{zz,r} \end{bmatrix} \\
= \;& \frac{1}{X_+^{\mathbf{q}} - X_-^{\mathbf{q}}} \left[\frac{1}{X - X_+^{\mathbf{q}}} - \frac{1}{X - X_-^{\mathbf{q}}} \right] \\
& \times \begin{bmatrix} \{X - \Gamma_{00}\} \tilde{E}_{00}^{\mathbf{q}} & \{X - \Gamma_{01}\} \tilde{E}_{01}^{\mathbf{q}} \phi_{01}(\mathbf{q}) \\ \{X - \Gamma_{10}\} \tilde{E}_{10}^{\mathbf{q}} \phi_{10}(\mathbf{q}) & \{X - \Gamma_{11}\} \tilde{E}_{11}^{\mathbf{q}} \end{bmatrix}.
\end{aligned}
$$

And capital X are $(\omega\hbar)^2$and

$$
\Gamma_{ss'} = E_{\bar{s}\bar{s}}^{\mathbf{q}} + \frac{E_{s\bar{s}}^{\mathbf{q}} \tilde{E}_{\bar{s}s'}^{\mathbf{q}}}{\tilde{E}_{ss'}^{q}}
$$

$$
X_{\pm}^{\mathbf{q}} = \frac{(E_{00}^{\mathbf{q}} + E_{11}^{\mathbf{q}}) \pm \sqrt{(E_{00}^{\mathbf{q}} - E_{11}^{\mathbf{q}})^2 + 4E_{01}^{\mathbf{q}} E_{10}^{\mathbf{q}}}}{2}.
$$

Green's function for longitudinal part are finally written explicitly

$$
\begin{aligned}
& D_{ss'}^{zz,r}(\omega) \qquad (4.17) \\
= \;& -\frac{i}{\hbar} \tilde{E}_{ss'}^{\mathbf{q}} \phi_{ss'}(\mathbf{q}) \begin{cases} & A_{ss'}^{\mathbf{q}} \left(\frac{1}{\tilde{\omega}\hbar - \sqrt{X_+}} - \frac{1}{\tilde{\omega}\hbar + \sqrt{X_+}} \right) \frac{1}{2\sqrt{X_+}} \\ + & B_{ss'}^{\mathbf{q}} \left(\frac{1}{\tilde{\omega}\hbar - \sqrt{X_-}} - \frac{1}{\tilde{\omega}\hbar + \sqrt{X_-}} \right) \frac{1}{2\sqrt{X_-}} \end{cases},
\end{aligned}
$$

in which

$$
\begin{aligned}
A_{ss'}^{\mathbf{q}} &= \frac{\Gamma_{ss'}^{\mathbf{q}} - X_+^{\mathbf{q}}}{X_-^{q} - X_+^{q}} \qquad (4.18) \\
B_{ss'}^{\mathbf{q}} &= \frac{\Gamma_{ss'}^{\mathbf{q}} - X_-^{\mathbf{q}}}{X_+^{q} - X_-^{q}}. \qquad (4.19)
\end{aligned}
$$

Noted, $\phi_{ss'}(\mathbf{q})$ is 1 for diagonal $\phi_{ss}(\mathbf{q})$. Greater and less Green's function is given by fluctuation-dissipation theorem,

$$D_{ss'}^{zz,<}(\mathbf{q},\omega) = -2\pi i \left\{ \begin{array}{l} A_{ss'}^{\mathbf{q}} \left(\frac{1}{e^{\beta\sqrt{X_+}}-1}\delta(\omega\hbar - \sqrt{X_+}) - \frac{1}{e^{-\beta\sqrt{X_+}}-1}\delta(\omega\hbar + \sqrt{X_+}) \right) \frac{1}{2\sqrt{X_+}} \\ +B_{ss'}^{\mathbf{q}} \left(\frac{1}{e^{\beta\sqrt{X_-}}-1}\delta(\omega\hbar - \sqrt{X_-}) - \frac{1}{e^{-\beta\sqrt{X_-}}-1}\delta(\omega\hbar + \sqrt{X_-}) \right) \frac{1}{2\sqrt{X_-}} \end{array} \right. \tag{4.20}$$

4.2.3 Interaction

Non-interactive Green's function is easily obtained from non-interactive Hamiltonian Eq. 4.3. To investigate the influence of interaction, we firstly rewrite the interaction part Eq. 4.4 to

$$H_{es} = -J_{es} \sum_{i,j} \left[S_i^+ C_{j\downarrow}^\dagger C_{j\uparrow} + S_i^- C_{j\uparrow}^\dagger C_{j\downarrow} + S_i^z \left(C_{j\uparrow}^\dagger C_{j\uparrow} - C_{j\downarrow}^\dagger C_{j\downarrow} \right) \right]. \tag{4.21}$$

In following part of this section, calculation is done in reciprocal space,

$$H_{es} = \frac{1}{\sqrt{N}} \sum_{k,k'} J(k,-k') \left\{ C_{k\downarrow}^\dagger C_{k'\uparrow} S_{k'-k}^+ + C_{k\uparrow}^\dagger C_{k'\downarrow} S_{k'-k}^- + (C_{k\uparrow}^\dagger C_{k'\uparrow} - C_{k\downarrow}^\dagger C_{k'\downarrow}) S_{k'-k}^z \right\} \tag{4.22}$$

in which

$$J(k,-k') = -8J_{es} \cos\left[\frac{(k-k')_x}{2}a\right] \cos\left[\frac{(k-k')_y}{2}a\right] \cos\left[\frac{(k-k')_z}{2}a\right].$$

Noted, for spin operators in reciprocal space are transformed over full reciprocal space, but Green's functions solved previously (Eq. 4.17 & 4.20) are all transformed over sub-lattice. Assuming both sub-lattice is of N_2

local spin, and total number $N = 2N_2$,

$$\begin{aligned} S_k^\alpha &= \frac{1}{\sqrt{N}} \sum_l e^{-ik\cdot R_l} S_l^\alpha \\ &= \frac{1}{\sqrt{2N_2}} \sum_{l,s'} e^{-ik\cdot R_{l,s'}} \phi_{s\bar{s}}(k) S_{l,\bar{s}}^\alpha \\ &= \frac{1}{\sqrt{2}} \left(S_{k,s}^\alpha + \phi_{s\bar{s}}(\mathbf{k}) S_{k,\bar{s}}^\alpha \right). \end{aligned}$$

It is a little bit ambiguous unless take both N and N_2 to infinite. and sub-lattice s is the sub-lattice that share the same original point with full lattice, and surely $\bar{s}$ is another sub-lattice. According to the definition of phase factor $\phi_{s\bar{s}}(k)$ in last section. it depend on the definition of original point of sub-lattice $\bar{s}$ and it is arbitrary, but fortunately, it do not change our targeting quantities. All the interesting quantities are in form of pair or commutation,

$$S_k^\alpha(t) S_{-k}^\beta(t') = \frac{1}{2} \left[S_{q,s}^\alpha(t) S_{-q,s}^\beta(t') + S_{q,\bar{s}}^\alpha(t) S_{-q,\bar{s}}^\beta(t') + \phi_{s\bar{s}}(-k) S_{q,s}^\alpha(t) S_{-q,\bar{s}}^\beta(t') + \phi_{s\bar{s}}(k) S_{q,\bar{s}}^\alpha(t) S_{-q}^\beta \right.$$

$$\left[S_k^\alpha(t) \ , \ S_{-k}^\beta(t') \right] = \frac{1}{2} \begin{cases} \left[S_{q,s}^\alpha(t), S_{-q,s}^\beta(t') \right] + \left[S_{q,\bar{s}}^\alpha(t), S_{-q,\bar{s}}^\beta(t') \right] \\ + \ \phi_{s\bar{s}}(-k) \left[S_{q,s}^\alpha(t), S_{-q,\bar{s}}^\beta(t') \right] + \phi_{s\bar{s}}(k) \left[S_{q,\bar{s}}^\alpha(t), S_{-q,s}^\beta(t') \right] \end{cases} \tag{4.24}$$

And phase factor $\phi_{s\bar{s}}(k)$ is also in Eq. 4.13 and 4.17 and in greater(less) Green's functions as well. And according to $\phi_{s\bar{s}}(k)\phi_{s\bar{s}}(-k) = \phi_{s\bar{s}}(k)\phi_{\bar{s}s}(k) = 1$, phase factor is exactly canceled. So all following calculation is done in full sub-lattice. we start from Eq. 4.22 and perturbatively expand interactive electron Green's function,

$$G_{kk_0}(\tau, \tau_0) = -\frac{i}{\hbar} \left\langle T_c e^{-\frac{i}{\hbar}\int H_{es} dt} C_{k\sigma}(\tau) C_{k_0\sigma_0}^\dagger(\tau_0) \right\rangle,$$

up to second order,

$$G_{k\sigma}(\tau,\tau_0)=\left\{\begin{array}{l} -\frac{i}{\hbar}\left\langle T_c C_{k\sigma}(\tau)C^{\dagger}_{k\sigma}(\tau_0)\right\rangle+\frac{1}{2!}\left(-\frac{i}{\hbar}\right)^2\left\langle T_c\int dt H_{es}C_{k\sigma}(\tau)C^{\dagger}_{k\sigma}(\tau_0)\right\rangle \\ +\left(-\frac{i}{\hbar}\right)^3\left\langle T_c\int\int dt_1dt_2H_{es}(t_1)H_{es}(t_2)C_{k\sigma}(\tau)C^{\dagger}_{k\sigma}(\tau_0)\right\rangle \end{array}\right\},$$

we have self-energy for spin-up and spin-down electron,

$$\Sigma^r_{k\uparrow}(t)=\left\{\begin{array}{ll} - & \frac{8J_{es}}{\sqrt{2N}}\left\langle S^z_{k=0}(t)\right\rangle\delta(t) \\ + & \frac{2i\hbar}{2N}\sum_{k'}\left[J_{es}\left(k-k'\right)\right]^2\left\{\begin{array}{l} g^r_{k'\downarrow}(t)D^{-+,>}_{k'-k}(t)+g^<_{k'\downarrow}(t)D^{-+,r}_{k'-k}(t) \\ +g^r_{k'\uparrow}(t)D^{zz,>}_{k-k'}(t)+g^<_{k'\uparrow}(t)D^{zz,r}_{k-k'}(t) \end{array}\right\} \end{array}\right. \tag{4.25}$$

$$\Sigma^r_{k\downarrow}(t)=\left\{\begin{array}{ll} & \frac{8J_{es}}{\sqrt{N}}\left\langle S^z_{k=0}(t)\right\rangle\delta(t) \\ + & \frac{2i\hbar}{2N}\sum_{k'}\left[J_{es}\left(k-k'\right)\right]^2\left\{\begin{array}{l} g^r_{k'\uparrow}(t)D^{+-,>}_{k'-k}(t)+g^<_{k'\uparrow}(t)D^{+-,r}_{k'-k}(t) \\ +g^r_{k'\downarrow}(t)D^{zz,>}_{k'-k}(t)+g^<_{k'\downarrow}(t)D^{zz,r}_{k'-k}(t) \end{array}\right\} \end{array}\right. . \tag{4.26}$$

$g^{r(<)}_{k\sigma}(t)$ is non-interactive Green's function for electrons,

$$g^>_{k\sigma}(t) = -\frac{i}{\hbar}\left(1-n_{k\sigma}\right)e^{-i\varepsilon_{k\sigma}t} \tag{4.27}$$

$$g^<_{k\sigma}(t) = \frac{i}{\hbar}n_{k\sigma}e^{-i\varepsilon_{k\sigma}t} \tag{4.28}$$

$$g^r_{k\sigma}(t) = -\frac{i}{\hbar}\theta(t)e^{-i\varepsilon_{k\sigma}t} \tag{4.29}$$

By inserting Eq. 4.27 - 4.29 and 4.13, 4.14, 4.17, 4.20 into Eq. 4.25 and 4.26, and transformed into frequency space. And relaxation time is given by imaginary part of self energy,

$$\frac{1}{\tau_{k\sigma}}=-\frac{2}{\hbar}Im\Sigma^r_{k\sigma}(\varepsilon_{k\sigma}).$$

Explicitly,

$$
\begin{aligned}
\frac{1}{\tau_{k\uparrow}} &= \frac{\pi}{N\hbar}\sum_{k'}\left[J_{es}\left(k-k'\right)\right]^2 \\
&\times \begin{cases}
& \left[\delta\left(\varepsilon_{k\uparrow}-\varepsilon_{k'\downarrow}+\tilde{X_+^q}\right)\left(\frac{1}{e^{\beta\tilde{X_+^q}}-1}+n_{k'\downarrow}\right)\sum_{ss'}\tilde{A}^q_{ss'}\right]_{q=k-k'} \\
+ & \left[\delta\left(\varepsilon_{k\uparrow}-\varepsilon_{k'\downarrow}+\tilde{X_-^q}\right)\left(\frac{1}{e^{\beta\tilde{X_-^q}}-1}+n_{k'\downarrow}\right)\sum_{ss'}\tilde{B}^q_{ss'}\right]_{q=k-k'} \\
+ & \left[\delta\left(\varepsilon_{k\uparrow}-\varepsilon_{k'\uparrow}+\sqrt{X_+^q}\right)\left(\frac{1}{e^{\beta\sqrt{X_+^q}}-1}+n_{k'\uparrow}\right)\frac{\sum_{ss'}A^q_{ss'}\tilde{E}^q_{ss'}}{2\sqrt{X_+^q}}\right]_{q=k-k'} \\
- & \left[\delta\left(\varepsilon_{k\uparrow}-\varepsilon_{k'\uparrow}-\sqrt{X_+^q}\right)\left(\frac{1}{e^{-\beta\sqrt{X_+^q}}-1}+n_{k'\uparrow}\right)\frac{\sum_{ss'}A^q_{ss'}\tilde{E}^q_{ss'}}{2\sqrt{X_+^q}}\right]_{q=k-k'} \\
+ & \left[\delta\left(\varepsilon_{k\uparrow}-\varepsilon_{k'\uparrow}+\sqrt{X_-^q}\right)\left(\frac{1}{e^{\beta\sqrt{X_-^q}}-1}+n_{k'\uparrow}\right)\frac{\sum_{ss'}B^q_{ss'}\tilde{E}^q_{ss'}}{2\sqrt{X_-^q}}\right]_{q=k-k'} \\
- & \left[\delta\left(\varepsilon_{k\uparrow}-\varepsilon_{k'\uparrow}-\sqrt{X_-^q}\right)\left(\frac{1}{e^{-\beta\sqrt{X_-^q}}-1}+n_{k'\uparrow}\right)\frac{\sum_{ss'}B^q_{ss'}\tilde{E}^q_{ss'}}{2\sqrt{X_-^q}}\right]_{q=k-k'}
\end{cases}
\end{aligned}
$$

$$
\begin{aligned}
\frac{1}{\tau_{k\downarrow}} &= \frac{\pi}{N\hbar}\sum_{k'}\left[J_{es}\left(k-k'\right)\right]^2 \\
&\times \begin{cases}
& \left[\delta\left(\varepsilon_{k\downarrow}-\varepsilon_{k'\uparrow}-\tilde{X_+^q}\right)\left(1+\frac{1}{e^{\beta\tilde{X_+^q}}-1}-n_{k'\uparrow}\right)\sum_{ss'}\tilde{A}^q_{ss'}\right]_{q=k'-k} \\
+ & \left[\delta\left(\varepsilon_{k\downarrow}-\varepsilon_{k'\uparrow}-\tilde{X_-^q}\right)\left(1+\frac{1}{e^{\beta\tilde{X_-^q}}-1}-n_{k'\uparrow}\right)\sum_{ss'}\tilde{B}^q_{ss'}\right]_{q=k'-k} \\
+ & \left[\delta\left(\varepsilon_{k\downarrow}-\varepsilon_{k'\downarrow}+\sqrt{X_+^q}\right)\left(\frac{1}{e^{\beta\sqrt{X_+^q}}-1}+n_{k'\downarrow}\right)\frac{\sum_{ss'}A^q_{ss'}\tilde{E}^q_{ss'}}{2\sqrt{X_+^q}}\right]_{q=k'-k} \\
- & \left[\delta\left(\varepsilon_{k\downarrow}-\varepsilon_{k'\downarrow}-\sqrt{X_+^q}\right)\left(\frac{1}{e^{-\beta\sqrt{X_+^q}}-1}+n_{k'\downarrow}\right)\frac{\sum_{ss'}A^q_{ss'}\tilde{E}^q_{ss'}}{2\sqrt{X_+^q}}\right]_{q=k'-k} \\
+ & \left[\delta\left(\varepsilon_{k\downarrow}-\varepsilon_{k'\downarrow}+\sqrt{X_-^q}\right)\left(\frac{1}{e^{\beta\sqrt{X_-^q}}-1}+n_{k'\downarrow}\right)\frac{\sum_{ss'}B^q_{ss'}\tilde{E}^q_{ss'}}{2\sqrt{X_-^q}}\right]_{q=k'-k} \\
- & \left[\delta\left(\varepsilon_{k\downarrow}-\varepsilon_{k'\downarrow}-\sqrt{X_-^q}\right)\left(\frac{1}{e^{-\beta\sqrt{X_-^q}}-1}+n_{k'\downarrow}\right)\frac{\sum_{ss'}B^q_{ss'}\tilde{E}^q_{ss'}}{2\sqrt{X_-^q}}\right]_{q=k'-k}
\end{cases}.
\end{aligned}
$$

Six terms contribute to scattering process of both spin-up and spin-down electrons, first 2 lines are spin flipping scattering and last 4 lines come from non-flipping scattering. The delta function is calculated via adaptive Gaussian function[112]. Due the symmetry of cubic lattice, only $\frac{1}{6}$ of k points are necessary for actual calculation.

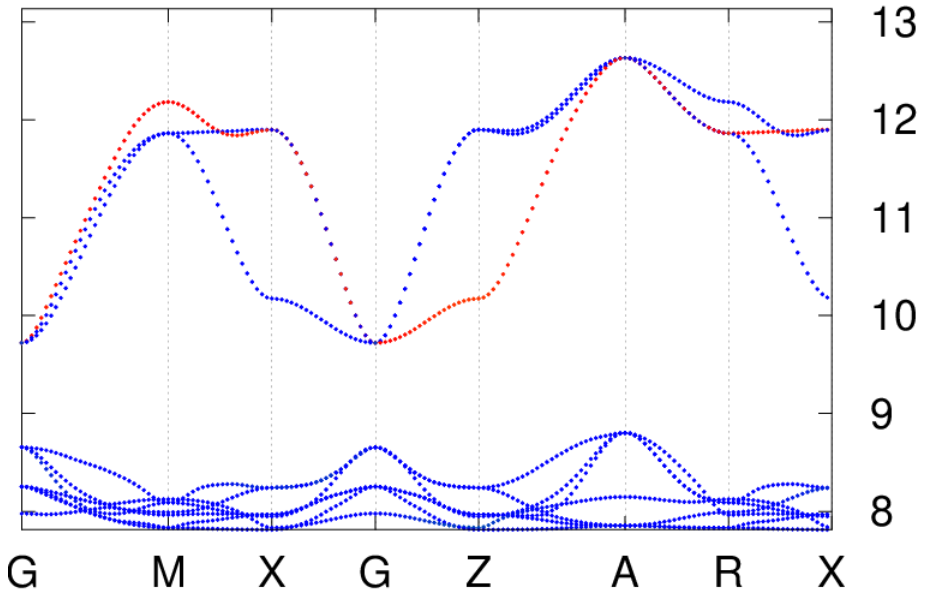

Fig. 4.5. Band structure of $EuTiO_3$

4.3 Result

Transport properties are calculated by the standard method of solving linearized Boltzmann's equation as Section 2.2.6. Since the conduction is contributed by 3d orbital of titanium, chemical potential is below band, The band is calculated by Quantum Espresso and three t2g bands are obtained, but we only consider one of them. As no experimental data of carrier density is obtained, chemical potential is chosen to be slightly below band, 0.017eV lower. Coupling strength J_{es} is $37.3K \cdot k_B$. In fact the choice of band didn't show much difference in terms of conductivity as only band bottom matters. To calculate it at low temperature, it is necessary to interpolate at band bottom to produce dense k points.

Fig. 4.6 shows the comparison of calculation and experiment. Magnetoresistivity are contributed by 4 aspects, Lorentz force, Zeeman splitting, molecular field effect, and spin-splited scattering rate.

Magnetization is calculated via RPA is shown in Fig. 4.7. The RPA magnetization(scatters) matches experimental data(solid line). However in ETO, the Heisenberg coupling in spin system is quite weak. both RPA and

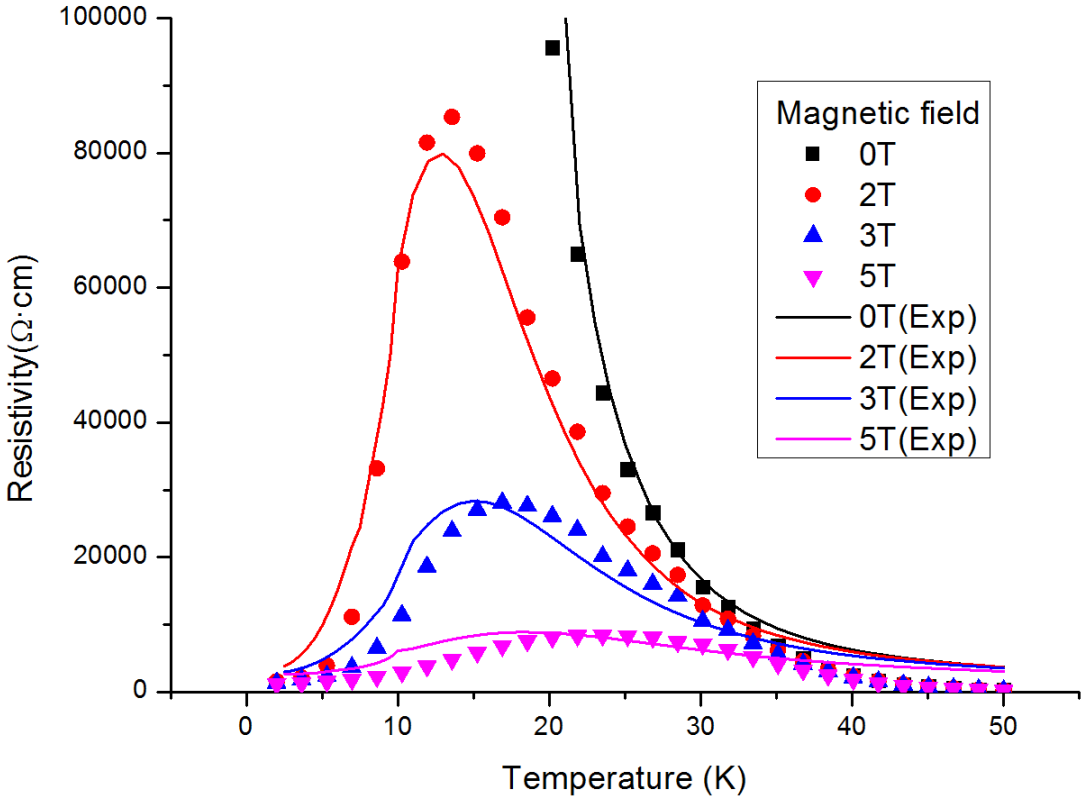

Fig. 4.6. Resistivity. Solid lines are experimental measurement and scatters are theoretical results.

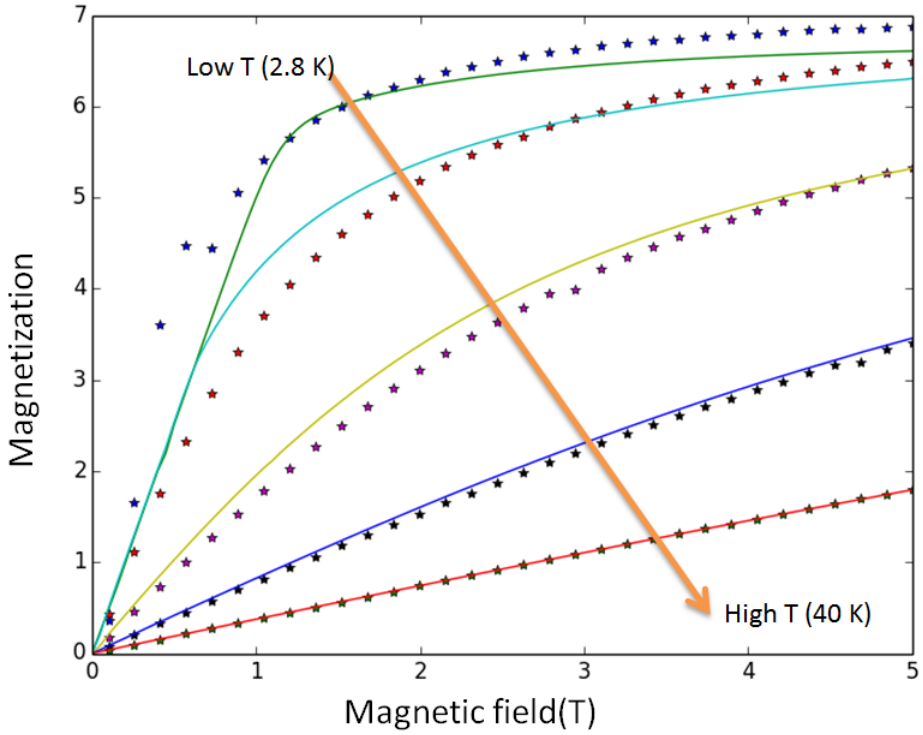

Fig. 4.7. Magnetization of 2.8K, 5K, 10K, 20K, 40K. Solid lines are experimental measurement, and stars are calculated by RPA.

mean-field produce applicable result. Nevertheless RPA have better result than mean field with stronger coupling and RPA give more information of dynamic details.

Relaxation time is shown in Fig. 4.8. Para lines are calculated at 30K ,with magnetic field of 0.1T. Ferro lines are calculated in ferromagnetic phase (10K & 5T). Anti Lines are calculated in antiferromagnetic phase (3K & 0T). Spin-splited scattering rates are degenerated in paramagnetic and anti-ferromagnetic phase. All of my results are calculated at low temperature, relaxation time do not vary a lot at most part of Brillouin zone , and the only difference is due to the differences of magnetic configuration. Two sub-bands are of considerable separation in ferromagnetic phase. The difference is usually smaller than 20%, but it have most significant differences near Γ(G) point, spin-up (parallel) electron have 3

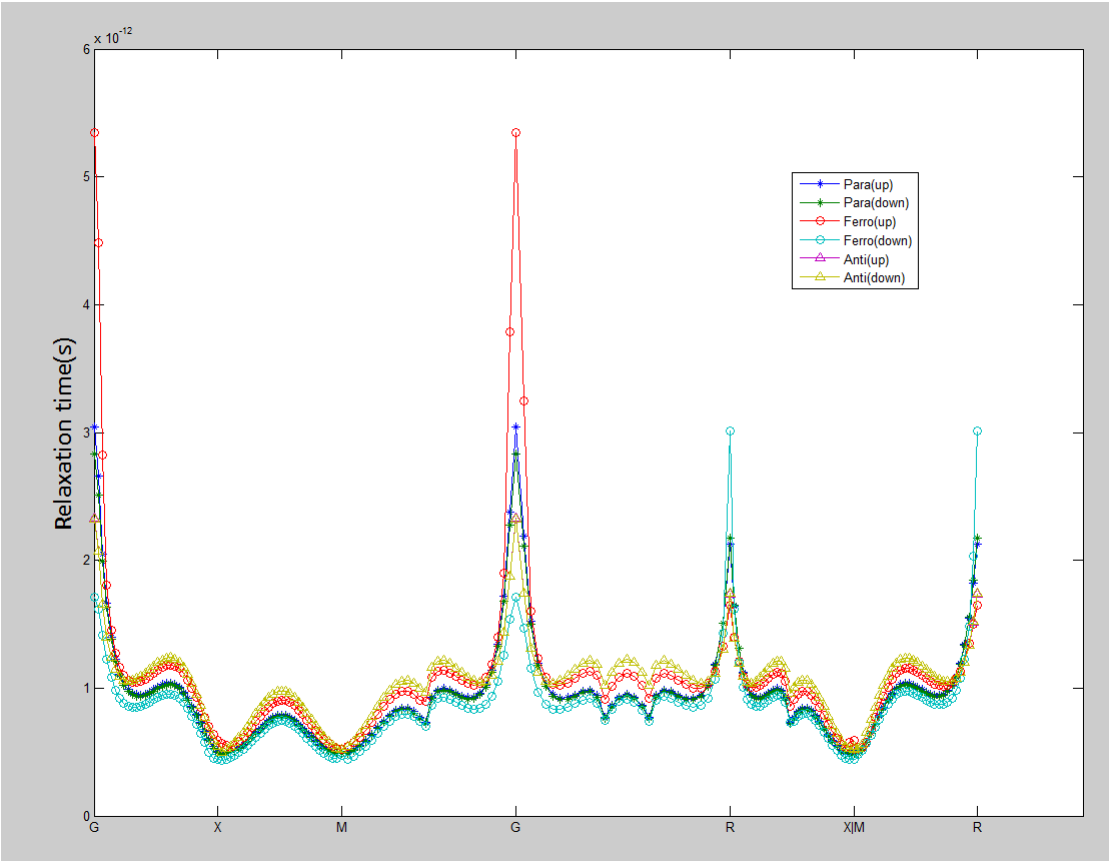

Fig. 4.8. k-dependent Relaxation time due to spin-splited scattering

times longer relaxation time than spin-down(anti-parallel) electron near Γ point. And electron-spin scattering, like normal electron-phonon scattering, have stronger scattering at high temperature. Nevertheless, the change in scattering rate cannot explain such large MR effect.

Carrier density of both spin-up and spin-down band is shown in Fig. 4.9, and it dramatically changes with temperature. molecular field caused band splitting make lower band shifted down. And temperature dependent magneto-response of carrier density is exactly corresponding to magnetoresistance. Actually, chemical potential is the most sensitive parameter and it's the key parameter to reproduce experimental result (Fig. 4.6). The fitted chemical potential is much smaller than calculated band gap 0.93eV. R.F. Chen found the small polaron effect will produce several sub-bands which explain the origin of small value of chemical potential[73]. My model always produce smaller resistivity at high temperature, and it is due to ig-

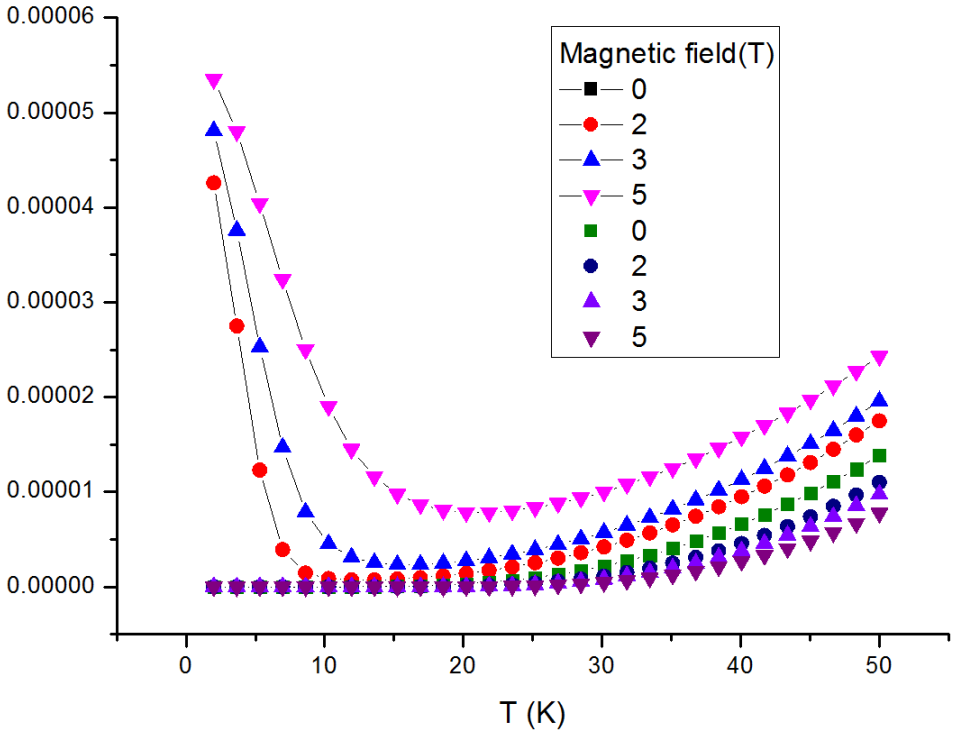

Fig. 4.9. Carrier density of each spin-splited bands(electrons per cell). solid-line-connected symbol are spin-up bands and disconnected lines are spin-down bands

norance of other scattering, e.g. phonon or impurity scattering.

In conclusion, the origin of such large CMR in ETO is primarily due to the molecular effect caused by off-site spin-electron coupling. However scattering rate changed with magnetic field, the contribution to CMR is so trivial compared to contribution from change of carrier density .

Chapter 5

Spin Green's Function for Finite Spin System

Double time temperature-dependent Green's function was initially used for spin-$\frac{1}{2}$ magnetic system in 1959 by S. V. Tyablikov [126, 79, 153]. And it was extended to higher spin by Tahir-Kheli and ter Harr[158] in 1962. Callen heavily simplified the method for higher spin case by proposing an explicit solution Eq. 2.23 . Recent year, some work have been done to investigate the infinite magnetic film or coupled bilayer structure with or without anisotropy[121, 68, 156].

Popularity of multiferroics aroused due to its potentially fascinating application. Particularly, a flurry of research focused on thin film multiferroics has been driven by the demand of seeking novel functional material for electronic industry. Although bulk ETO is an incipient ferroelectrics, thin film ETO demonstrate strain-induced ferroelectricity. To achieve better utilization of thin film ETO, it's necessary to have further understanding of coupling between spins,phonons and electrons. Current is the most common way to implement manipulation in microelectronic device, and NEGF is one of standard methods to investigate transport properties and other dynamics in nano-scale. Nowadays, nano device of electron and phonon

system have received extensive research[142, 86, 103, 76, 141, 96, 59, 104, 124, 115, 129, 145, 147, 71, 93, 67, 119, 108, 81, 143], but it's quite deficient in spin-electron system, which is useful for further modeling of spintronic nano-device. The probe into coupled system starts from full understanding isolated system. And non-equilibrium dynamics can be perturbatively studied via equilibrium Green's function. For spin system, which are normally difficult to be solved, the following method provide an approximation to obtain full set of Green's functions. It is a cornerstone to incorporate system into the framework of NEGF. Particularly, as improper multiferroics, multiferroicity in ETO excited in different ion site, which is ideal to construct isolated system by ignore coupling at beginning.

Spin Green's function have briefly discussed in Section 2.3, the method was limited to translational invariant infinite system. Although, mathematically, there is only minor modification for nano-size case, there are some technical difficulties to be resolved.

5.1 Method

5.1.1 First order

Starting from Eq. 2.16, homogeneous Heisenberg model can always obtain closed formula with transverse component only for first order case. And translational invariant infinite systems always lead to pole structure,

$$G_k(\omega) = \frac{2\langle S^z\rangle}{\omega - \omega_k}.$$

Transverse correlation is obtained by fluctuation-dissipation theorem,

$$G_k^<(\omega) = -\frac{1}{\pi}\frac{ImG_k(\omega)}{e^{\beta\omega}-1}\delta(\omega-\omega_k).$$

self-consistency procedure is closed via Callen's formula Eq. 2.23, as what I did in section 4.2.2. Due to the identity$(S^z)^2 = \frac{1}{4}$ for spin-$\frac{1}{2}$ system, simpler expression is achieved,

$$\begin{aligned}\langle S_i^z \rangle &= \frac{1}{2} - \langle S_i^- S_i^+ \rangle \\ &= \frac{1}{2} + \frac{1}{N\pi} \sum_k \int_{-\infty}^{\infty} d\omega \frac{ImG_k(\omega)}{e^{\beta\omega} - 1} \delta(\omega - \omega_k) \\ &= \frac{1}{2} - \frac{1}{8\pi^3} \int dk \frac{2\langle S^z \rangle}{e^{\beta\omega_k} - 1},\end{aligned}$$

with $\frac{2}{e^x - 1} = coth\left(\frac{x}{2}\right) - 1$,

$$\langle S_i^z \rangle = \frac{4\pi^2}{\int d\mathbf{k} \coth(\beta\omega_k)}. \tag{5.1}$$

Such formula is still self-consistent as ω_k is written in terms of $\langle S_i^z \rangle$, the explicit form of ω_k depending on Hamiltonian and choice of decoupling rule.

Decoupling Rule

I have discussed one of decoupling rule, Tyablikov decoupling (Eq. 2.20). Although, no rigorous justification for this rule, but validity was checked by comparison with other method and QMC result [161].

Callen proposed an improvement on RPA decoupling [40] for spin-$\frac{1}{2}$,

$$\left\langle\left\langle S_i^z S_j^+; S_l^- \right\rangle\right\rangle \approx \langle S_i^z \rangle \left\langle\left\langle S_j^+; S_l^- \right\rangle\right\rangle - \alpha \left\langle S_i^- S_j^+ \right\rangle \left\langle\left\langle S_i^+; S_l^- \right\rangle\right\rangle, \tag{5.2}$$

with correction factor $\alpha = \frac{\langle S^z \rangle}{S}$. The derivation starts from identities

$$S_i^z = S - S_i^- S_i^+ \tag{5.3}$$

$$S_i^z = \frac{1}{2}\left(S_i^+ S_i^- - S_i^- S_i^+\right), \tag{5.4}$$

and S_i^z is divided to 2 parts , $S_i^z = \alpha S_i^z + (1-\alpha) S_i^z$. each S_i^z at right-

hand-side is replace by 5.3 and 5.4 respectively,

$$\left\langle\left\langle S_i^z S_j^+; S_l^-\right\rangle\right\rangle = \alpha S \left\langle\left\langle S_j^+; S_l^-\right\rangle\right\rangle + \frac{1}{2}(1-\alpha)\left\langle\left\langle S_i^+ S_i^- S_j^+; S_l^-\right\rangle\right\rangle - \frac{1}{2}(1+\alpha)\left\langle\left\langle S_i^- S_i^+ S_j^+; S_l^-\right\rangle\right\rangle.$$

triple terms are decomposed symmetrically,

$$\left\langle\left\langle S_i^+ S_i^- S_j^+; S_l^-\right\rangle\right\rangle \approx \left\langle S_i^+ S_i^-\right\rangle \left\langle\left\langle S_j^+; S_l^-\right\rangle\right\rangle + \left\langle S_i^- S_j^+\right\rangle \left\langle\left\langle S_i^+; S_l^-\right\rangle\right\rangle + \left\langle S_i^+ S_j^+\right\rangle \left\langle\left\langle S_i^-; S_l^-\right\rangle\right\rangle \quad (5.5)$$

$$\left\langle\left\langle S_i^- S_i^+ S_j^+; S_l^-\right\rangle\right\rangle \approx \left\langle S_i^- S_i^+\right\rangle \left\langle\left\langle S_j^+; S_l^-\right\rangle\right\rangle + \left\langle S_i^+ S_j^+\right\rangle \left\langle\left\langle S_i^-; S_l^-\right\rangle\right\rangle + \left\langle S_i^- S_j^+\right\rangle \left\langle\left\langle S_i^+; S_l^-\right\rangle\right\rangle \quad (5.6)$$

it surely reasonable to assume $\left\langle S_i^+ S_j^+\right\rangle = \left\langle S_i^- S_j^-\right\rangle = 0$, and for on-site correlation term using relation $\left\langle S_i^+ S_i^-\right\rangle = 2\left\langle S_i^z\right\rangle + \left\langle S_i^- S_i^+\right\rangle$, Callen's decoupling Eq. 5.2 is arrived. When $\alpha \to 0$, Callen's decoupling will go back to RPA decoupling. And for fully magnetized limit , i.e. $\langle S^z\rangle = \frac{1}{2}$, $\alpha = 1$. It was able to generalized to arbitrary spin with $\alpha = \frac{\langle S^z\rangle}{2S^2}$ [40].

Mean field theory(MFT) is simplest method, but extensively used. Although MFT is usually worked out locally, but it can be also incorporated into Eq. 5.1 by considering constant $\omega_k = \omega^{MFT}$, rather than k-depended, and leads to iterative equation

$$\langle S^z\rangle = \frac{1}{2}\tanh\left(\frac{\beta\omega^{MFT}}{2}\right).$$

The methods were compared in mono-layer ferromagnetic film [105]. RPA turn out to be the best approximation, albeit it is simpler than Callen's decoupling. However the mean field method is less accurate than other method, but all method get better accuracy in week coupling case, i.e. J/B is small. Since in weak coupling limit, coupled Heisenberg system restore to paramagnetic system, and all the decoupling is trivial compared to Zeeman term. This is also consistent with our bulk Heisenberg model for $EuTiO_3$, which both RPA and MFT give quite accurate result compared to experimental result [105].

5.1.2 Second Order

I have analyzed first order case, but first order is not always enough. For example, when anisotropy is considered or other case that longitudinal component and transverse component are coupled, I have to consider longitudinal Green's function function, and it is necessary to extend the method to second order. For pure longitudinal part, first term of right-hand-side of Eq. 2.17 vanished,

$$\omega^2\hbar^2 \langle\langle A; B\rangle\rangle_\omega = \left\langle \left[i\hbar\dot{A}, B \right] \right\rangle + \left\langle \left\langle -\hbar^2 \ddot{A}; B \right\rangle \right\rangle_\omega , \tag{5.7}$$

which gives pole structure,

$$G_k(\omega) = \frac{A}{\omega - \omega_k^+} + \frac{B}{\omega - \omega_k^-}.$$

During this process, both terms in right-hand-side of Eq. 5.7 have vertex terms to be decoupled. As shown in Eq. 5.5 and 5.6, symmetrical decoupling is the easiest rule.

Decoupling Rules

The applicability of Wick's theorem for spin operator is not proven yet. Modified Wich's expansion is given for spin-$\frac{1}{2}$ system at zero temperature[110, 92, 39], but for general spin operators at Keldysh contour, a set of decoupling rules are used for approximation. In 2.3.3, two simple decoupling rules have been mentioned. Except simple symmetric decoupling, vertex correction was introduced in [155, 113, 132],

$$S_i^\alpha S_j^\beta S_l^\gamma \approx \lambda_{i,j,l}^{a,\beta,\gamma} \left\langle S_i^\alpha S_j^\beta \right\rangle S_l^\gamma + \eta_{i,j,l}^{a,\beta,\gamma} \left\langle S_j^\beta S_l^\gamma \right\rangle S_i^\alpha + \mu_{i,j,l}^{a,\beta,\gamma} \langle S_i^\alpha S_l^\gamma \rangle S_j^\beta . \tag{5.8}$$

The determination of correction factor depends on both type and site of each operators. It's impossible to properly choose all correction factor.

Usually it's reasonable to assume $\langle S_i^+ S_j^+ \rangle = \langle S_i^- S_j^- \rangle = 0$, and correction factors associated with are surely 0. Kondo and Yamaji [155] usually choose a uniform factor for all non-zero correction factor. However site index i, j, l are arbitrary, but the span of vertex depends on Hamiltonian. For example, a Heisenberg model with only nearest neighboring coupling, the largest possible span for second order expansion is next-nearest site. For this reason decoupling rules can also be chosen as [121, 68],

$$\begin{aligned}
S_i^+ S_j^- S_j^+ &= \langle S_j^- S_j^+ \rangle S_i^+ + \alpha_{i,j}^{+-} \langle S_i^+ S_j^- \rangle S_j^+ \\
\left(S_j^z\right)^2 S_i^+ &= \left\langle \left(S_j^z\right)^2 \right\rangle S_i^+ \\
S_i^+ S_i^z S_j^z &= \lambda_{i,j}^{+-} \langle S_i^z S_j^z \rangle S_i^+ \\
S_i^+ S_j^+ S_l^- &= \alpha_{j,l}^{+-} \langle S_j^+ S_l^- \rangle S_i^+ + \alpha_{i,l}^{+-} \langle S_i^+ S_l^- \rangle S_j^+ .
\end{aligned}$$

Only $\langle S_i^+ S_j^- \rangle$ and $\langle S_i^z S_j^z \rangle$ terms are retained, transverse vertex parameter $\alpha_{i,j}^{+-}$ and longitudinal vertex parameter $\lambda_{i,j}^{+-}$ both depend on site of correlation $\langle S_i^+ S_j^- \rangle$ and $\langle S_i^z S_j^z \rangle$ respectively. For nearest coupled Heisenberg model, Further approximation can simplify parameters to 3 cases, α_1^{+-},λ_1^{+-} for nearest i, j ,α_2^{+-},λ_2^{+-} for next-nearest i, j, and 1 for on-site case (i.e. $i = j$). The value of parameters are determined via fitting with QMC result[156, 82, 97, 68, 66, 121].

5.1.3 Finite System

Infinite system are usually decoupled in k space, especially for isotropic system, transverse and longitudinal component are decoupled. The Hamiltonian can be written as

$$H = \sum_{i,j,\alpha,\beta} J_{i,j}^{\alpha\beta} S_i^\alpha S_j^\beta , \tag{5.9}$$

where site index i, j must be or can be mapped into 1-D countable index(e.g. $0, 1, 2, \cdots, N-1$), rather than an generalized index(e.g. 2-D or 3-D vector). and α, β are $\pm$ or x, y, z component. In the case that α, β are x,y, spin operators should be converted into ladder form via relation $S^{\pm} = S^x \pm iS^y$.

Because both transverse and longitudinal parts are included in unified formalism, original equation of motion(Eq. (2.17)) is used here, rather than simplified Eq. 5.7,

$$\omega^2\hbar^2 \left\langle\left\langle S_i^\alpha; S_j^\beta \right\rangle\right\rangle_\omega = \omega \left\langle\left[i\hbar S_i^\alpha, S_j^\beta\right]\right\rangle + \left\langle\left[i\hbar \dot{S}_i^\alpha, S_j^\beta\right]\right\rangle + \left\langle\left\langle -\hbar^2 \ddot{S}_i^\alpha; S_j^\beta \right\rangle\right\rangle_\omega .$$

The details of decoupling will be discussed later. I just assume some decoupling rule is applied already, and a closed form is obtained. Since different sites are coupled after decoupling, and Eq. 5.10 is written in matrix form,

$$\omega^2\hbar^2 G^r = \omega\hbar T + \Gamma_1 + \Gamma_2 G^r. \tag{5.10}$$

where T, Γ_1,Γ_2, G^r are matrix, the entry $G^r_{m,n} = \langle\langle S_m; S_n\rangle\rangle_\omega$, S_m and S_n is 1-D series of spin operator S_i^α. In this section, I can assume the layout of each spin are symmetrical ,i.e. both m,n are mapped in same way, and be mapped as $m = 3 \times i + \alpha$, $\pm$ and z are mapped to 1,2,3. So aforementioned matrices are of size 3N $\times$ 3N. It is easily to be grouped in terms of G^r, and replace $\omega\hbar = \tilde{\omega}$

$$\left(\tilde{\omega}^2 I - \Gamma_2\right) G^r = \left(\tilde{\omega} T + \Gamma_1\right). \tag{5.11}$$

Non-singular Case

If Γ_2 it's invertible, Eq.5.11 is easy to be solved. Although G^r is easy to be obtained by multiplying inverse of $(\tilde{\omega}^2 I - \Gamma_2)$, disorganization is still

compulsory. Assuming diagonal $\Omega = L\Gamma_2 R$, and $LR = I$, Eq. 5.11 is

$$\left(\tilde{\omega}^2 I - R\Omega L\right) G^r_\omega = \left(\tilde{\omega} T + \Gamma_1\right),$$

left multiply matrix L,

$$\left(\tilde{\omega}^2 I - \Omega\right) L G^r_\omega = \left(\tilde{\omega} L T + L\Gamma_1\right),$$

and $(\tilde{\omega}^2 I - \Omega)$ is diagonal, the inverse $(\tilde{\omega}^2 I - \Omega)^{-1}$ is diagonal as well ,

$$G^r_\omega = R \begin{bmatrix} \ddots & 0 & 0 \\ 0 & \frac{1}{\tilde{\omega}^2 - \Omega} & 0 \\ 0 & 0 & \ddots \end{bmatrix} \left(\tilde{\omega} L T + L\Gamma_1\right). \tag{5.12}$$

Fluctuation-dissipation theorem is applied ,

$$G^<_\omega = \frac{-i}{2\pi} R \begin{bmatrix} \ddots & 0 & 0 \\ 0 & \frac{1}{2\sqrt{\Omega}} \frac{\delta\left(\tilde{\omega} - \sqrt{\Omega}\right) - \delta\left(\tilde{\omega} + \sqrt{\Omega}\right)}{e^{\beta\tilde{\omega}} - 1} & 0 \\ 0 & 0 & \ddots \end{bmatrix} \left(\tilde{\omega} L T + L\Gamma_1\right).$$

All correlation in Γ_1 and Γ_2 is obtained from $G^<_\omega$, but earlier formula for $\langle S^z \rangle$ (Eq.2.23) is not valid here. And have to turn back to original identity,

$$\left\langle S^+_i S^-_i \right\rangle + \left\langle S^z_i S^z_i \right\rangle - \left\langle S^z_i \right\rangle = S\left(S + 1\right). \tag{5.13}$$

Singular case

In the case of zero eigenvalue appears , boson function $\frac{1}{e^{\beta\tilde{\omega}} - 1}$ diverge. Along with diagonalization , both Ω,L,R will be partitioned to non-zero and zero

eigenvalue space.

$$L = \begin{bmatrix} L^1 \\ \\ L^0 \end{bmatrix}$$
$$R = \begin{bmatrix} R^1 & R^0 \end{bmatrix}$$

$$\Omega = \begin{bmatrix} \Omega_1 & 0 \\ \\ 0 & \Omega_0 \end{bmatrix}.$$

Assuming there are n zero eigenvalues, so L^0, L^1 are $n\times(3N)$ and $(3N-n)\times(3N)$ matrix respectively, and R^0, R^1 are $(3N)\times n$ and $(3N)\times(3N-n)$ matrix. Ω^1 is diagonal matrix of size $(3N-n)\times(3N-n)$, and Ω^0 is actually zero matrix of size n×n. Although inverse of Ω_0 is ill-defined, inversion of $(\tilde{\omega}^2 I_{n\times n} - \Omega_0)$ is still valid. So Eq. 5.12 is written as

$$G^r_\omega = \begin{bmatrix} R^1 & R^0 \end{bmatrix} \begin{bmatrix} \begin{bmatrix} \frac{1}{\tilde{\omega}^2-\Omega_1} \end{bmatrix} & 0 \\ 0 & \begin{bmatrix} \frac{1}{\tilde{\omega}^2-\Omega_0} \end{bmatrix} \end{bmatrix} \left(\begin{bmatrix} L^1 \\ \\ L^0 \end{bmatrix} \tilde{\omega} T + \begin{bmatrix} L^1 \\ \\ L^0 \end{bmatrix} \Gamma_1 \right), \quad (5.14)$$

where $\begin{bmatrix} \frac{1}{\tilde{\omega}^2-\Omega_1} \end{bmatrix}$ diagonal matrix with all diagonal entries in the form of $\frac{1}{\tilde{\omega}^2-\Omega_1}$, Ω_1 in denominator refers to one of the eigenvalue of matrix Ω_1, the same for $\begin{bmatrix} \frac{1}{\tilde{\omega}^2-\Omega_0} \end{bmatrix}$. Expanding Eq. 5.14, and considering $L^0R^1 = L^0R^1 = 0$,

$$G^r_\omega = R^1 \begin{bmatrix} \frac{1}{\tilde{\omega}^2-\Omega_1} \end{bmatrix} (L^1\tilde{\omega}T + L^1\Gamma_1) + R^0 \begin{bmatrix} \frac{1}{\tilde{\omega}^2-\Omega_0} \end{bmatrix} (L^0\tilde{\omega}T + L^0\Gamma_1).$$

Applying fluctuation-dissipation theorem on first term, but the behavior of singular $\frac{1}{e^{\beta\tilde{\omega}}-1}$ is unknown.To overcome this obstacle, it is not needed to

know details and just used notation $\left[\frac{1}{\tilde{\omega}^2-\Omega_0}\right]^<$.

$$G^<_\omega = R^1 \tfrac{-i}{2\pi}\left[\tfrac{1}{\sqrt{\Omega_1}}\tfrac{\delta\left(\tilde{\omega}-\sqrt{\Omega_1}\right)-\delta\left(\tilde{\omega}+\sqrt{\Omega_1}\right)}{e^{\beta\tilde{\omega}}-1}\right](L^1\tilde{\omega}T + L^1\Gamma_1)+R^0\left[\tfrac{1}{\tilde{\omega}^2-\Omega_0}\right]^<(L^0\tilde{\omega}T + L^0\Gamma_1). \tag{5.15}$$

The trickiest part is to left multiply matrix $\begin{bmatrix}0 & R^0\end{bmatrix}\begin{bmatrix}0\\ L^0\end{bmatrix}$ and due to $L^0R^1 = 0$ and $L^0R^0 = I_{n\times n}$,

$$\begin{bmatrix}0 & R^0\end{bmatrix}\begin{bmatrix}0\\ L^0\end{bmatrix}G^<_\omega = R^0\left[\tfrac{1}{\tilde{\omega}^2-\Omega_0}\right]^<\left(L^0\tilde{\omega}T + L^0\Gamma_1\right). \tag{5.16}$$

Unknown second term in Eq. 5.15 is replaced by Eq. 5.16,

$$G^<_\omega = R^1 \tfrac{-i}{2\pi}\left[\tfrac{1}{\sqrt{\Omega_1}}\tfrac{\delta\left(\tilde{\omega}-\sqrt{\Omega_1}\right)-\delta\left(\tilde{\omega}+\sqrt{\Omega_1}\right)}{e^{\beta\tilde{\omega}}-1}\right](L^1\tilde{\omega}T + L^1\Gamma_1)+\begin{bmatrix}0 & R^0\end{bmatrix}\begin{bmatrix}0\\ L^0\end{bmatrix}G^<_\omega. \tag{5.17}$$

$G^<_\omega$ is obtained by calculating Eq. 5.17 iteratively. $\langle S^z\rangle$ is obtained as non-singular case (Eq. 5.13). Because singular formula will be reinstated to non-singular case with empty zero eigenvalue space (n=0), Eq. 5.17 covers both singular and non-singular case.

5.2 Algorithm

In last section I worked out iterative formula , but I just assume the higher order vertex are properly decoupled and skipped the details. And I also saw the formalism for finite system is mathematically straightforward and of only little difference from infinite system, but the decoupling process for finite system is more complicated than infinite system. The immense complexity for finite system has been the largest obstacle to implementation of such method. It almost impossible to manually decouple for finite system. The number of terms for each site after decoupling may be as many as

$(3Z)^2$, Z is coordination number. For this reason , a algorithm is proposed to work out this symbolic decoupling rule automatically.

5.2.1 Matrix Representation

Hamiltonian Eq. 5.9 only considered coupling among local spins. People always interest in system coupled to magnetic field. Hamiltonian to be discussed is,

$$H = \sum_{i,j,\alpha,\beta} J_{i,j}^{\alpha\beta} S_i^{\alpha} S_j^{\beta} + \sum_{i,\alpha} \left(B_i^{\alpha}\right)^{\star} S_i^{\alpha}. \tag{5.18}$$

Defining vector $S_i = \left[S_i^+, S_i^-, S_i^z\right]$, sub-matrix $H\left(i,j\right)$, the interaction between site i and j is

$$H\left(i,j\right) = \begin{bmatrix} J_{i,j}^{+,+} & J_{i,j}^{+,-} & J_{i,j}^{+,z} \\ J_{i,j}^{-,+} & J_{i,j}^{-,-} & J_{i,j}^{-,z} \\ J_{i,j}^{z,+} & J_{i,j}^{z,-} & J_{i,j}^{z,z} \end{bmatrix}.$$

So, $H_{i,j} = \sum_{\alpha,\beta} J_{i,j}^{\alpha\beta} S_i^{\alpha} S_j^{\beta} = S_i H\left(i,j\right) S_j^T$. I can define a super-operator,

$$L_l^{\gamma} \star = \left[S_l^{\alpha}, \star\right]_L, \tag{5.19}$$

subscript L means to commute with left operator. For example, $L_l^{\gamma} \star H_{i,j} = \sum_{\alpha,\beta} J_{i,j}^{\alpha\beta} \left[S_l^{\gamma}, S_i^{\alpha}\right] S_j^{\beta}$, and similarly, $R_l^{\alpha}\star$ is defined as

$$R_l^{\gamma} \star = \left[S_l^{\alpha}, \star\right]_R s$$

$R_l^{\gamma} \star H_{i,j} = \sum_{\alpha,\beta} J_{i,j}^{\alpha\beta} S_i^{\alpha} \left[S_l^{\gamma}, S_j^{\beta}\right]$. It's easy to have

$$\begin{aligned} -L_l^{\gamma}\star &= \left[\star, S_l^{\alpha}\right]_L \\ -R_l^{\gamma}\star &= \left[\star, S_l^{\alpha}\right]_R. \end{aligned}$$

$\left[S_l^{\gamma}, H\right]$ can be written as $\left[S_l^{\gamma}, H\right] = L_l^{\gamma} \star H + R_l^{\gamma} \star H = \sum_{i,j} L_l^{\gamma} \star H_{i,j} +$

$\sum_{i,j} R_l^\gamma \star H_{i,j}$. Due to commutation relation

$$\begin{aligned}\left[S_i^\pm, S_j^z\right] &= \mp\delta_{i,j} S_i^\pm \\ \left[S_i^+, S_j^-\right] &= 2\delta_{i,j} S_i^z,\end{aligned}$$

the first derivative of a single operator is in binary form as Hamiltonian (Eq. 5.18). Super operator $L_l^\gamma\star$ on binary Hamiltonian is indeed a mapping from a matrix to another matrix. For example, Considering a isotropic Heisenberg model, oupling strength between site i and j is J,

$$\begin{aligned}\tilde{H}_{i,j} &= J\mathbf{S}_i \cdot \mathbf{S}_j \\ &= \frac{J}{2}\left(S_i^+ S_j^- + S_i^- S_j^+\right) + J S_i^z S_j^z \\ &= S_i \begin{bmatrix} 0 & \frac{J}{2} & 0 \\ \frac{J}{2} & 0 & 0 \\ 0 & 0 & J \end{bmatrix} S_j^T.\end{aligned}$$

Applying super-operator $L_i^+\star$,

$$\begin{aligned}L_i^+ \star \tilde{H}_{i,j} &= J S_i^z S_j^+ - J S_i^+ S_j^z \\ &= S_i \begin{bmatrix} 0 & 0 & -J \\ 0 & 0 & 0 \\ J & 0 & 0 \end{bmatrix} S_j^T,\end{aligned}$$

find,

$$\begin{bmatrix} 0 & 0 & -1 \\ 0 & 0 & 0 \\ 0 & 2 & 0 \end{bmatrix} \begin{bmatrix} 0 & \frac{J}{2} & 0 \\ \frac{J}{2} & 0 & 0 \\ 0 & 0 & J \end{bmatrix} = \begin{bmatrix} 0 & 0 & -J \\ 0 & 0 & 0 \\ J & 0 & 0 \end{bmatrix}.$$

Commutator operator can be written in matrix form

$$L_i^+\star = \begin{bmatrix} 0 & 0 & -1 \\ 0 & 0 & 0 \\ 0 & 2 & 0 \end{bmatrix},$$

and similarly for $-$and z component,

$$\begin{aligned} L_i^-\star &= \begin{bmatrix} 0 & 0 & 0 \\ 0 & 0 & 1 \\ -2 & 0 & 0 \end{bmatrix} \\ L_i^z\star &= \begin{bmatrix} 1 & 0 & 0 \\ 0 & -1 & 0 \\ 0 & 0 & 0 \end{bmatrix}. \end{aligned}$$

$R_l^\gamma\star$ is also given as,

$$\begin{aligned} R_i^+\star &= \begin{bmatrix} 0 & 0 & 0 \\ 0 & 0 & 2 \\ -1 & 0 & 0 \end{bmatrix} \\ R_i^-\star &= \begin{bmatrix} 0 & 0 & -2 \\ 0 & 0 & 0 \\ 0 & 1 & 0 \end{bmatrix} \\ R_i^z\star &= \begin{bmatrix} 1 & 0 & 0 \\ 0 & -1 & 0 \\ 0 & 0 & 0 \end{bmatrix} \end{aligned}$$

Be noted, $L_l^\gamma\star$ matrix is just transpose of corresponding $R_l^\gamma\star$ matrix. And $L_l^\gamma\star$ is left multiplication on coefficient matrix, meanwhile $R_l^\alpha\star$ is right

multiplication,

$$L_i^+ \star \tilde{H}_{i,j} = S_i \begin{bmatrix} 0 & 0 & -1 \\ 0 & 0 & 0 \\ 0 & 2 & 0 \end{bmatrix} H(i,j) S_j^T$$

and

$$R_j^+ \star \tilde{H}_{i,j} = S_i H(i,j) \begin{bmatrix} 0 & 0 & 0 \\ 0 & 0 & 2 \\ -1 & 0 & 0 \end{bmatrix} S_j^T.$$

Ssymbolic commutation operation can be locally implemented in computer by matrix multiplication. Due to $\left[S_i^\alpha, S_j^\beta\right] = 0$ for all $i \neq j$, Full Hamiltonian is of size $(3N+3) \times (3N)$.

The site index of spins are $0, 1, \cdots, N-1$. The lowest 3 rows are coupling to magnetic field, corresponding column vector of operators are,

$$\mathbf{h} = \begin{bmatrix} h^+ \\ h^- \\ h^z \end{bmatrix} = \mu_B \mathbf{B} = \mu_B \begin{bmatrix} B^+ \\ B^- \\ B^z \end{bmatrix} = \mu_B \begin{bmatrix} \frac{B^x + iB^y}{2} \\ \frac{B^x - iB^y}{2} \\ B^z \end{bmatrix}.$$

Although it is mathematically more reasonable to construct large commutation super-operator matrix, it is computationally more efficient to use 3×3 sub-matrix. For $L_l^+ \star \tilde{H}_{i,j}$ operation, only $i = l$ or $j = l$ produce non-zero matrix. For each operator S_i^α, only the sub-matrices in the belt associated with site i need to be consider (in Fig. 5.1). L_i^α is used for horizontal part of sub-matrices, and R_i^α for vertical part. Diagonal sub-matrix is in considered for both horizontal and vertical part and are added up.

Following the same way, commuting column operator and row operators with full Hamiltonian again individually, a 3rd-dimension tensor is

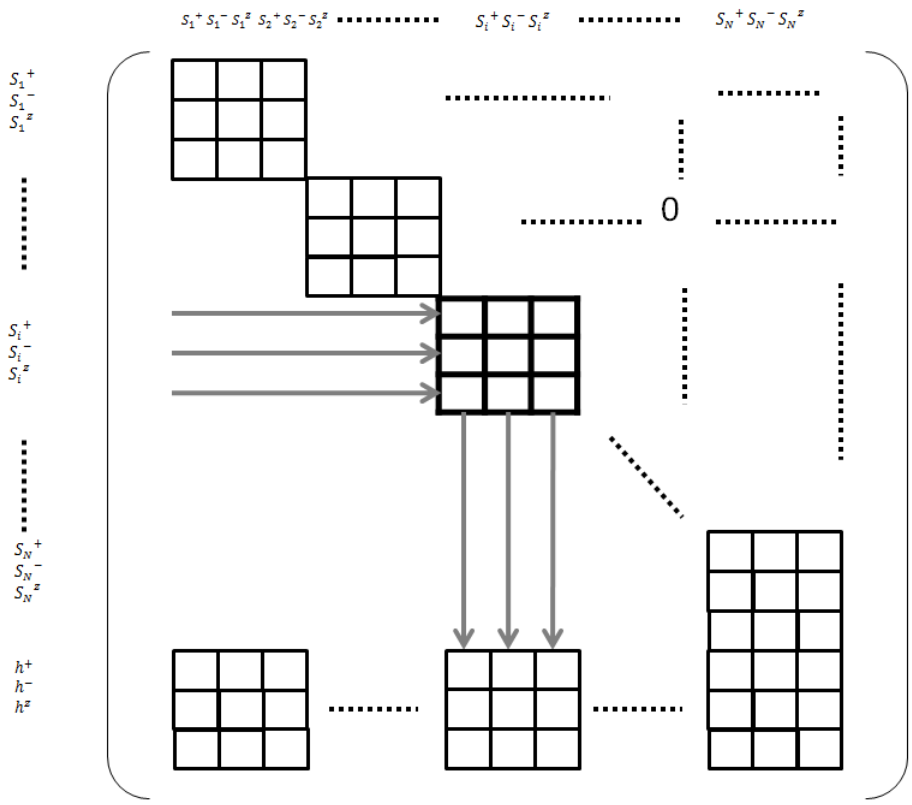

Fig. 5.1. Belt of non-zero sub-matrix associated with S_i^α

obtained. This 3rd-dimension tensor described coefficients of all triple operator terms, however it's quite sparse.

Decoupling rule Eq.5.8 is applied, and a customized linked list is constructed to store the expression of all non-zero entries of Γ_2 in Eq. 5.10. one have symbolic Γ_2, which describe how each entries of numerical Γ_2 is calculated from G. The similar procedure is adopted for Γ_1. So after every iteration of Eq.5.17, numerical matrix T, Γ_1, Γ_2 are updated according to corresponding symbolic matrix.

Linked list structure is shown in Fig. 5.2, symbolic matrix can be either Γ_1 or Γ_2 matrix as they are of same form. Each entry is a pointer to the beginning of a list or null pointer for zero entry. 3 components in each node, c_i is the pre-factor and either complex number or real number. Ptr_c is the pointer pointing to either element of correlation or element of array of $\langle S^z \rangle$ accordingly. Because a lot of inserting operation during the generation of symbolic matrix, list is preferred at beginning. But it is better to use a simple array generated from the aforementioned linked list to achieve higher computational efficiency.

The complete procedure is shown in Fig. 5.3.

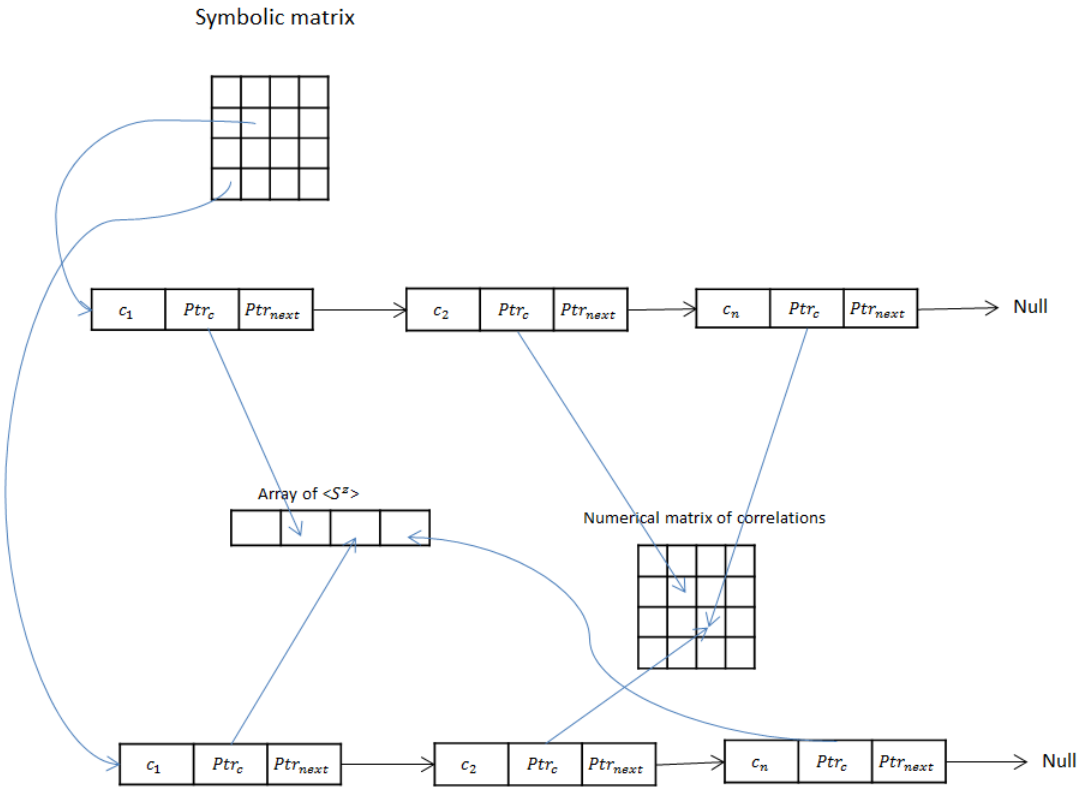

Fig. 5.2. Linked list structure.

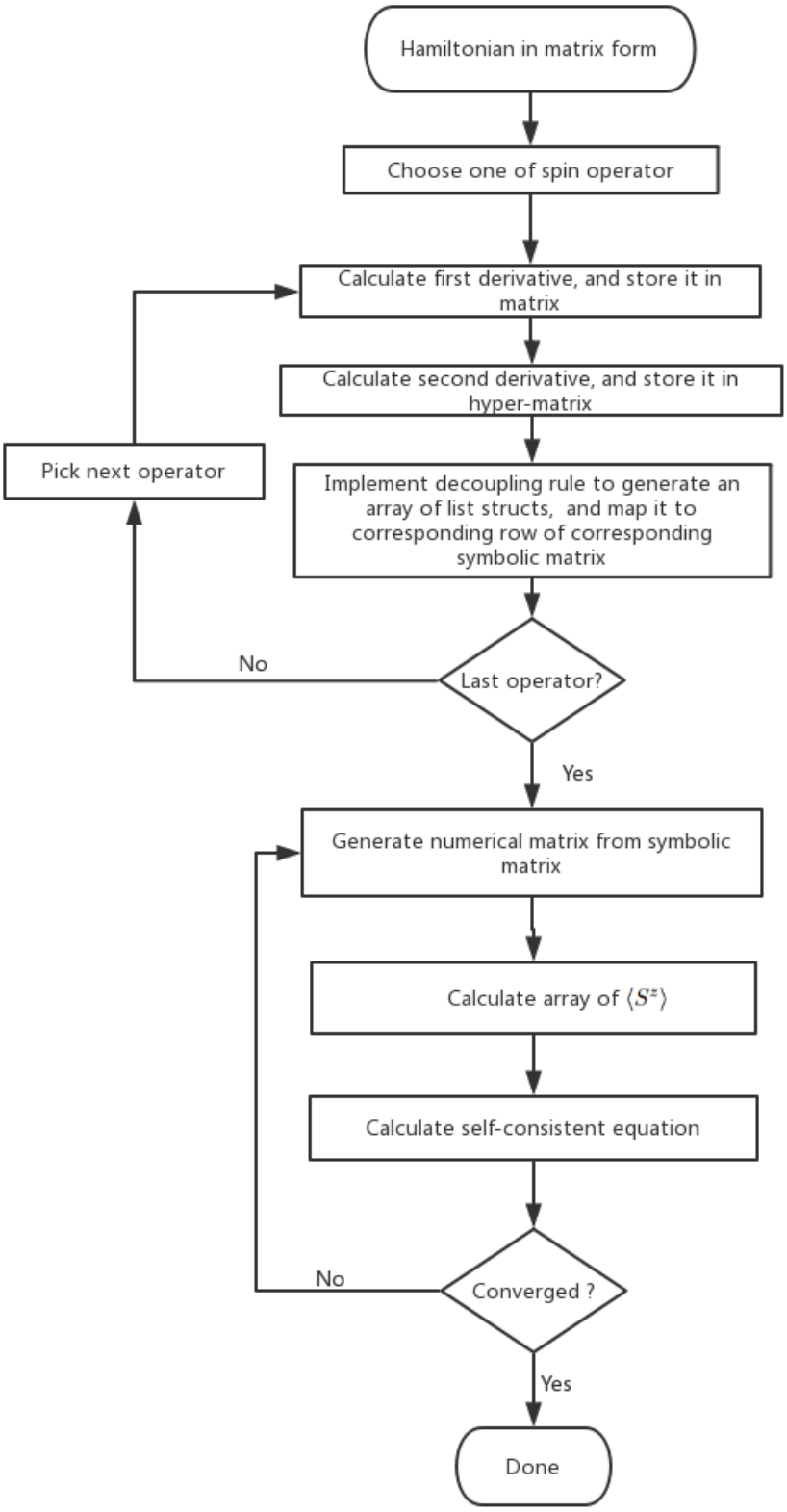

Fig. 5.3. Flowchart of algorithm.

Chapter 6

Summary

In Chapter 3, I studied soft phonon due to second-order Jahn-Teller effect. And my calculation manifested its enhancement on softness of soft mode. It also shown second order coupling can stabilize anharmonic oscillation. Although I didn't investigate structural phase transition, the stabilization indicate coupling may increase the temperature of transition. It partially supports Bersuker's argument of local origin of displasive ferroelectricity from dynamic point of view. Such model didn't contain direct long-range coupling between ions and it contains acoustic zone-center features. The incorporation with polarizability model to investigate whole phonon band should be next step, and it may provide deeper understanding about soft-mode condensation in $EuTiO_3$.

In Chapter 4, I investigated the magnetoresistance of $EuTiO_3$ bulk system. I derived formula to study spin-disorder scattering in detail. Although it looks complicated, it approximately considered full spin dynamics in three magnetic phases, including critical region. Hence it is able to uniformly study both spin-disorder scattering and molecular field effect over critical region. Finally, its numerical results matched experiments during magneto-region, however with few fitting parameters. It exhibited dramatical huge CMR effect in $EuTiO_3$ are dominated by carrier change due to

molecular field caused band shift, and spin-disorder scattering play minor role in CMR.

In Chapter 5, I derived the self-consistent formula for spin Green's function of nano-size system and proposed an algorithm to do expansion automatically. It's possible to be used for modeling nano-scale functional device of multiferroic ETO layer.

Bibliography

[1] D. Fu and M. Itoh, "Role of Ca off-centering in tuning the ferroelectric phase transitions in Ba(Zr,Ti)O_3 system," *Ferroelectr. Mater.*, 2015.

[2] M. E. Lines and A. M. Glass, *Principles and Applications of Ferroelectrics and Related Materials*, ser. International series of monographs on physics. OUP Oxford, 1977.

[3] H. Bilz, G. Benedek, and A. Bussmann-Holder, "Theory of ferroelectricity: The polarizability model," *Phys. Rev. B*, vol. 35, no. 10, pp. 4840–4849, apr 1987.

[4] V. Goian, S. Kamba, J. Hlinka, P. Vaněk, a. a. Belik, T. Kolodiazhnyi, and J. Petzelt, "Polar phonon mixing in magnetoelectric $EuTiO_3$," *Eur. Phys. J. B*, vol. 71, no. 3, pp. 429–433, oct 2009.

[5] H. Wu and W. Z. Shen, "Magnetoelectric effect in perovskite quantum paraelectric $EuTiO_3$," *Solid State Commun.*, vol. 133, no. 8, pp. 487–491, 2005.

[6] A. Bussmann-Holder, J. Kohler, R. K. Kremer, and J. M. Law, "Relation between structural instabilities in $EuTiO_3$ and $SrTiO_3$," *Phys. Rev. B*, vol. 83, no. 21, pp. 1–4, 2011.

[7] J. G. Bednorz and K. A. Müller, "Possible highTc superconductivity in the Ba-La-Cu-O system," *Zeitschrift für Phys. B Condens. Matter*, vol. 64, no. 2, pp. 189–193, jun 1986.

[8] G. Binasch, P. Grünberg, F. Saurenbach, and W. Zinn, "Enhanced magnetoresistance in layered magnetic structures with antiferromagnetic interlayer exchange," *Phys. Rev. B*, vol. 39, no. 7, pp. 4828–4830, mar 1989.

[9] M. N. Baibich, J. M. Broto, A. Fert, F. N. Van Dau, F. Petroff, P. Etienne, G. Creuzet, A. Friederich, and J. Chazelas, "Giant Magnetoresistance of (001)Fe/(001)Cr Magnetic Superlattices," *Phys. Rev. Lett.*, vol. 61, no. 21, pp. 2472–2475, nov 1988.

[10] W. Zhang, G. E. Eperon, and H. J. Snaith, "Metal halide perovskites for energy applications," vol. 1, p. 16048, may 2016.

[11] A. S. Bhalla, R. Guo, and R. Roy, "The perovskite structurea review of its role in ceramic science and technology," *Mater. Res. Innov.*, vol. 4, no. 1, pp. 3–26, 2000.

[12] H. D. Megaw, "Crystal Structure of Barium Titanate," *Nature*, vol. 155, no. 3938, pp. 484–485, 1945.

[13] A. von Hippel, "Ferroelectricity, Domain Structure, and Phase Transitions of Barium Titanate," *Rev. Mod. Phys.*, vol. 22, no. 3, pp. 221–237, jul 1950.

[14] M. Yashima and R. Ali, "Structural phase transition and octahedral tilting in the calcium titanate perovskite $CaTiO_3$," *Solid State Ionics*, vol. 180, no. 2-3, pp. 120–126, 2009.

[15] E. Tosatti and R. Martoák, "Rotational melting in displacive quantum paraelectrics," *Solid State Commun.*, vol. 92, no. 1, pp. 167–180, 1994.

[16] S. K. Mishra and D. Pandey, "Low temperature x-ray diffraction study of the phase transitions in $Sr_{1-x}Ca_xTiO_3$ (x=0.02,0.04): Evi-

dence for ferrielectric ordering," *Appl. Phys. Lett.*, vol. 95, no. 23, p. 232910, 2009.

[17] F. W. Lytle, "XRay Diffractometry of LowTemperature Phase Transformations in Strontium Titanate," *J. Appl. Phys.*, vol. 35, no. 7, pp. 2212–2215, jul 1964.

[18] M. Itoh, R. Wang, Y. Inaguma, T. Yamaguchi, Y.-J. Shan, and T. Nakamura, "Ferroelectricity Induced by Oxygen Isotope Exchange in Strontium Titanate Perovskite," *Phys. Rev. Lett.*, vol. 82, no. 17, pp. 3540–3543, apr 1999.

[19] J. G. Bednorz and K. A. Müller, "$Sr_{1-x}Ca_xTiO_3$: An XY Quantum Ferroelectric with Transition to Randomness," *Phys. Rev. Lett.*, vol. 52, no. 25, pp. 2289–2292, jun 1984.

[20] J. H. Haeni, P. Irvin, W. Chang, R. Uecker, P. Reiche, Y. L. Li, S. Choudhury, W. Tian, M. E. Hawley, B. Craigo, A. K. Tagantsev, X. Q. Pan, S. K. Streiffer, L. Q. Chen, S. W. Kirchoefer, J. Levy, and D. G. Schlom, "Room-temperature ferroelectricity in strained $SrTiO_3$," *Nature*, vol. 430, no. 7001, pp. 758–761, aug 2004.

[21] H. Uwe and T. Sakudo, "Stress-induced ferroelectricity and soft phonon modes in $SrTiO_3$," *Phys. Rev. B*, vol. 13, no. 1, pp. 271–286, jan 1976.

[22] Y. Taguchi, Y. Tokura, T. Arima, and F. Inaba, "Change of electronic structures with carrier doping in the highly correlated electron system $Y_{1-x}Ca_xTiO_3$," *Phys. Rev. B*, vol. 48, no. 1, pp. 511–518, jul 1993.

[23] Y. Tokura, Y. Taguchi, Y. Okada, Y. Fujishima, T. Arima, K. Kumagai, and Y. Iye, "Filling dependence of electronic properties on the verge of metalMott-insulator transition in $Sr_{1-x}La_xTiO_3$," *Phys. Rev. Lett.*, vol. 70, no. 14, pp. 2126–2129, apr 1993.

[24] T. Katsufuji, Y. Taguchi, and Y. Tokura, "Transport and magnetic properties of a Mott-Hubbard system whose bandwidth and band filling are both controllable: $R_{1-x}Ca_xTiO_{3+y/2}$," *Phys. Rev. B*, vol. 56, no. 16, pp. 10 145–10 153, oct 1997.

[25] H. Akamatsu, Y. Kumagai, F. Oba, K. Fujita, H. Murakami, K. Tanaka, and I. Tanaka, "Antiferromagnetic superexchange via 3d states of titanium in $EuTiO_3$ as seen from hybrid Hartree-Fock density functional calculations," *Phys. Rev. B*, vol. 83, no. 21, p. 214421, jun 2011.

[26] J. H. Lee, L. Fang, E. Vlahos, X. Ke, Y. W. Jung, L. F. Kourkoutis, J.-W. Kim, P. J. Ryan, T. Heeg, M. Roeckerath, V. Goian, M. Bernhagen, R. Uecker, P. C. Hammel, K. M. Rabe, S. Kamba, J. Schubert, J. W. Freeland, D. A. Muller, C. J. Fennie, P. Schiffer, V. Gopalan, E. Johnston-Halperin, and D. G. Schlom, "A strong ferroelectric ferromagnet created by means of spin-lattice coupling," *Nature*, vol. 466, no. 7309, pp. 954–958, aug 2010.

[27] A. N. Morozovska, M. D. Glinchuk, R. K. Behera, B. Zaulychny, C. S. Deo, and E. A. Eliseev, "Ferroelectricity and ferromagnetism in $EuTiO_3$ nanowires," *Phys. Rev. B*, vol. 84, no. 20, p. 205403, nov 2011.

[28] G.-m. Zhao, V. Smolyaninova, W. Prellier, and H. Keller, "Electrical Transport in the Ferromagnetic State of Manganites: Small-Polaron Metallic Conduction at Low Temperatures," *Phys. Rev. Lett.*, vol. 84, no. 26, pp. 6086–6089, jun 2000.

[29] R. Shen and Z.-Z. Li, "Magnetic phase diagram and transport properties of the mixed-valence manganites," *Solid State Commun.*, vol. 110, no. 4, pp. 237–242, 1999.

[30] Q. Li, J. Zang, A. R. Bishop, and C. M. Soukoulis, "Charge localization in disordered colossal-magnetoresistance manganites," *Phys. Rev. B*, vol. 56, no. 8, pp. 4541–4544, aug 1997.

[31] H. Röder, J. Zang, and A. R. Bishop, "Lattice Effects in the Colossal-Magnetoresistance Manganites," *Phys. Rev. Lett.*, vol. 76, no. 8, pp. 1356–1359, feb 1996.

[32] J. Zang, A. R. Bishop, and H. Röder, "Double degeneracy and Jahn-Teller effects in colossal-magnetoresistance perovskites," *Phys. Rev. B*, vol. 53, no. 14, pp. R8840—-R8843, apr 1996.

[33] A. J. Millis, "Lattice effects in magnetoresistive manganese perovskites," *Nature*, vol. 392, no. 6672, pp. 147–150, mar 1998.

[34] A. J. Millis, R. Mueller, and B. I. Shraiman, "Fermi-liquid-to-polaron crossover. II. Double exchange and the physics of colossal magnetoresistance," *Phys. Rev. B*, vol. 54, no. 8, pp. 5405–5417, aug 1996.

[35] A. J. Millis, P. B. Littlewood, and B. I. Shraiman, "Double Exchange Alone Does Not Explain the Resistivity of $La_{1-x}Sr_xMnO_3$," *Phys. Rev. Lett.*, vol. 74, no. 25, pp. 5144–5147, jun 1995.

[36] K. M. RUBI and O. B. SINGH, "MAGNETOCALORIC, MAGNETORESISTANCE AND MAGNETODIELECTRIC EFFECTS IN UNDOPED AND DOPED $EuTiO_3$," Ph.D. dissertation, 2016.

[37] P. Drude, "Zur Elektronentheorie der Metalle; II. Teil. Galvanomagnetische und thermomagnetische Effecte," *Ann. Phys.*, vol. 308, no. 11, pp. 369–402, 1900.

[38] Drude, P, "Zur Elektronentheorie der Metalle," *Ann. Phys.*, vol. 306, no. 3, pp. 566–613, 1900.

[39] J. Sólyom, "A proof of Wick's theorem for spin operators," *Phys. Lett. A*, vol. 28, no. 2, pp. 99–100, 1968.

[40] H. Callen, "Green Function Theory of Ferromagnetism," *Phys. Rev.*, vol. 130, no. 3, pp. 890–898, 1963.

[41] F. Suzuki, N. Shibata, and C. Ishii, "Thermodynamics of low-dimensional Heisenberg ferromagnets by the Green's function method," *J. Phys. Soc. Japan*, vol. 63, no. 4, pp. 1539–1547, 1994.

[42] H. Shimahara and S. Takada, "Green's Function Theory of the Two-DimensionalHeisenberg ModelSpin Wave in Short Range Order," *J. Phys. Soc. Japan*, vol. 60, no. 7, pp. 2394–2405, 1991.

[43] C. P. J. Curie, *Comput Rend Acad Sci Paris*, no. 91, pp. 294–297, 1880.

[44] G. Busch and P. Scherrer, *Naturwiss*, no. 23, pp. 737–738, 1935.

[45] A. von Hippel, R. G. Breckenridge, F. G. Chesley, and L. Tisza, "High dielectric constant ceramics," *Ind. Eng. Chem.*, vol. 38, no. 11, pp. 1097–1109, 1946.

[46] Wul, B. and Goldman, J. M., *C. R. Acad. Sci. URRS*, no. 51, p. 21, 1946.

[47] Wul, B. and Goldman, J. M., *C. R. Acad. Sci. URRS*, no. 49, p. 177, 1945.

[48] Wul, B. and Goldman, J. M., *C. R. Acad. Sci. URRS*, no. 46, p. 139, 1945.

[49] T. M. K. Nedungadi, "Effect of temperature on the raman spectrum of quartz," *Proc. Indian Acad. Sci. - Sect. A*, vol. 11, no. 2, pp. 86–95, feb 1940.

[50] A. Bussmann-Holder, "The polarizability model for ferroelectricity in perovskite oxides," *J. Phys. Condens. Matter*, vol. 24, no. 27, p. 273202, jul 2012.

[51] G. Benedek, H. Bilz, and B. Mokross, "MICROSCOPIC POLARIZABILITY MODEL OF FERROELECTRIC SOFT MODES," 1981.

[52] A. Bussmann-Holder, H. Bilz, and G. Benedek, "Applications of the polarizability model to various displacive-type ferroelectric systems," *Phys. Rev. B*, vol. 39, no. 13, pp. 9214–9223, 1989.

[53] W. Cochran, "Crystal stability and the theory of ferroelectricity," *Phys. Rev. Lett.*, vol. 3, no. 9, pp. 412–414, 1959.

[54] A. Bussmann-Holder and J. Köhler, "Revisiting the fascinating properties of $EuTiO_3$ and its mixed crystals with $SrTiO_3$: Possible candidates for novel functionalities," *J. Phys. Chem. Solids*, vol. 84, pp. 2–12, 2014.

[55] J. L. Bettis, M.-H. Whangbo, J. Köhler, A. Bussmann-Holder, and A. R. Bishop, "Lattice dynamical analogies and differences between $SrTiO_3$ revealed by phonon-dispersion relations and double-well," *Phys. Rev. B*, vol. 84, no. 18, p. 184114, nov 2011.

[56] H. Bilz, H. Buttner, A. Bussmann-holder, and P. Vogl, "Phonon anomalies in ferroelectrics and superconductors," *Ferroelectrics*, vol. 73, no. 1, pp. 493–500, 1987.

[57] I. B. Bersuker, "Pseudo Jahn-teller origin of perovskite multiferroics, magnetic- ferroelectric crossover, and magnetoelectric effects: The d0-d10 problem," *Phys. Rev. Lett.*, vol. 108, no. 13, pp. 1–5, 2012.

[58] W. Thomson, "On the Electro-Dynamic Qualities of Metals:–Effects of Magnetization on the Electric Conductivity of Nickel and of Iron," *Proc. R. Soc. London*, vol. 8, pp. 546–550, jan 1856.

[59] M. Galperin, A. Nitzan, and M. A. Ratner, "Inelastic effects in molecular junctions in the Coulomb and Kondo regimes: Nonequilibrium equation-of-motion approach," *Phys. Rev. B*, vol. 76, no. 3, p. 35301, jul 2007.

[60] P. Fröbrich, P. Jensen, P. Kuntz, and A. Ecker, "Many-body Green's function theory for the magnetic reorientation of thin ferromagnetic films," *Eur. Phys. J.*, vol. 594, pp. 579–594, 2000.

[61] J. B. Torrance, M. W. Shafer, and T. R. McGuire, "Bound Magnetic Polarons and the Insulator-Metal Transition in EuO," *Phys. Rev. Lett.*, vol. 29, no. 17, pp. 1168–1171, oct 1972.

[62] H. G. Bohn, W. Zinn, B. Dorner, and A. Kollmar, "Neutron scattering study of spin waves and exchange interactions in ferromagnetic and paramagnetic EuS," *J. Appl. Phys.*, vol. 52, no. 3, pp. 2228–2230, 1981.

[63] T. Kolodiazhnyi, M. Valant, J. R. Williams, M. Bugnet, G. a. Botton, N. Ohashi, and Y. Sakka, "Evidence of Eu^{2+} 4f electrons in the valence band spectra of $EuTiO_3$ and $EuZrO_3$," *J. Appl. Phys.*, vol. 112, no. 8, p. 083719, 2012.

[64] P. Fröbrich and P. J. Kuntz, "Spectral theorem of many-body Green's function theory when there are zero eigenvalues of the matrix governing the equations of motion," *Phys. Rev. B*, vol. 68, no. 1, p. 14410, jul 2003.

[65] S. V. Molnar and S. Methfessel, "Giant Negative Magnetoresistance in Ferromagnetic Eu1xGdxSe," *J. Appl. Phys.*, vol. 38, no. 3, pp. 959–964, 1967.

[66] Winterfeldt, S. and Ihle, D., "Theory of antiferromagnetic short-range order in the two-dimensional Heisenberg model," *Phys. Rev. B*, vol. 56, no. 9, p. 5535, 1997.

[67] Y. Dubi and M. Di Ventra, "Thermoelectric Effects in Nanoscale Junctions," *Nano Lett.*, vol. 9, no. 1, pp. 97–101, 2009.

[68] D. Ihle, C. Schindelin, and H. Fehske, "Magnetic order in the quasi-two-dimensional easy-plane XXZ model," *Phys. Rev. B*, vol. 64, no. 5, p. 054419, jul 2001.

[69] F. B. Anderson and H. B. Callen, "Statistical Mechanics and Field-Induced Phase Transitions of the Heisenberg Antiferromagnet," *Phys. Rev.*, vol. 136, no. 1959, 1964.

[70] J. Hlinka, J. Petzelt, S. Kamba, D. Noujni, and T. Ostapchuk, "Infrared dielectric response of relaxor ferroelectrics," *Phase Transitions*, vol. 79, no. February 2015, pp. 41–78, 2006.

[71] M. Tahir and A. MacKinnon, "Quantum transport in a resonant tunnel junction coupled to a nanomechanical oscillator," *Phys. Rev. B*, vol. 77, no. 22, p. 224305, jun 2008.

[72] Y. Shapira and R. L. Kautz, "Effect of spin splitting of the conduction band on the resistivity and Hall coefficient: Model for the positive magnetoresistance in EuSe," *Phys. Rev. B*, vol. 10, no. 11, pp. 4781–4794, dec 1974.

[73] R. Chen, J.-C. Ren, K. Rubi, R. Mahendiran, and J.-S. Wang, "Small Polaron Transport and Colossal Magnetoresistance in $EuTiO_3$," *Arxiv*, pp. 1–5, 2017.

[74] Y. Shapira, S. Foner, and N. F. Oliveira, "Effect of antiferromagnetic ordering on the resistivity of EuTe," *Phys. Rev. A*, vol. 32, no. 5, pp. 323–324, 1970.

[75] Junger, "Green-function theory of anisotropic Heisenberg magnets with arbitrary spin," Ph.D. dissertation, 1973.

[76] J.-T. Lü, H. Zhou, J.-W. Jiang, and J.-S. Wang, "Effects of electron-phonon interaction on thermal and electrical transport through molecular nano-conductors," *AIP Adv.*, vol. 5, no. 5, p. 53204, 2015.

[77] P. Liu and J. Tang, "A magnetic polaron model for the enhanced Curie temperature of EuO_{1x}," *J. Phys. Condens. Matter*, vol. 25, no. 12, p. 125802, 2013.

[78] J. Varignon, N. C. Bristowe, and P. Ghosez, "Electric Field Control of Jahn-Teller Distortions in Bulk Perovskites," *Phys. Rev. Lett.*, vol. 116, no. 5, pp. 1–6, 2016.

[79] S. Tyablicov and V. Bonch-Brevich, *The Green Function Method in Statistical Mechanics*. Amsterdam: North-Holland, 1962.

[80] H. Wu, Q. Jiang, and W. Z. Shen, "Coupling between the magnetism and dielectric properties in $Eu_{1x}Ba_xTiO_3$," *Phys. Rev. B*, vol. 69, no. 1, p. 014104, 2004.

[81] K. Flensberg, "Tunneling broadening of vibrational sidebands in molecular transistors," *Phys. Rev. B*, vol. 68, no. 20, p. 205323, nov 2003.

[82] C. Schindelin, H. Fehske, H. Büttner, and D. Ihle, "Spin-correlation functions and susceptibilities in the easy-plane XXZ chain," *Phys. Rev. B*, vol. 62, no. 18, pp. 12 141–12 145, 2000.

[83] D. S. Ellis, H. Uchiyama, S. Tsutsui, K. Sugimoto, K. Kato, D. Ishikawa, and A. Q. R. Baron, "Phonon softening and dispersion in $EuTiO_3$," *Phys. Rev. B*, vol. 86, no. 22, pp. 1–5, 2012.

[84] W. Zhong and D. Vanderbilt, "Effect of quantum fluctuations on structural phase transitions in $SrTiO_3$ and $BaTiO_3$," *Phys. Rev. B*, vol. 53, no. 9, pp. 5047–5050, 1996.

[85] Z. J. Mo, Z. H. Hao, J. Shen, L. Li, J. F. Wu, F. X. Hu, J. R. Sun, and B. G. Shen, "Observation of giant magnetocaloric effect in $EuTiO_3$," *J. Alloys Compd.*, vol. 649, pp. 674–678, 2015.

[86] X. Zianni, "Effect of electron-phonon coupling on the thermoelectric efficiency of single-quantum-dot devices," *Phys. Rev. B*, vol. 82, no. 16, p. 165302, oct 2010.

[87] B. Matthias and A. von Hippel, "Domain Structure and Dielectric Response of Barium Titanate Single Crystals," *Phys. Rev.*, vol. 73, no. 11, pp. 1378–1384, jun 1948.

[88] Y. Shapira, S. Foner, T. B. Reed, H. Birecki, and H. E. Stanley, "Dependence of the insulator-metal transition in EuO on magnetic order," *Phys. Rev. A*, vol. 41, no. 5, pp. 471–472, 1972.

[89] W. Haubenreisser, "A Status Report of Green ' s Function Theory in Uniaxial Ferro- magnetic Unpinned Thin Films," vol. 9, 1972.

[90] E. Haller, H. Köppel, L. S. Cederbaum, W. von Niessen, and G. Bieri, "Multimode Jahn-Teller and pseudo-Jahn-Teller effects in BF3," *J. Chem. Phys.*, vol. 78, no. 3, p. 1359, 1983.

[91] D. Nascimento and B. H. Bernhard, "The magnetocaloric effect in itinerant antiferromagnetic materials," *Solid State Commun.*, vol. 167, pp. 40–45, 2013.

[92] H. J. Spencer, "A Wick Theorem for Spin-One Operators," *Phys. Rev.*, vol. 167, no. 2, pp. 430–433, mar 1968.

[93] G. A. Steele, A. K. Hüttel, B. Witkamp, M. Poot, H. B. Meerwaldt, L. P. Kouwenhoven, and H. S. J. van der Zant, "Strong Coupling Between Single-Electron Tunneling and Nanomechanical Motion," *Science (80-.).*, vol. 325, no. 5944, pp. 1103–1107, 2009.

[94] P. J. Ryan, J.-W. Kim, T. Birol, P. Thompson, J.-H. Lee, X. Ke, P. S. Normile, E. Karapetrova, P. Schiffer, S. D. Brown, C. J. Fennie, and D. G. Schlom, "Reversible control of magnetic interactions by electric field in a single-phase material." *Nat. Commun.*, vol. 4, p. 1334, jan 2013.

[95] R. von Helmolt, J. Wecker, B. Holzapfel, L. Schultz, and K. Samwer, "Giant negative magnetoresistance in perovskitelike La 2 / 3 Ba 1 / 3 MnO x ferromagnetic films," *Phys. Rev. Lett.*, vol. 71, no. 14, pp. 2331–2333, oct 1993.

[96] D. Segal and A. Nitzan, "Heating in current carrying molecular junctions," *J. Chem. Phys.*, vol. 117, no. 8, pp. 3915–3927, 2002.

[97] S. Winterfeldt and D. Ihle, "Spin dynamics and antiferromagnetic short-range order in the two-dimensional Heisenberg model," *Phys. Rev. B*, vol. 59, no. 9, pp. 6010–6012, 1999.

[98] K. Z. Rushchanskii, N. a. Spaldin, and M. Ležaić, "First-principles prediction of oxygen octahedral rotations in perovskite-structure EuTiO," *Phys. Rev. B*, vol. 85, no. 10, p. 104109, mar 2012.

[99] S. Süllow, I. Prasad, M. C. Aronson, S. Bogdanovich, J. L. Sarrao, and Z. Fisk, "Metallization and magnetic order in EuB6," *Phys. Rev. B*, vol. 62, no. 17, pp. 11 626–11 632, nov 2000.

[100] S. Kamba, D. Nuzhnyy, P. Vaněk, M. Savinov, K. Knížek, Z. Shen, E. Šantavá, K. Maca, M. Sadowski, and J. Petzelt, "Magnetodielec-

tric effect and optic soft mode behaviour in quantum paraelectric $EuTiO_3$ ceramics," *Europhys. Lett.*, vol. 80, no. 2, p. 27002, 2007.

[101] Y. Kususe, H. Murakami, K. Fujita, I. Kakeya, M. Suzuki, S. Murai, and K. Tanaka, "Magnetic and transport properties of $EuTiO_3$ thin films doped with Nb," *Jpn. J. Appl. Phys.*, vol. 53, pp. 1–7, 2014.

[102] M. Gaudin, "Une démonstration simplifiée du théorème de wick en mécanique statistique," *Nucl. Phys.*, vol. 15, pp. 89–91, feb 1960.

[103] A. Ueda, O. Entin-Wohlman, and A. Aharony, "Effect of phonons on the ac conductance of molecular junctions," *Nanoscale Res. Lett.*, vol. 6, no. 1, p. 204, mar 2011.

[104] Galperin, Michael and Nitzan, Abraham and Ratner, Mark A, "Inelastic tunneling effects on noise properties of molecular junctions," *Phys. Rev. B*, vol. 74, no. 7, p. 75326, aug 2006.

[105] A. Ecker, P. Fröbrich, P. J. Jensen, and P. J. Kuntz, "Temperature dependence of the single-ion lattice anisotropy coefficients of a ferromagnetic Heisenberg monolayer," *J. Phys. Condens. Matter*, vol. 11, no. 6, p. 1557, 1999.

[106] M. R. Oliver, J. O. Dimmock, A. L. McWhorter, and T. B. Reed, "Conductivity Studies in Europium Oxide," *Phys. Rev. B*, vol. 5, no. 3, pp. 1078–1098, feb 1972.

[107] D. Stanek, O. P. Sushkov, and G. S. Uhrig, "Self-consistent spin-wave theory for a frustrated Heisenberg model with biquadratic exchange in the columnar phase and its application to iron pnictides," *Phys. Rev. B*, vol. 84, no. 6, p. 064505, aug 2011.

[108] J. Ren, J.-X. Zhu, J. E. Gubernatis, C. Wang, and B. Li, "Thermoelectric transport with electron-phonon coupling and electron-

electron interaction in molecular junctions," *Phys. Rev. B*, vol. 85, no. 15, p. 155443, apr 2012.

[109] R. A. Tahir-Kheli and D. T. Haar, "Use of Green Functions in the Theory of Ferromagnetism ." *Phys. Rev.*, vol. 41, no. 1961, 1962.

[110] T. Arai and B. Goodman, "Cumulant expansion and Wick's theorem for spins. Application to the antiferromagnetic ground state," *Phys. Rev.*, vol. 155, no. 2, pp. 514–527, 1967.

[111] A. Von Hippel, "Ferroelectricity, domain structure, and phase transitions of barium titanate," *Rev. Mod. Phys.*, vol. 22, no. 3, pp. 221–237, 1950.

[112] J. Yates, X. Wang, D. Vanderbilt, and I. Souza, "Spectral and Fermi surface properties from Wannier interpolation," *Phys. Rev. B*, vol. 75, no. 19, p. 195121, may 2007.

[113] H. Shimahara and S. Takada, "Fragility of AF long-range-order in two dimensional t-J model," 1992.

[114] M. E. Zhitomirsky and A. L. Chernyshev, "Colloquium: Spontaneous magnon decays," *Rev. Mod. Phys.*, vol. 85, no. 1, pp. 219–242, jan 2013.

[115] Z. Huang, F. Chen, R. D'agosta, P. A. Bennett, M. Di Ventra, and N. Tao, "Local ionic and electron heating in single-molecule junctions," *Nat Nano*, vol. 2, no. 11, pp. 698–703, nov 2007.

[116] P. W. Anderson and H. Hasegawa, "Considerations on double exchange," *Phys. Rev.*, vol. 100, no. 2, p. 675, 1955.

[117] B. P. Alho, a. M. G. Carvalho, and P. J. von Ranke, "Anisotropic magnetocaloric effect in antiferromagnetic systems: Application to $EuTiO_3$," *J. Appl. Phys.*, vol. 116, no. 11, p. 113907, 2014.

[118] S. Jin, T. H. Tiefel, M. McCormack, R. A. Fastnacht, R. Ramesh, and L. H. Chen, "Thousandfold Change in Resistivity in Magnetoresistive La-Ca-Mn-O Films," *Science (80-.).*, vol. 264, no. 5157, pp. 413–415, 1994.

[119] H. Zhou, J. Thingna, J.-S. Wang, and B. Li, "Thermoelectric transport through a quantum nanoelectromechanical system and its backaction," *Phys. Rev. B*, vol. 91, no. 4, p. 45410, jan 2015.

[120] N. F. Mott, "The Electrical Conductivity of Transition Metals," *Proc. R. Soc. London A*, vol. 153, no. 880, pp. 699–717, 1936.

[121] D. Ihle, C. Schindelin, A. Weisse, and H. Fehske, "Magnetic order-disorder transition in the two-dimensional spatially anisotropic Heisenberg model at zero temperature," *Phys. Rev. B*, vol. 60, no. 13, pp. 9240–9243, 1999.

[122] P. G. Steeneken, L. H. Tjeng, I. Elfimov, G. A. Sawatzky, G. Ghiringhelli, N. B. Brookes, and D.-J. Huang, "Exchange Splitting and Charge Carrier Spin Polarization in EuO," *Phys. Rev. Lett.*, vol. 88, no. 4, p. 47201, jan 2002.

[123] Y. a. Tserkovnikov, "Equations for two-temperature Green's functions for a Heisenberg ferromagnet in the mode-coupling approximation," *Theor. Math. Phys.*, vol. 154, no. 1, pp. 165–174, 2008.

[124] M. B. Tagani and H. R. Soleimani, "Influence of electron-phonon interaction on the thermoelectric properties of a serially coupled double quantum dot system," *J. Appl. Phys.*, vol. 112, no. 10, p. 103719, 2012.

[125] H.-S. Lu, T.-Y. Cai, S. Ju, and C.-D. Gong, "Half-Metallic p -Type $LaAlO_3$ / $EuTiO_3$ Heterointerface from Density-Functional Theor," *Phys. Rev. Appl.*, vol. 3, no. 3, p. 034011, 2015.

[126] N. Bogolyubov and S. Tyablikov, "Retarded and Advanced Green Functions in Statistical Physics," *Sov. Phys. Dokl.*, vol. 4, p. 589, dec 1959.

[127] L. Bellaiche and J. Íñiguez, "Universal collaborative couplings between oxygen-octahedral rotations and antiferroelectric distortions in perovskites," *Phys. Rev. B*, vol. 88, no. 1, pp. 1–9, 2013.

[128] A. Schilling, M. Cantoni, J. D. Guo, and H. R. Ott, "Superconductivity above 130 K in the Hg-Ba-Ca-Cu-O system," *Nature*, vol. 363, no. 6424, pp. 56–58, may 1993.

[129] G. D. Mahan, *Many-Particle Physics*, ser. Physics of Solids and Liquids. Springer US, 2013.

[130] A.-y. Hu and H.-y. Wang, "The exchange interaction values of perovskite-type materials $EuTiO_3$ and $EuZrO_3$," *J. Appl. Phys.*, vol. 193903, pp. 1–8, 2014.

[131] R. Bastardis, U. Atxitia, O. Chubykalo-Fesenko, and H. Kachkachi, "Unified decoupling scheme for exchange and anisotropy contributions and temperature-dependent spectral properties of anisotropic spin systems," *Phys. Rev. B*, vol. 86, pp. 1–18, 2012.

[132] E. Rhodes and S. Scales, "Second-Order Green's-Function Theory of the Infinite-Chain Heisenberg Ferromagnet," *Phys. Rev. B*, vol. 8, no. 5, pp. 1994–2003, 1973.

[133] C. J. Fennie and K. M. Rabe, "Magnetic and electric phase control in epitaxial $EuTiO_3$ from first principles," *Phys. Rev. Lett.*, vol. 97, no. 26, pp. 1–4, 2006.

[134] Y. Yang, W. Ren, D. Wang, and L. Bellaiche, "Understanding and revisiting properties of $EuTiO_3$ bulk material and films from first principles," *Phys. Rev. Lett.*, vol. 109, no. 26, pp. 1–5, 2012.

[135] C. Zener, "Interaction between the d-shells in the transition metals. II. Ferromagnetic compounds of manganese with Perovskite structure," *Phys. Rev.*, vol. 82, no. 3, pp. 403–405, 1951.

[136] Y. Shapira, S. Foner, and T. B. Reed, "EuO. I. Resistivity and Hall Effect in Fields up to 150 kOe," *Phys. Rev. B*, vol. 8, no. 5, pp. 2299–2315, sep 1973.

[137] T. Birol and C. Fennie, "Origin of giant spin-lattice coupling and the suppression of ferroelectricity in $EuTiO_3$ from first principles," *Phys. Rev. B*, vol. 88, no. 9, p. 094103, sep 2013.

[138] W. Capra, "The magnetic phase diagram of the magnetoelectric $EuTiO_3$ studied by neutron powder diffraction," *PhD Thesis*, 2013.

[139] Y. Shapira, R. L. Kautz, and T. B. Reed, *Positive Magnetoresistance Due to Conduction-Band Splitting in the Eu — Chalcogenides*. Wiesbaden: Vieweg+Teubner Verlag, 1974, pp. 894–898.

[140] H. Haberlandt and A. Kohnel, "Diagram Technique for the Green Function of a Heisenberg Ferromagnet with Arbitrary Spin," *Phys. Status Solidi*, vol. 60, no. 2, pp. 625–632, 1973.

[141] J. M. Ziman, *Electrons and Phonons: The Theory of Transport Phenomena in Solids*, ser. International series of monographs on physics. OUP Oxford, 1960.

[142] B. Lassagne, Y. Tarakanov, J. Kinaret, D. Garcia-Sanchez, and A. Bachtold, "Coupling Mechanics to Charge Transport in Carbon Nanotube Mechanical Resonators," *Science (80-.).*, vol. 325, no. 5944, pp. 1107–1110, 2009.

[143] L. Simine and D. Segal, "Vibrational cooling, heating, and instability in molecular conducting junctions: full counting statistics analysis," *Phys. Chem. Chem. Phys.*, vol. 14, no. 40, pp. 13 820–13 834, 2012.

[144] a. L. Kuzemsky, "Irreducible green functions method and many-particle interacting systems on a lattice," *Riv. del Nuovo Cim.*, vol. 25, no. 1, pp. 1–91, 2001.

[145] H. Park, J. Park, A. K. L. Lim, E. H. Anderson, A. P. Alivisatos, and P. L. McEuen, "Nanomechanical oscillations in a single-C60 transistor," *Nature*, vol. 407, no. 6800, pp. 57–60, sep 2000.

[146] N. M. Plakida, "Dyson equation for Heisenberg ferromagnet," *Phys. Lett. A*, vol. 43, no. 6, pp. 481–482, 1973.

[147] A. Mitra, I. Aleiner, and A. J. Millis, "Phonon effects in molecular transistors: Quantal and classical treatment," *Phys. Rev. B*, vol. 69, no. 24, pp. 1–21, 2004.

[148] H. Akamatsu, Y. Kumagai, F. Oba, K. Fujita, H. Murakami, K. Tanaka, and I. Tanaka, "Antiferromagnetic superexchange via 3d states of titanium in $EuTiO_3$ as seen from hybrid hartree-fock density functional calculations," *Phys. Rev. B*, no. 21, p. 214421, jun.

[149] P. M. Woodward, "Octahedral Tilting in Perovskites. II. Structure Stabilizing Forces," *Acta Crystallogr. B*, vol. 53, no. 1, pp. 44–66, 1997.

[150] J. F. Cooke and H. H. Hahn, "Rigorous Boson Formulation for Calculating Time-Dependent Thermal Properties of Localized Spin Systems," *Phys. Rev.*, vol. 184, no. 2, pp. 509–517, aug 1969.

[151] Z. Nussinov, A. Shnirman, D. P. Arovas, A. V. Balatsky, and J. X. Zhu, "Spin and spin-wave dynamics in Josephson junctions," *Phys. Rev. B*, vol. 71, no. 21, pp. 1–14, 2005.

[152] K. Rubi, P. Kumar, D. V. Maheswar Repaka, R. Chen, J.-S. Wang, and R. Mahendiran, "Giant magnetocaloric effect in magnetoelectric $Eu_{1-x}Ba_xTiO_3$," *Appl. Phys. Lett.*, vol. 104, no. 3, p. 032407, 2014.

[153] S. Tyablicov, *Methods in the Quantum Theory of Magnetism.* New York: Plenum Press, 1967.

[154] B. T. Matthias, R. M. Bozorth, and J. H. Van Vleck, "Ferromagnetic Interaction in EuO," *Phys. Rev. Lett.*, vol. 7, no. 5, pp. 160–161, sep 1961.

[155] J. Kondo and K. Yamaji, "Green's-Function Formalism of the One-Dimensional Heisenberg Spin System," *Prog. Theor. Phys.*, vol. 47, no. 3, p. 807, 1972.

[156] L. Siurakshina, D. Ihle, and R. Hayn, "Theory of magnetic order in the three-dimensional spatially anisotropic Heisenberg model," *Phys. Rev. B*, vol. 61, no. 21, pp. 14 601–14 606, 2000.

[157] P. FROBRICH and P. KUNTZ, "Many-body Green's function theory of Heisenberg films," *Phys. Rep.*, vol. 432, no. 5-6, pp. 223–304, oct 2006.

[158] R. A. Tahir-Kheli and D. ter Haar, "Use of Green Functions in the Theory of Ferromagnetism. III. s-d Interactions," *Phys. Rev.*, vol. 130, no. 1, pp. 108–112, apr 1963.

[159] A. B. Harris, D. Kumar, B. I. Halperin, and P. C. Hohenberg, "Dynamics of an antiferromagnet at low temperatures: Spin-wave damping and hydrodynamics," *Phys. Rev. B*, vol. 3, no. 3, pp. 961–1024, 1971.

[160] D. Levy and O. Nagai, "Effects of Surface Spin Waves and Surface Anisotropy in Magnetic Thin Films at Finite Temperatures," *Phys. Status Solidi*, vol. 351, pp. 351–361, 1979.

[161] C. Timm, S. M. Girvin, P. Henelius, and A. W. Sandvik, "1/N expansion for two-dimensional quantum ferromagnets," *Phys. Rev. B*, vol. 58, no. 3, pp. 1464–1484, 1998.